CARBON MOLECULAR SIEVE AND CERAMIC MEMBRANES FOR BLACK LIQUOR CONCENTRATION

A Thesis
Presented to
The Academic Faculty

By

Nikita Sergeevich Kevlich

In Partial Fulfillment
Of the Requirements for the Degree
Master of Science in Chemical Engineering

Georgia Institute of Technology

December 2015

CARBON MOLECULAR SIEVE AND CERAMIC MEMBRANES FOR BLACK LIQUOR CONCENTRATION

Approved by:

Dr. Sankar Nair, Advisor
School of Chemical & Biomolecular Engineering
Georgia Institute of Technology

Dr. Meisha Shofner, Co-Advisor
School of Materials Science and Engineering
Georgia Institute of Technology

Dr. Ryan Lively, Committee Member
School of Chemical & Biomolecular Engineering
Georgia Institute of Technology

Date Approved: November 2, 2015

ACKNOWLEDGEMENTS

There have been many persons without whom this thesis would not be possible. In particular, I would like to thank Dr. Sinquefield, Dr. Ketki Sharma, Dr. Fereshteh Rashidi, Dr. Jason Bentley, Mr. Steve Lien, Phillip Crawford, Kiwon Eum, Dr. Fawen Wu, Krishna Chandran Jayachandrababu, Dr. Seok-Jhin Kim, Matthew Orr, Dr. Crawford, Major Henry White, my parents, and all the others who have given assistance, advised, listened, and encouraged me in this endeavor. The advice and resources provided by my advisor, Dr. Nair and my co-advisor, Dr. Shofner, were invaluable. I also wish to thank Christ for the grace to make it through.

Thanks to Dr. Reichmanis' lab (particularly Dalsu Choi and Ping-Hsun Chu) for allowing us to use their UV-Vis and spin-coater, to Dr. Dong-Yeun Koh for providing the Hg porosimetery data, to Ms. Yolande Berta for her training and assistance in using the SEM, EDX, and Au coater, Jeff Andrews and Parker Bradley for their machine-shop assistance, for the ChemE glass-shop; Manny Gonzales, Jamshad Mahmood, Peter Marshall, Dr. Radhakrishnaiah Parachuru for their guidance on equipment for pressing, firing, and polishing of alumina supports; Dr. Santamarina and Marco Terzariol for their high-pressure module safety assistance; and Ellis Kilgore (Swagelok) for his assistance with designing and purchasing proper parts,

Finally, many thanks to the Renewable Bioproducts Institute for financial support through the PSE Fellowship.

TABLE OF CONTENTS

LIST OF TABLES

LIST OF FIGURES

LIST OF SYMBOLS OR ABBREVIATIONS [NOMENCLATURE]

Greek Symbols:

μ	dynamic viscosity
υ	kinematic viscosity
π	osmotic pressure
σ	reflection coefficient
ω	angular velocity

Abbreviations and Nomenclature

a	solution/fitting constant for osmotic pressure
BL	black liquor
BPR	backpressure regulator
C_b	bulk or feed concentration
C_m	concentration at the membrane wall/interface
CMS	carbon molecular sieve
C_p	permeate concentration
D	diffusion coefficient
DI	distilled
EPDM	ethylene propylene diene monomer
FTIR	fourier transform infrared spectroscopy
J	water (or solvent) flux
J_v	the volumetric flux of the permeate through the membrane

k	solute mass transfer coefficient
KCL	Kymen Laboratories Ltd
KK	Kedem–Katchalsky
m_b	initial mass of the bulk/feed solution
MF	microfiltration
m_p	mass of the permeate
MW	molecular weight
MW_w	weight-average molecular weight
MWCO	molecular weight cut off
n	solution/fitting constant for osmotic pressure
NF	nanofiltration
NMP	1-Methyl-2-pyrrolidinone
$\bar{P}$	permeance
PEG	polyethylene glycol
PES	polyethersulfone
PVA	polyvinyl alcohol
P_m	solute permeability
r	membrane radius
R_a	resistance from adsorption of solutes onto the membrane surface
R_{cp}	resistance from concentration polarization
Re	Reynold's number
R_g	gel layer resistance
R_m	hydraulic membrane resistance

RO	reverse osmosis
R_{obs}	observed rejection
RPM	rotations per minute
R_{int}	intrinsic (real) rejection
r_s	Stokes radius
RT	room temperature
SBL	strong black liquor
SCAN	Scandinavian Pulp, Paper, and Board Testing Committee
SEM	scanning electron microscope
SK	Spiegler–Kedem
SS316	stainless steel 316
TAPPI	Technological Association of the Pulp and Paper Industry
TDS	total dissolved solids
TGA	thermogravimetric analysis
TMP	transmembrane pressure
TS	total solids
UF	ultrafiltration
V_0	initial volume
V_p	permeate volume
V_R	retentate volume
VR	volume reduction
WAXD	wide angle x-ray diffraction
WBL	weak black liquor

XRD	X-ray diffraction

SUMMARY

The concentration of Kraft black liquor is an energy-intensive process requiring 6-7 multiple effect evaporators. Membranes have the potential to replace the first 1-2 of these evaporator effects (stages) by concentrating black liquor to 30-35%, resulting in significant energy savings. There are no membranes in industrial use for this purpose today, though both polymeric and ceramic (metal oxide) have been studied in the laboratory and on a pilot scale. These membranes face issues of sufficient stability (polymers) and larger costs and pore sizes (ceramics), resulting in inadequate performance. This work addresses improvements in the performance of ceramic (α-alumina and γ-alumina) membranes by adding coatings with smaller pore sizes onto supports with larger pores (for high fluxes). These coated supports are able to serve as both prefilters and as adequate supports for the coating of Matrimid-based carbon molecular sieves (CMSs) to achieve reverse osmosis-quality filtrates. Ceramic coatings achieved a maximum lignin rejection of 60%, which is inadequate for good filtration based on the state-of the art commercial membranes. However, for CMS coatings, the alumina-coated layer yielded a CMS membrane with flux and ~68% lignin rejection. Though defects in the CMS layer are present, the initial results are promising. Future work would address the mitigation of defects and incorporate sacrificial nanoparticles into the CMS layer to improve liquid flux performance.

CHAPTER 1

INTRODUCTION AND LITERATURE REVIEW

1.1 Motivation

The objective of this work was to develop improved non-polymeric membranes for the concentration of Kraft black liquor (BL). BL is a very caustic fluid (pH>12) that exits digesters at high temperatures (80-90 °C) and contains numerous organic and inorganic fouling species. The paper industry recovers the organic and inorganic species in BL by multiple-effect evaporation. However, this is very energy-intensive and membranes offer the promise to replace 1-2 evaporators by concentrating BL from about 15% solids to about 35% solids.

Work has been carried out using both polymeric and ceramic (metal oxide) membranes. Polymeric membranes are cheaper, but suffer from lack of long-term stability under the harsh BL conditions. Ceramic membranes are more stable, but are more expensive and lack the small pore-sizes to achieve high-rejections. Furthermore, a literature survey showed that most of the membranes tested were commercial membranes; little has been done to improve the performance of non-polymeric membranes to increase their rejection performance (by decreasing pore sizes) yet maintaining high stability and minimizing costs.

This project addressed some of these issues by attempting to design and characterize improved ceramic (α-alumina and γ-alumina) and zeolite and/or carbon molecular sieve (CMS) membranes that can withstand the harsh operating conditions

associated with black liquor (BL) while efficiently concentrating BL from about 15% solids to about 35% solids.

1.2 Basics of BL and Kraft pulping

The production of forest-based products such as paper involves highly energy-intensive pulping processes. Three key types of pulping processes are used in the production of paper products: soda, sulfite, and sulfate (Kraft). Soda pulping uses primarily NaOH and is used to handle bagasse, straw, grass, bamboo and similar non-wood based sources. Sulfite pulping uses sulfite or bisulfite salts (e.g., ammonium sulfite) to break up wood chips. The Kraft process (Figure 1) is the dominant pulping process. In the Kraft process, NaOH is used as the primary pulping chemical, but Na_2S is also added to assist removal of lignin from the cellulose fibers and to mechanically strengthen the resulting pulp. In this process, wood chips and Kraft pulping chemicals are mixed in a pressurized, heated digester to break up the woody biomass and remove the pulp, which is used for paper production. The incoming pulping chemical stream is known as cooking liquor or white liquor and the pulp waste stream is known as black liquor (BL). The BL stream that exits the digester is called weak BL (WBL) and is at a typical temperature of 90°C, high pH (>10.5), and about 15 wt.% solids concentration. It contains a number of inorganic and organic compounds, the most important of which are the pulping chemicals and lignin. The weak BL stream is concentrated in multiple-effect evaporators to strong BL (SBL) that contains 50-75 wt.% solids. The concentrated BL is then burned to provide energy to the Kraft process and to recover the inorganic chemicals.[1, 2]

With more than 500 million tons/year of BL generated worldwide and almost 200 trillion BTUs/year (0.2 Quads/year) of energy used for BL concentration in the US alone, the recovery of BL is an important industrial and environmental issue.[3] BL is a valuable byproduct from which one can recover the pulping chemicals, produce energy from recovery and combustion of lignin, and recover other organic BL components as feedstocks for higher-value bio-based products.[4-6] For example, lignin has many functional groups which can be used in place of petroleum-derived molecules as building blocks for higher-value chemicals. The most common commercial uses of lignin are as dispersants, as binders, and in steam/power production.[6-15] Other BL components, like hydroxyacids could be used for manufacture of cosmetics, film packaging, and biodegradable plastics, while hemicellulose could be used in hydrogels and as a paper additive.[10, 16, 17]

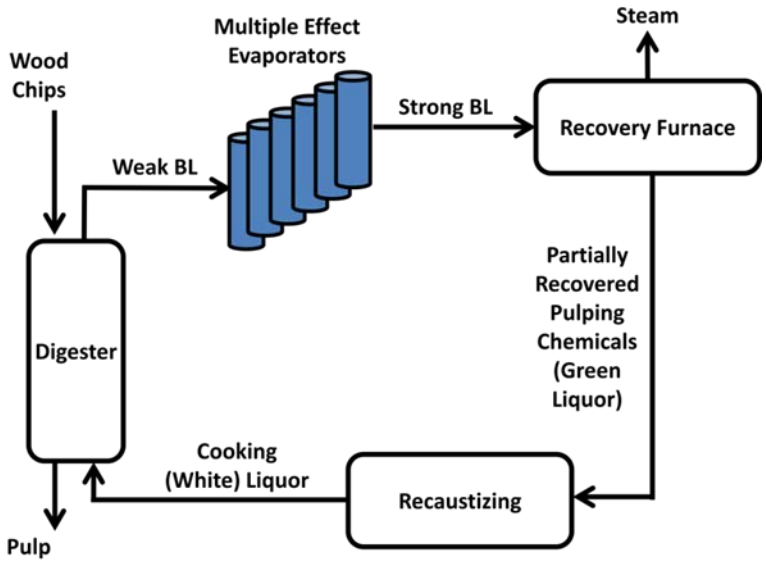

Figure 1: Simplified schematic of the Kraft pulping process and Black Liquor (BL) recycling. Adapted from Refs.[1, 2]

Conventionally, BL concentration from WBL to SBL is carried out in multiple-effect evaporators, which convert BL from about 15% solids up to about 75% solids.[18] This concentrated slurry can be combusted to generate electricity, and the resultant ash is causticized to recover the pulping chemicals, which are sent back to the digester.[1, 19] The multiple-effect evaporation process is very energy intensive and has a large CO_2 emissions footprint. This process is the second largest energy consumer in the paper plant.[16] Globally, the pulp and paper industry is the fourth largest industrial energy user, consuming more than 6 Quads/yr in 2005.[20] Membranes are a potential alternative for the energy-efficient concentration of BL and for recovering valuable organic and inorganic components. Because of the high fouling potential and high viscosity of concentrated BL, a complete replacement of the entire evaporation process with membranes is likely not feasible. However, even partial concentration (up to about 30% solids) would considerably improve the process and result in a major reduction in energy usage. Membranes also have advantages over alternate approaches for lignin removal that rely upon inducing its precipitation via acidification or electrochemical techniques (to precipitate lignin by lowering the pH via an electrical current).[16, 21] One relevant example of the acid precipitation technique is the Lignoboost process, which has been scaled-up in a demonstration plant owned by Inventia. This process focuses on lignin recovery post-precipitation by utilizing membrane filtration and resuspension of the filtrate cake to achieve high purity and high recovery of lignin.[22] However, experimental comparisons of the acidification or electrochemical techniques support the general conclusion that while acidification processes can achieve a high degree of lignin removal, they also involve high costs of acidifying chemicals, anti-corrosion and process safety measures, and

electrical energy, as well as degradation of the lignin.[5, 13, 14, 23-26] In light of these drawbacks, membranes offer the potential of a lower-cost, easily scalable process in existing pulp mills to concentrate BL as well as to separate valuable organic and inorganic dissolved. It is also possible that acid precipitation of lignin could still be used as a pre-treatment step in conjunction with membrane separation, like in the Lignoboost process.[22, 27, 28]

Given the challenging operational conditions for using membranes in BL concentration, there are two main purposes of this chapter. First, an overview is provided regarding the current state-of-the-art in membrane science and engineering for BL concentration and related applications. Second, the key challenged are identified related to membrane materials, membrane processing, development of structure-performance relationships, and operational requirements that must be addressed in order to obtain membranes that are viable for BL treatment. In addition to the ubiquitous challenge of achieving high membrane flux and good selectivity for desired components, a number of important issues exist in relation to the long-term stability of membranes under harsh operating conditions (especially pH > 10.5 and temperature ~90°C), the complex composition of BL, and its fouling characteristics. This chapter discusses the key composition and properties of BL, the general membrane characteristics and materials that have been used, a detailed consideration of the membrane performance that has been achieved with different modules, effects of fouling and. a discussion on the economics of different BL concentration membrane configurations. This chapter concludes with an introduction to CMSs, which could potentially be used as novel membranes for BL concentration.

1.3 Composition and Physicochemical Properties of Black Liquor

BL composition depends significantly on the pulping process and on the type of biomass feedstock used. Common wood sources include softwoods (such as pine), hardwoods (such as eucalyptus), and fibrous plants (such as bamboo).[18] The solids content in BL can be represented either as the total dissolved solids (TDS) or as the total solids (TS). TS includes both the dissolved solids and the suspended solids that exist as particles or colloids in BL. Tables 9-11 (Appendix A) give a detailed overview of the inorganic and organic composition of BL feeds. Table 1 and Table 2 summarize key information relevant to the discussion in this section. The main inorganics (Table 1) include NaOH, Na_2S, Na_2CO_3, Na_2SO_4, $Na_2S_2O_3$, and NaCl, with most of the sodium present in BL bound to the phenolic hydroxyl groups in lignin.[27, 29-32] BL also contains impurities like silica, lime, iron oxide, alumina, potash and sodium chloride.[33] Silica is important because it causes abrasion of process equipment, and is a challenge during processing of straw BL which has higher silica content.[9] Another important BL component is ash (total inorganic content post BL combustion). The ash content in American and European BL is low, but is high for pulps that come from grass-like materials, including those in China, India, and Brazil. For example, the ash content of wheat straw BL is 10 times that of wood, 5 times that of bamboo, and 2 times that of reed and bagasse.[33]

Table 1: Main inorganic solutes in black liquor.

Compound	Birch BL (% TDS Basis)[30]	Pine BL (%TDS Basis)[31, 32]
NaOH	2.4	1.3
Na_2SO_4	4.8	2.6
Na_2CO_3 and K_2CO_3	9.2	7.0 (Na_2CO_3 only)
$Na_2S_2O_3$, Na_2SO_3, and Na_2S_x	0.5	1.5 (Na_2SO_3), 3.1 ($Na_2S_2O_3$)
NaHS	3.6	3.7 (Na_2S)
NaCl	0.5	-

Table 2: Main types of organic species in black liquor.

Compound	(wt. % of dry solids)	Avg. MW_w (Da)	Typical MW_w range (Da)	References
Lignin	28.9-43	3821	820-9860	6, 15, 18, 34, 35
Hemicellulose	0.11-1.3	-	1,000-100,000	36
Extractives	0.3-6.69	on order of 10^2	-	37, 38

Table 2 summarizes the typical relative amounts and weight-average molecular weights (MW_w) of the three major organic components in BL.[6, 15, 18, 34-38] The most abundant organic component in BL is lignin, which exists in BL as colloidal macromolecules that have a high degree of cross-linking. [39, 40] The phenolic hydroxyl (R-OH) and carboxyl (R-COOH) functional groups in lignin help to stabilize it in BL.[18, 39] The stabilization is due to reactions such as in Equation (1), wherein free alkali reacts with the hydroxyl groups of lignin:[39]

$$R-OH + NaOH \rightarrow R-ONa + H_2O \qquad (1)$$

Because BL is highly alkaline, the hydroxyl groups dissociate at higher pH, making the usually hydrophobic lignin more hydrophilic with a negative surface charge.[41] If a hydrophilic membrane is used, lignin can interact strongly with the membrane surface and decrease the water flux.[41] At pH above 12.5, enough phenolic groups have become ionized to enable lignin to take a more compact and spherical particle shape, thus making it easier to handle in feed streams.[18] Pure lignin suspensions tend to have low viscosity, which is useful for improving fluid flow characteristics in membrane modules.[42] Even though the molecular weight (MW) of lignin in BL can vary widely (with extremes <1 kDa and >50 kDa), the MW_w is usually 0.82-9.86 kDa (Table 2), and a polydispersity index of 3.6-4.5.[15, 19, 34] The MW distribution of lignin changes with temperature; at higher temperature, there is a wider distribution of lignin particle sizes.[23]

In addition to lignin, the other main organic compounds in BL are hemicelluloses and wood extractives. As seen in Table 2, hemicellulose is generally larger in MW than lignin (though much of the hemicelluloses are broken down into saccharinic acids).[43] The kinds and amounts of hemicelluloses differ between different wood species. For example, the main hemicellulose in hardwood is glucuronoxylan, while it is galactoglucomannan in softwoods.[32] The dominant polysaccharides that make up hemicelluloses are glucose, mannose, galactose, xylose, and arabinose.[5] Extractives are the much lower MW compounds that come from the wood itself and include resins, fats, waxes, oils, proteins, terpenes, and other small organic species.[5] Some of these extractives can in themselves be used for higher value added products. BL also contains a number of low-MW organic

acids such as acetic and formic acid.[29] Table 12 in Appendix B gives a comprehensive account of the methods and standards used to determine varied BL components. Notable testing standards include those developed by the Technological Association of the Pulp and Paper Industry (TAPPI methods), the Scandinavian Pulp, Paper, and Board Testing Committee (SCAN methods), and the Kymen Laboratories Ltd (KCL methods).[44-46] For example, concentration of lignin is typically determined by measuring is absorbance at 280 nm using UV-Vis spectrophotometry. TS/TDS amounts are measured by weighing dried BL samples, while the ash (inorganic) mass is determined by combusting the dried BL samples and measuring the sulfated ash content. The amount of mass lost is the organic content. Total ion content can be measured from conductivity readings.

Wood-based BL is mostly a Newtonian fluid until the solids content approaches ~50%, at which point it behaves like a shear thinning fluid (Figure 2) in which the viscosity decreases with increasing shear rate.[18, 29] Non-wood-based BL can be shear thinning even at lower solids concentrations (e.g., bagasse BL becomes shear thinning at ~40%).[18, 47] As the BL concentration increases, BL viscosity also increases significantly (Figure 2). Higher BL concentrations also result in greater osmotic pressure, which lowers the flux drastically at a given transmembrane pressure differential (TMP).[27] Because of the above factors, membrane concentration of BL is practically limited to about 30-40 wt. % solids.

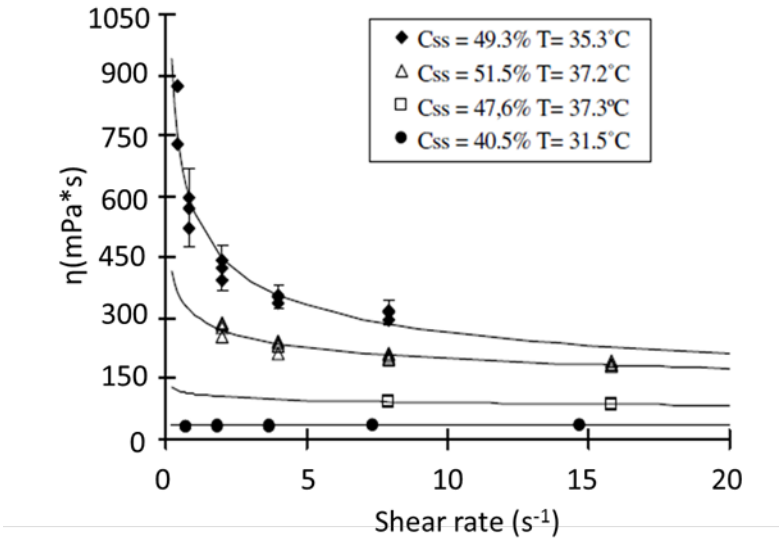

Figure 2: Viscosity of hardwood black liquor as a function of shear rate and solids concentration C_{ss}. Adapted from Ref.[18]

1.4 Membranes for BL Treatment: General Characteristics

Different types of membrane processes have been investigated for BL treatment: microfiltration (MF), ultrafiltration (UF), nanofiltration (NF), and reverse osmosis (RO). Table 3 summarizes the approximate range of membrane molecular weight cut-off (MWCO) values, pore sizes, and transmembrane pressures (TMPs) that can be used for BL treatment.[11, 48-53] Note that there is some ambiguity between the transition regions. MF membranes investigated for BL treatment are typically symmetric and have a single layer.[54] This is in contrast to UF, NF, and RO membranes, which are asymmetric and consist of a thin, active membrane layer on top of a thicker and highly porous support which provides mechanical strength and stability.[54] The different types of membrane pores can be functionally characterized by their MWCO values, which correspond to the MW of a test species that has a rejection coefficient of about 0.90-0.95.[41, 54, 55] Species

above the MWCO will not be significantly permeated through the membrane.[41] To ascertain the MWCO of a membrane, a typical method involves determining the rejection coefficients of several test species like polysaccharides and dextrans of known MW.[54, 55] If different test-species are used, it is best to determine the MWCO by first converting the MWs into hydrodynamic Stokes radii, r_s (nm), to give greater consistency between different types of test species (Equation 2).[56] The radii can then be plotted versus the observed rejection and the corresponding MWCO determined from the radii that have about 0.90-0.95 rejection.

$$\log_{10} r_s = 0.377 log_{10} MW_w - 1.328 \qquad (2)$$

Table 3: Some characteristics of MF, UF, NF, and RO membranes for BL concentration applications.[11, 48-53]

	MF	**UF**	**NF**	**RO**
Pore Size (nm)	20-10,000	1-50	0.5-4	0.2-1.5
MWCO (kDa)	100-5000	15-400	0.1-20	< 0.8
TMP (MPa)	0.1-0.5	0.1-1	1-3	3-20

In BL concentration studies, membranes have been operated either in dead-end mode (wherein the direction of fluid-phase flow is perpendicular to the membrane surface) or cross-flow/tangential-flow mode (in which the direction of fluid flow is parallel to the membrane surface).[54] In most fundamental investigations, BL concentration membranes have been operated in stirred-cell,[9, 56-64] unstirred-cell,[14] or rotated-cell modules,[62, 63] whereas larger-scale tests have been carried out in flat-sheet, [9,

[17, 27, 61, 65-67] spiral-wound,[28] plate-and-frame,[15, 19, 24, 25, 68, 69] and shell-and-tube (including hollow fiber[15, 70]) modules.[4, 7, 9, 11, 13, 16, 28, 33, 41, 71-79] Two common types of laboratory-scale setups are shown in Figure 3a (for cross-flow operation using either tubular or flat-sheet membranes) and Figure 3b for dead-end operation (typically with stirring and small disc membranes).[4, 7-9, 14, 16, 24, 27, 58, 62, 64, 69, 79] The complementary equipment for both operational modes is similar. BL is stored in a reservoir (either as part of the module itself or in a separate feed tank) and is then sent to the module either using a pump (for continuous or dead-end modes) or under inert gas (e.g. N_2) pressure (for the dead-end cells). Most pumps require dampeners to ensure smooth and consistent flow in the module. In continuous systems, the retentate is usually recycled while for both modes, the collected permeate is analyzed to determine its composition and to calculate the rejections of solutes of interest. Permeate flux is determined either via a mass balance for benchtop systems or from a flow meter if the volumetric flow-rates are high or if the permeate is recycled. To ensure accurate TMP, pressure gauges/transducers are placed as close as possible to the feed, retentate, and/or permeate sides of the membrane. For continuous mode operation, the retentate requires a backpressure regulator (BPR) to ensure sufficient feed pressure. The permeate stream is usually open to the atmosphere.

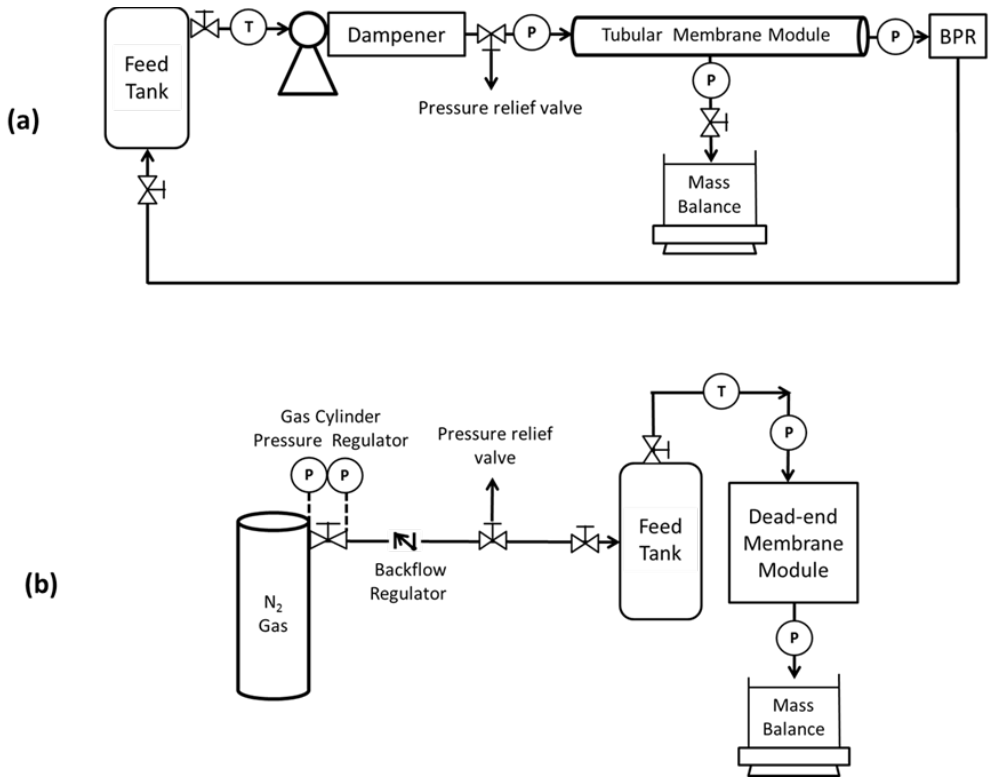

Figure 3: Membrane permeation setups commonly used in the literature for concentration of black liquor using (a) cross-flow (tubular shown here) or (b) dead-end operational modes . Adapted from Refs.[41, 80]

Safety considerations are important since the caustic system operates under high pressures and temperatures. Check valves are typically placed before important components (e.g. gas cylinder pressure regulators) to prevent their damage in case normal flow is reversed. Relief valves prevent accidental over-pressurization of components and to relieve pressure when replacing the membrane or removing other components, especially if clogging had occurred. Periodic inspection and replacement of corroded components is important and additional piping, tank, and valves can be added to aid in cleaning and maintaining the system. Because of the corrosiveness of BL, special care must also be taken to ensure that the equipment and parts used in membrane modules are

resistant to degradation by BL. Several works have reported the use of stainless steel 316 (SS316) membrane modules in their studies.[58-60, 62-64, 81] For gaskets like O-rings, ethylene propylene diene monomer (EPDM), EPDM is found to be more stable than Viton (a fluoroelastomer from DuPont™), though neoprene has also been used.[7, 65]

Additionally, to make membranes applicable to BL concentration, they must be (a) stable (capable of surviving BL for long operation), (b) have high solute rejections (else there is little concentration), and (c) achieve high fluxes to minimize surface area requirements (by minimizing fouling, increasing porosity, and having thin membrane layers). Note also that for BL, membrane filtration is limited to ~25-35% TS because of the great reduction in flux due to fouling, concentration polarization, and high osmotic pressure (Figure 4) and the very large energy costs to pump the denser fluid to the high pressures needed to maintain flux (Figure 5)

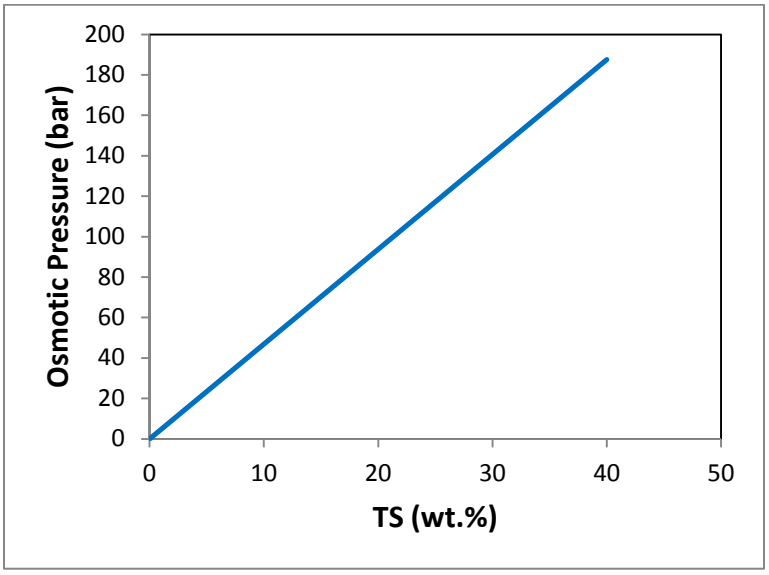

Figure 4: Osmotic Pressure of BL as a function of total solids content. Adapted from Ref.[49]

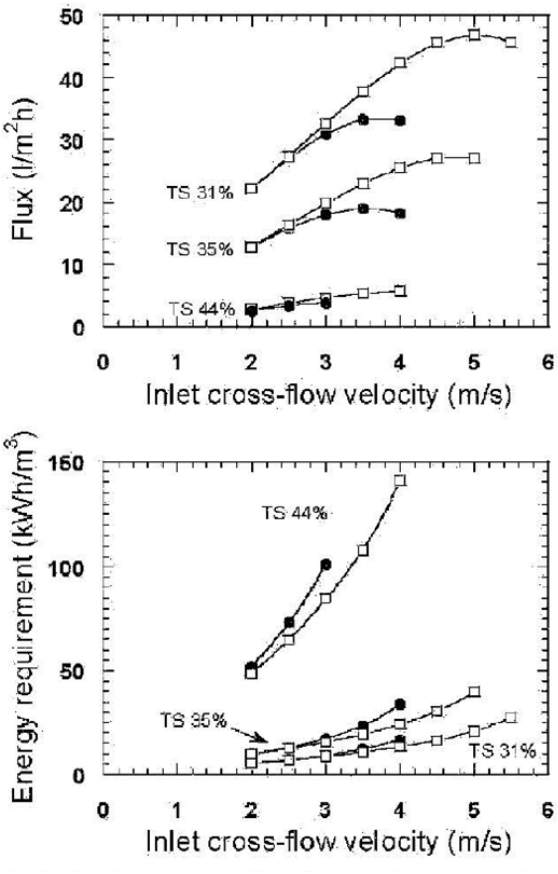

Figure 5: Flux and energy trends for different cross-flow velocities and TS at a TMP of 200 (filled-in points) and 300 kPa (unshaded points). From Ref.[79] (http://www.tandfonline.com)

1.5 Membrane Materials for BL Concentration

Figure 6 illustrates important milestones in the history of development or evaluation of membrane materials for BL concentration. Primarily polymeric membranes and ceramic (metal oxide) membranes have been investigated. Tables 13-14 (Appendix C) give a comprehensive overview of polymeric and ceramic membranes, respectively, that have been investigated for MF, UF, and NF, and RO concentration of BL. Some of the key developments are discussed in more detail in this section. In the 1970s, DDS

Corporation explored membrane-based methods for BL concentration.[33] Early work by DDS included the application of cellulose acetate RO membranes in a sulfide mill in Norway, concentrating TS from 6 to 12 wt.%.[33] This trial was followed by another usage of DDS cellulose acetate membranes in 1978 in Quebec, Canada, which achieved concentrations of TS from 12 to 18%.[33] The organic (cellulose acetate) RO membranes used in both of the above plants had lifetimes of about 1 year because of degradation in the high pH and temperature conditions. Additionally, these membranes required cleaning 2-6 times per week because the high TS content of BL clogged the pores and fouled the membranes.[33, 82] About a decade later, Ross et al. studied UF concentration of BL with 10 kDa and 20 kDa MWCO polysulfone membranes.[14] However, these membranes displayed very low rejection of lignin above pH 10.2, likely due to membrane degradation.[14]

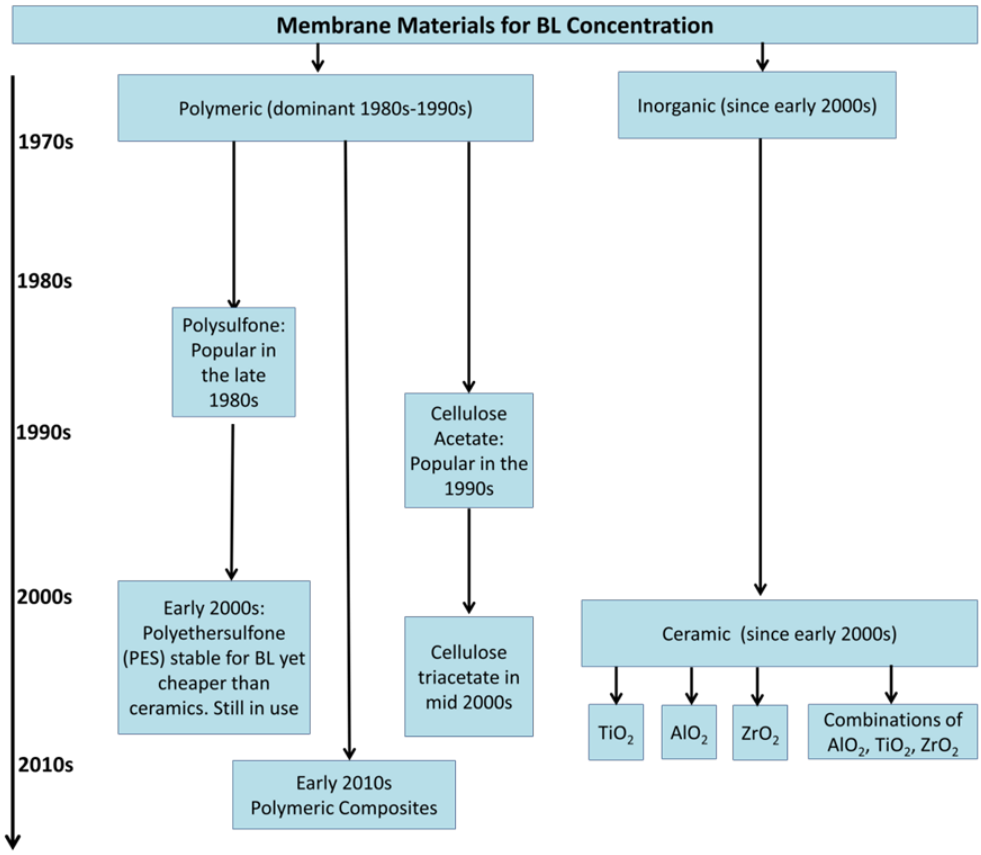

Figure 6: Milestones in the development or use of different membrane materials for black liquor concentration.

As can be seen from Table 13 in Appendix C, cellulose acetate and polysulfone-based membranes have been widely used, likely due to their commercial availability. However, while some of these membranes could provide fairly high rejections (e.g. up to 75% rejection of lignin[14]), their major drawback has been long-term stability. In recent years, polyethersulfone (PES) membranes have gained prominence because of their higher stability, yet the challenge is still to achieve high rejections of organics and ideally even inorganics. Arkell showed that these objectives could be achieved by combining ceramic UF with some of the more stable polymeric NF membranes to achieve up to 90%

lignin rejection.[16] Others have proposed combining carbonation with UF and/or NF to achieve higher rejections.[27, 28] Nevertheless, it is expected that salt rejections are lower than those of organics because of the smaller MW and size of the inorganic ions. There is a need for stable membranes that can perform RO to separate not only the organics, but also the inorganic species, from water in BL.

A general problem with many polymeric membranes used to date is their short (< 1.5 years) lifetime and requirement for frequent cleaning, thereby leading to high capital and maintenance costs.[33] To address these issues, there has been considerable focus in recent years on inorganic (specifically metal oxide) membranes that are more robust and resistant to the high pH and temperature of BL feeds.[33] Ceramic membranes, such as the commercially available Kerasep membranes (made from Al_2O_3–TiO_2) have a general lifetime of about 6 years.[13, 74] Inorganic membranes also need to be cleaned less frequently and generally have higher fluxes.[9] Kang et al. compared the fouling characteristics of an inorganic membrane (zirconia) and a polymeric membrane (polypropylene), and found that the polymeric membrane was prone to a large build-up of cake on the membrane surface whereas the inorganic membrane experienced fouling primarily due to deposition of inorganic solids inside the pores.[83] This difference was attributed to differences in surface roughness and surface charge of the two different materials.[83] Unlike the inorganic membrane, the polymeric membrane was incapable of adsorption of charged species from the solute and hence was less prone to deposition of solids in the pores. Kang et al. plotted the normalized flux decline for each type of membrane (Figure 7) and observed that the inorganic membrane experienced only ~50% flux decline from its initial flux at steady-state compared to ~65% for the polymeric

membrane over the same time period of about 150 hours.[83] Ceramic membranes also have higher mechanical strength and have been operated successfully at feed pressures up to 100 bar.[33] Typically, these commercially available membranes are Al_2O_3, TiO_2, or ZrO_2 membrane layers on top of ceramic supports. All of these membranes, however, have pore sizes that are too large for NF or RO applications. For example, aluminum oxide membranes synthesized using anodic oxidation can achieve a minimum pore size of 10 nm, which is not sufficient for very good NF or any RO separation.[84]

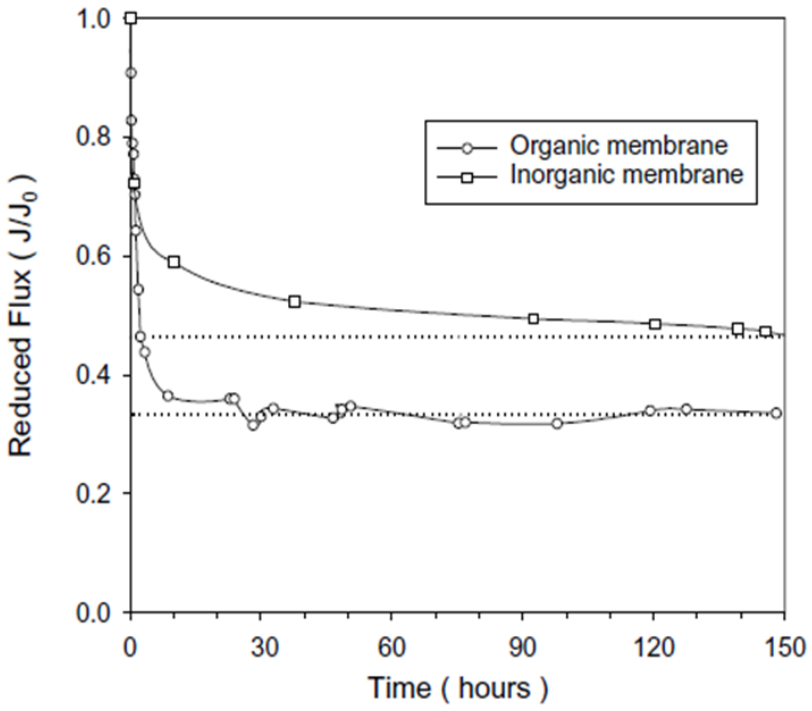

Figure 7: Normalized flux decline for a polymeric (organic) membrane compared to an inorganic membrane. From Ref.[83]

Though ceramics are generally considered to be functionally better membrane materials than polymer membranes for BL concentration, the membrane cost must also

be considered. Ceramic membranes are typically more expensive that polymeric membranes albeit delivering better performance and extended lifetime in comparison to polymer membranes. As an example, Arkell et al. applied their laboratory-scale results of lignin rejection by both ceramic and polymeric NF membranes to estimate the economics of an industrial-scale process.[16] The polymeric NF membranes used in their study cost only about 9.5% of the ceramic NF membrane. On the other hand, the ceramic membrane had a rated life-time of four times that of the polymeric membrane. Though the ceramic membrane was more stable, calculations showed that the higher lignin rejection of the polymeric NF and its low cost resulted in it being the optimum BL concentration choice. In comparsion to using just the NF polymeric membrane, the ceramic NF membrane was 48% more expensive and the combination of a ceramic UF and the polymeric NF was 161% more expensive.[16] These estimates indicate the need for non-polymeric membranes with better rejection and flux properties if they are to be competitive with current polymeric membranes.

It is noteworthy that there is a gap in proper material science knowledge in the published membranes for BL usage. Almost all literature studies commercially available membranes. Just testing more commercial membranes will not be sufficient. There is a great need to improve inorganic and even polymeric membranes, with significant opportunities to use novel materials for BL filtration

1.6 Separation of BL components

Figure 8 shows the three main types of membrane separations (i.e., UF, NF, and RO) that have been investigated for concentration of BL. All of these separations have

been previously investigated with both polymeric and ceramic membranes, as detailed in the previous section and in Tables 13-14 (Appendix C). Ceramic-based membranes have pore sizes only in the MF/UF range and at best, the high MW-end of NF. Consequently, polymeric membranes are still used for NF, sometimes in combination with ceramic UF. Future research is likely to move towards introduction of non-polymeric NF and even RO membranes that could offer the advantages of stability and efficient operation at every MW range. RO would be particularly beneficial since it would allow the full capabilities of separation of BL components. Today, UF and NF are the primary types of membranes considered for lignin rejection. Having better NF and RO membranes would permit not only the almost complete rejection of lignin (and all other organics), but would also allow the separation of free salts, further reducing the energy load and scale formation issues in the downstream evaporators and boilers. Below we discuss some of the key advances in the literature regarding the separation of each of the major components in BL.

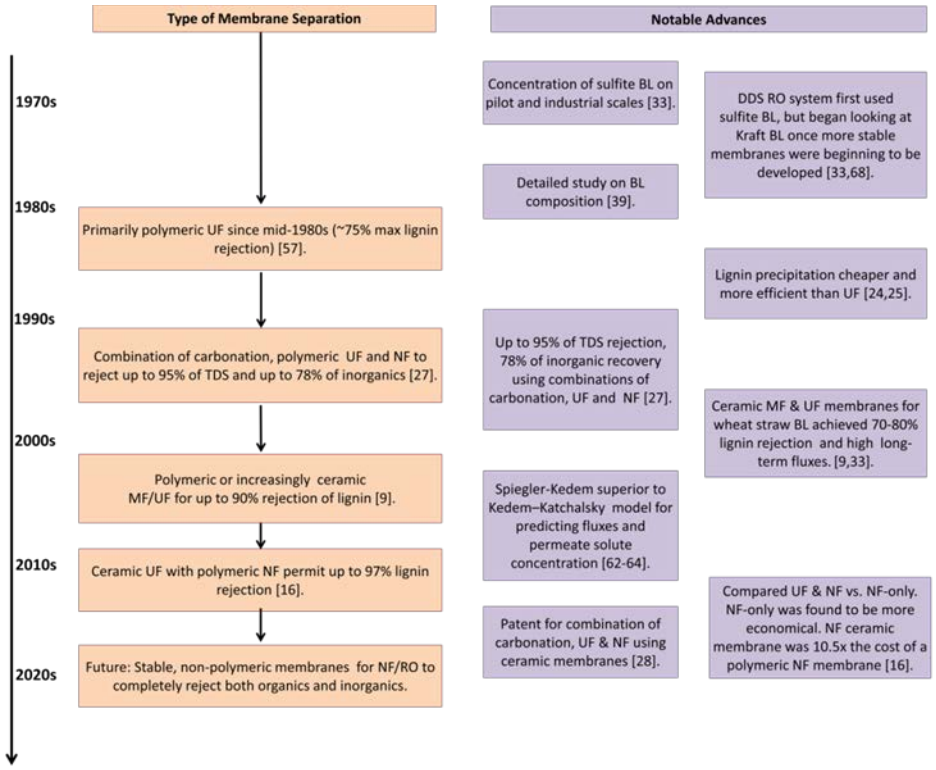

Figure 8: Milestones in the development of membrane processes for black liquor concentration.

1.6.1 Concentration of Lignin

The concentration of low-solids WBL to a high-solids SBL is the most common objective in the BL separation literature. This involves the use of MF, UF or NF membranes to transport water and other low-MW BL components into the permeate stream, thus producing a retentate stream concentrated in lignin. Table 15 (Appendix C) provides a detailed overview of the results of experimental studies on lignin concentration with different UF and NF membranes. Selected results representative of the main findings are discussed below. Liu et al. investigated the effects of membrane pore size on lignin rejection. They used three different tubular α-alumina (Al_2O_3) membranes

with pore sizes of 50 nm, 0.2 μm, and 0.8 μm (i.e., UF and MF range).[33] These membrane achieve a similar lignin rejection of about 75% while also maintaning high long-term fluxes. Interestingly, the flux of the 0.2 um membrane was the highest (200-300 L/[h m^2] for most of the concentration range), while the 50 nm and 0.8 um membrane had similar lower fluxes. The reason for this is not known. Also, the 0.2 um membrane had high long-term fluxes, not experiencing major fouling for up to 35 days.[33] Arkell et al. examined the flux, lignin retention, and overall cost of removing lignin from softwood kraft BL.[16] Specifically, they were interested to examine the results of a UF and NF combination compared to a NF only. The UF membrane was ceramic (Al_2O_3 with a surface layer of TiO_2), while one ceramic (TiO_2) and 3 polymeric composite membranes were tested for NF. At the same MWCO of 1 kDa, the polymeric NF membrane outperformed the ceramic membrane, achieving lignin retention of 90% compared to 80% with the ceramic membrane (with no UF pretreatment).[16] This was because the cereamic NF membrane was known to have a larger pore size, despite the same MWCO.[16] This ambiguity in the MWCO has been observed before. Causserand et al. showed that the observed rejection (used to determine the MWCO) can vary strongly with the operating conditions (which are rarely specified), as shown in Figure 9. For example, the observed rejection decreased from 90% to 40% for a 20 kDa PEG as the flux increased (from increasing the TMP).[55] Interestingly, adding an UF prefiltration step decreased the lignin rejection of the ceramic NF membrane from 80% to 56%, while little change was observed with the polymeric membrane of similar MWCO. Again, this was likely because of the larger pore size (larger moleules were retained by the UF but passed through the ceramic NF more easily than the smaller pore-sized polymeric NF).

However, the permeate flux was always higher in the NF membranes after a UF pretreatment, likely from the reduction in fouling species and osmotic pressure.[16]

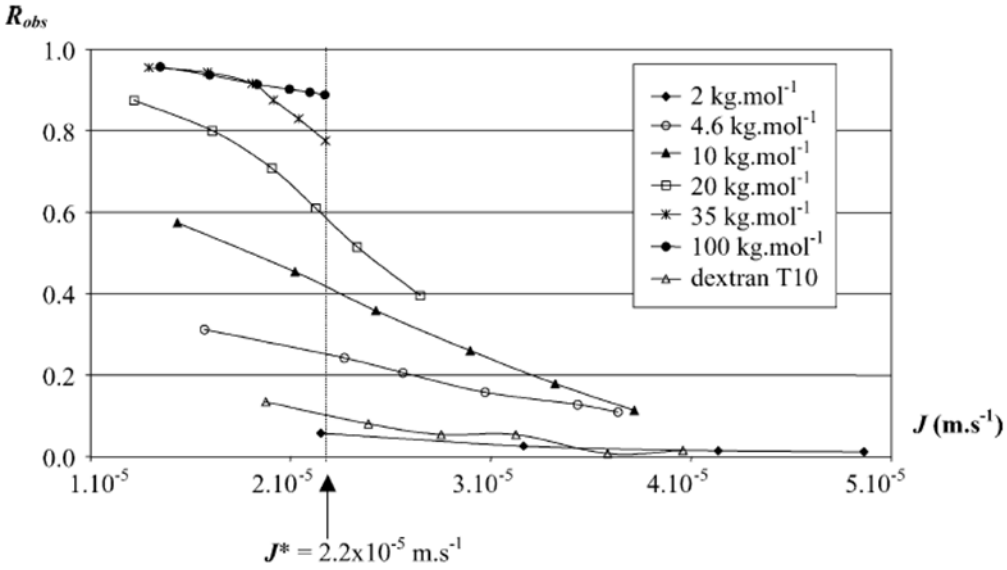

Figure 9: MWCO changes because R_{obs} changes as flux (TMP) changes. From Ref.[55]

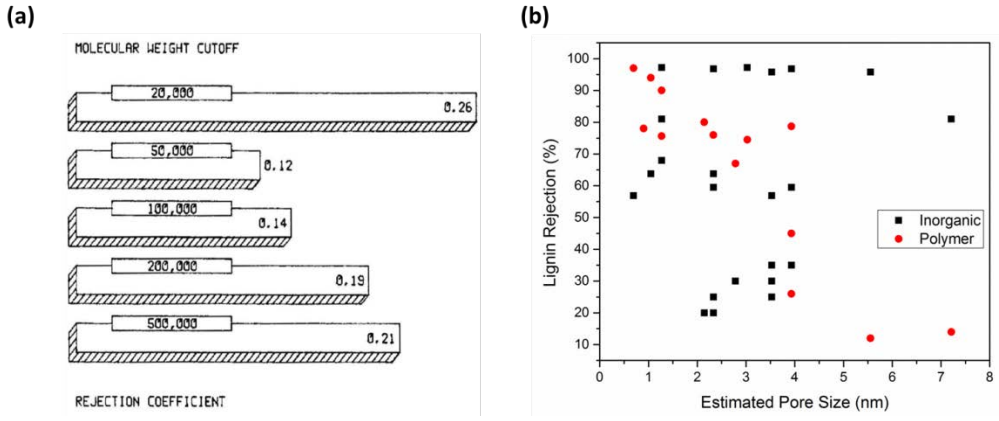

Figure 10: (a) Non-monotonic dependence of lignin rejection upon UF membrane MWCO (reprinted by permission of Taylor & Francis LLC [http://www.tandfonline.com] from Ref.[15]), and (b) Non-monotonic dependence of lignin rejection of NF membranes (plotted using the data in Tables 13-15 in Appendix C) upon the estimated pore sizes, based on MWCOs and Equation (2).

Several authors have reported the interesting observation of a non-monotonic behavior of lignin rejection as a function of membrane MWCO in MF and UF. For example, the results of Hill et al. on polymeric membranes are shown in Figure 10a.[15] The rejection value passes through a minimum as a function of MWCO, with a 500 kDa membrane having almost as high rejection coefficient as a 20 kDa membrane. It is also surprising that membranes with very high MWCOs have any lignin rejection at all. This trend is also reported in other works and has been attributed to gel layer formation.[15, 41, 78] Lignin is hypothesized to form a relatively dense, dynamic gel layer either at the membrane surface or within the large pores of high-MWCO membranes, resulting in a lower effective MWCO and an unexpectedly high rejection.[58] For lower-end UF and NF, the trend is more clear, as shown in Figure 10b which plots data from Tables 13-15 in Appendix C for different types of polymeric and ceramic membranes. The pore sizes of the membranes were not reported in these studies, but were estimated using Equation (2) and the reported MWCOs. In the case of polymeric membranes, lignin rejection sharply increased at a critical pore size of ~4 nm (~21 kDa MWCO), with smaller pore sizes having high rejections. It is also worth mentioning here that hemicellulose was easily retained in most UF and NF membranes due to its higher MW than lignin. For example, Jonsson et al. reported greater than 80% retention of hemicellulose even with a 100 kDa membrane, whereas a lignin retention of 61% was observed with a 4 kDa membrane.[78]

An alternative process for lignin separation involving membrane electrodialysis and acid precipitation has also been demonstrated. Membrane electrodialysis using polymeric membranes can first remove the alkali (NaOH) from BL, thus lowering its pH to 6-7, allowing some of the BL to be used as an emulsifier for catalytic cracking of

heavy oil.[10] Next, further electrodialysis was performed until the BL pH was reduced to 5, at which point the pH was further reduced to 3 using nitric acid. This allowed almost all of the lignin to finally be precipitated. The remaining liquid is rich in xylan which can be used for production of other chemicals (see Section 5.2).[10] However, membrane electrodialysis is likely constrained by scalability issues when handling large BL flow rates, and may involve high electricity costs.

1.6.2 Separation of Valuable Components and Value-Added Products

As discussed earlier, BL contains a large number of organic species (Tables 9, 11 in Appendix A). Due to the lack of appropriate separations technology, many of the valuable BL components are not industrially usable at the moment. Lignin has several direct uses and potential uses for higher value added products.[85] Concentrated lignin can be gasified to H_2, CH_4, and CO for use as energy-efficient and low-carbon fuels.[21] Lignin is non-toxic and has FDA approval for usage in food and packaging.[85] The biggest usage of lignin is in commodity markets while specialty markets have less market share because they require additional processing or modification of lignin.[85] Actual uses in commodity markets include as cement/concrete additives (~50% of lignin goes to this use alone), binders, for animal feeds, and viscosity reducers in molasses and oil well drilling muds.[7, 9-12, 14, 85] Specialty market uses have included production of vanillin, pesticides, oil well cement retarders, gypsum board, dispersants, carbon black, inks, industrial cleaners, micronutrients, and lead acid batteries.[7-11, 13-15, 41, 85] Hemicellulose has been used in barrier films, hydrogels, paper additives.[16]

BL also contains a number of low-MW dissolved organic compounds (Table 11 in Appendix A) that appear in the permeate streams of UF or NF membranes. These low-MW organics include saccharinic acids, formic and acetic acids, and extractives such as tall oil and resins.[28, 80, 86] New membrane technology for separation of dissolved lower-MW BL components from each other may allow increased usage of these BL components as feedstocks. For example, hydroxyacids present as dissolved organics in BL can be used in the production of cosmetics, film packaging, and as building blocks for synthesis of biodegradable plastics.[17] To accomplish the recovery of hydroxylacids from soda BL, Hellstèn et al. demonstrated a separation process combining UF, size-exclusion chromatography, ion-exchange, adsorption, and evaporation (Figure 11).[17] UF removed up to 75% of the lignin, with the remainder being removed by an adsorption column. These two unit operations combined resulted in 99% removal of lignin. Alkalis are removed by size-exclusion chromatography and ion-exchange. In the final step, evaporation is used to separate volatile acids and water from hydroxyacids. Specifically, hydroxyacid purities of up to 81 wt.% and yields of up to 91% could be obtained. The final separation step could potentially be carried out using organophilic membranes to permeate the hydroxyacids or a hydrophilic membrane that permeates water, but no working example of such membranes is currently demonstrated.

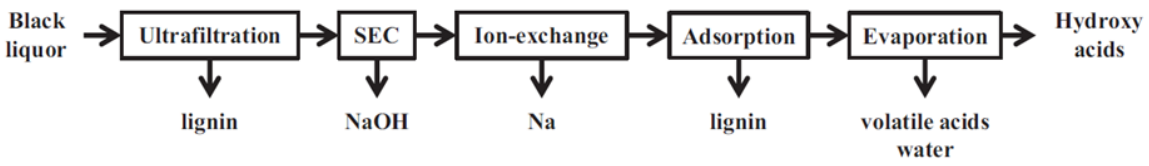

Figure 11: Separation process for recovery of hydroxyacids from soda black liquor. From Ref.[17]

Xylan (a dominant hemicellulose in hardwood) can be used as a feedstock for production of building-block chemicals like furfural, as a colorant, and as a viscosity reducer in drilling fluids.[10, 87] In 2013, the world market for furfural was approximately 300,000 tons per year and is forecast to reach about 650,000 tons by 2020.[88, 89] Lake proposed the use of acid precipitation in conjunction with membranes and other unit operations to purify the xylan component in BL for use in furfural synthesis (Figure 12).[28] The process begins by conventional acid precipitation of lignin using CO_2, until the pH is reduced to 8.5-9.5. This would remove most of the lignin, which would be retained along with the xylan hemicellulose in membrane separation processes. Furthermore, the reduced pH allows greater flexibility in the choice of membrane materials, since many membrane materials are quite stable at pH 8.5-9.5 but unstable at the high pH (> 10.5) of raw BL. However, as mentioned previously, acidification may have high chemical costs and other supporting costs (e.g. piping and storing pressurized CO_2).[5] The next step is a tubular UF membrane (MWCO 1.5-2 kDa) process to concentrate the xylan hemicellulose as retentate while allowing most of the water, salts, and low-MW organics to permeate. A spiral-wound NF membrane (MWCO 0.15-0.5 kDa) is then used to purify the xylan-rich retentate by completely rejecting xylan while permeating water, salts, and the lowest MW organics. It is noted that while the NF membrane alone could achieve the desired xylan purity and concentration without UF pre-treatment, this may be difficult in practice due to low fluxes and severe fouling. UF pre-treatment helps to eliminate most of the undesired fouling components as well as decrease the volume of liquid for processing by the NF unit operation. The concentrated and high- purity hemicellulose solution is then sent to a catalytic reactor wherein xylan is converted to furfural. A final

step involves production of pure furfural by separation from water and xylan. This can be done using distillation or extraction, but could also potentially be carried out by nanoporous membranes.

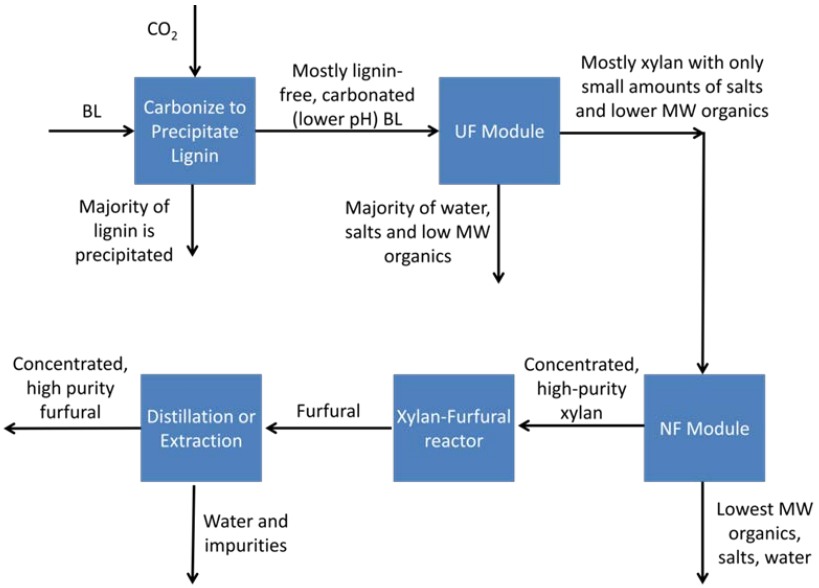

Figure 12: Process combining acid precipitation of lignin with membrane (UF and NF) separations to produce a feedstock for subsequent furfural production. Adapted from Ref.[28]

1.6.3 Separation of BL Inorganics from Organics

Conventionally, the inorganic salts present in BL (Table 1) are recovered as ash after combustion of the SBL stream exiting the evaporators (Figure 1).[77] The main monovalent ions are sodium (Na^+) and potassium (K^+). Current studies on BL concentration membranes focus on UF or NF to concentrate lignin and hemicelluloses while permeating water and ions. An energy-efficient membrane process for BL concentration and inorganics recycling would include a downstream RO system that

permeates water and produces concentrated alkaline brine containing the inorganic ions and dissolved low-MW organic solutes. In addition to the usual requirements of high salt rejection, good water flux, and fouling resistance, these membranes should be fabricated from materials capable of withstanding the high pH of the UF/NF permeate stream. This requirement is beyond the capabilities of current polymeric RO membranes, and there are significant opportunities and challenges in the development of such membranes. The monovalent ions tend to be free in the bulk solution, while the multivalent ions tend to be bound to lignin or other colloids.[19, 27, 75, 90] The total concentration of monovalent ions is in the range of 3.1-42.3 g/L (Tables 9-10 in Appendix A). Kirbawy showed that multivalent ions are mainly located in the retentate (and not the permeate) of UF membranes.[19] The main multivalent inorganic ions that have been typically retained are Mg, Mn, Fe and Ca, with Mg and Mn typically having higher retentions (70-90% [77]) and Fe and Ca having lower retentions (40-60%[77]).[7, 74-77, 91] These inorganics make up only a small portion of the solids in BL (Tables 9-10 in Appendix A). Typical rejections for multivalent ions have been 80-100% for Mg, 45-85% for Mn, 40-71% for Fe, and 40-81% for Ca, while the monovalent inorganics had rejections in the range of 6-19% since they are permeated by UF/NF membranes.[7, 75, 77] Typical good recoveries have been 37-70% for Mg, 25-60% for Mn, 35-60% for Fe, 20-40% for Ca, while the monovalent inorganics had rejections below 10-17%.[74, 77, 91]

1.6.4 Water Separation

The paper industry is water-intensive.[92] It would thus be desirable to separate water from BL and recycle it, while recovering the inorganic components as concentrated

brine that would place a lower load on the inorganics recycling boiler. To our knowledge, there are no works exploring the production of 'pure' water from BL using membranes. The direct production of water from raw BL appears prohibitively challenging for two main reasons. First, the osmotic pressure of WBL (15 wt.% solids) is about 70 bar as estimated from the correlation for BL based on TS (Figure 4).[49] This is a high osmotic pressure compared to, *e.g*. that encountered in the desalination of seawater (about 25 bar[93]), and would likely require significant energy costs for pressurization of the BL feed. Second, the presence of large quantities of organic solids (such as lignin and hemicellulose) and dissolved organic molecules in raw BL will certainly lead to high concentration polarization and fouling effects in RO membranes. Thus, it is more reasonable to consider RO membranes for separation of water from the permeate stream of an efficient NF pre-treatment membrane. Thus, the industrial use of RO membranes for BL applications is likely to be contingent on the development and acceptance of NF membranes in the Kraft process. Assuming that the NF membrane can achieve near-complete retention of lignin and higher-MW organics while allowing permeation of nearly all monovalent inorganics and low-MW organics, the solids content of the NF permeate would be lowered to ~8 wt.% which corresponds to an osmotic pressure of ~ 40 bars. The pH of this stream would likely be unchanged. This represents a feasible opportunity for development of inorganic/non-polymeric RO membranes that can produce water suitable for recycle while concentrating the inorganics. It is also noted that the salt rejection requirements for such membranes could be somewhat lower than those of desalination membranes, since this application would not require the RO membrane to produce a water stream of potable quality.

1.7 BL Membrane Flux and Rejection: Theory and Experimental Analysis

In this section and the next, the currently accepted theoretical description and experimental understanding of the key performance parameters of BL concentration membranes: flux, rejection (selectivity), and fouling behavior (including concentration polarization effects) are summarized. In UF, NF, and RO membranes for BL concentration, the transmembrane pressure differential (TMP) is the driving force that pushes the permeate through the membrane pores. In cross-flow modules, the TMP is defined as the average of the difference between the feed and retentate pressures minus the permeate pressure.[13, 54, 77] In dead-end modules that have no retentate stream, the TMP is simply the difference between the feed and retentate pressures. The osmotic differential, caused by the presence of different solute concentrations on the feed and permeate sides, opposes permeation. As a result, the flux of the solvent can be written in the well-known form of Equation (3):[49, 94, 95]

$$J = \overline{P}\,(\Delta P - \sigma\Delta\Pi) \qquad (3)$$

In the simplest case, without any fouling or resistance to flow other than that of water through the membrane, BL literature commonly expresses Equation (3) as Equation (4):[62, 96]

$$J = \frac{\Delta P - \sigma\Delta\Pi}{\mu R_m} \qquad (4)$$

In the above two equations, J is the solvent flux, $\overline{P}$ is the effective membrane permeance (permeability divided by the membrane thickness), Π is the osmotic pressure, $(\Delta P - \sigma\Delta\Pi)$ is the net driving force, R_m is the hydraulic membrane resistance (resistance to flow of pure solvent in the membrane itself), μ is the dynamic viscosity, and σ is the osmotic reflection coefficient. The reflection coefficient couples the solvent transport to the rejection of the solutes. A σ value of unity implies complete solute rejection, while a σ value of zero implies that all of the solute passes through the membrane.[96] The reflection coefficient is generally expected to be independent of solute concentration but is strongly dependent on the solute molecule size (or molecular weight) and membrane pore size (or MWCO).[97] The osmotic pressure is directly related to the solute concentration. Various correlations exist in the literature, the simplest of which is the linear proportionality of osmotic pressure and solute concentration obtained from the van't Hoff equation and which is valid for dilute solutions.[27] In more concentrated solutions, the osmotic pressure is often correlated to power-law or polynomial functions of the solute concentrations in which the constant parameters are fitted experimentally.[96, 98]

The BL membrane literature usually reports solute rejection values/percentages or solute recoveries as a measure of the membrane selectivity towards (or against) that solute. The 'observed (or apparent) rejection' (also called 'retention' in some works) is defined as R_{obs} =1-C_p/C_b, where C_p and C_b denote the permeate and bulk feed concentrations respectively.[27, 41, 57, 58, 99] Some authors also use the retentate concentration in place of bulk concentration.[9, 54, 99, 100] The 'real' or 'intrinsic' rejection is R_{int} = 1-C_p/C_m, where C_m denotes the actual concentration of the solute near the membrane-feed

interface. For solutes with a high reflection coefficient, $R_{int} > R_{obs}$ because the solute concentration at the membrane surface is greater than in the bulk feed due to concentration polarization.[58] A useful relationship between the two rejections, the volumetric flux of the permeate through the membrane (J_v), and the solute mass-transfer coefficient, k, can be derived that accounts for the back-diffusion of a polarized solute into the bulk feed as shown in Equation (5). A plot of the right side versus the volumetric flux gives a linear relationship, allowing R_{int} and k to be determined.[55, 57, 64]

$$\ln\left(\frac{1-R_{obs}}{R_{obs}}\right) = \ln\left(\frac{1-R_{\text{int}}}{R_{\text{int}}}\right) + \frac{J_v}{k} \qquad (5)$$

The solute recovery (yield) is the ratio of solute concentrations in the retentate and feed streams, and for UF is given by Equation (6):[74, 75, 77, 100]

$$\text{Recovery} = \frac{m_r}{m_b} = (1-VR)^{1-R_{obs}} \qquad (6)$$

with $VR = \frac{V_{\text{p}}}{V_0}$. Here VR is the volume reduction, V_0 is the initial feed volume, V_P is the permeate volume, m_r is the retentate mass, and m_b is the initial mass of the bulk/feed solution.[41, 74, 75, 77]

In UF membranes with negligible concentration polarization effects, the solvent flux of Equation (2) reduces to Darcy's law by setting $\Delta\Pi \sim 0$.[58, 81, 96] The membrane resistance R_m depends on properties such as the pore size, membrane thickness, porosity,

and pore tortuosity, and is usually determined from experimental flux data. The viscosity of BL is obtained from a correlation as a function of TDS or TS concentration.[58, 62] The Darcy equation is not valid for conditions with solutes, since they can foul membranes and is also not used for RO and some NF studies.[96] A generalized form of Equation (6) can be written for the solvent flux as shown in Equation (7), and includes the additional resistance terms: R_a is the resistance from adsorption of solutes onto the membrane surface, R_g is the resistance created by a fouling gel layer at the membrane surface, and R_{cp} is the concentration polarization resistance.[48, 96]

$$J = \frac{\Delta P}{\mu(\mathrm{R_m} + \mathrm{R_a} + \mathrm{R}_{cp} + \mathrm{R_g})} \qquad (7)$$

Bhattacharjee et al. examined models based upon irreversible (nonequilibrium) thermodynamics[64, 94, 101, 102] for predicting solvent and solute fluxes as well as the solute rejection in BL concentration membranes. The Spiegler-Kedem (SK) model shown in Equation (8) relates the observed solute rejection R_o to the mass transfer coefficient of TDS or TS (k), solvent volumetric flux (J_v), solute permeability (P_m), and osmotic reflection coefficient (σ):[64]

$$\frac{R_{obs}}{1-R_{obs}} = \frac{\sigma}{1-\sigma}\left[1-\exp\left\{-\frac{J_v(1-\sigma)}{P_m}\right\}\right] * \exp\left(\frac{-J_v}{k}\right) \qquad (8)$$

This study examined how well the widely used SK and Kedem–Katchalsky (KK) models matched the experimental data pertaining to: (1) flux versus time (and steady-

state flux) at different TMPs, (2) flux versus time at different stirring speeds (i.e., different Reynold's numbers), and (3) C_p (the permeate concentration of TS or TDS) as a function of TMP for different stirring speeds. Figure 13a shows the flux decline over time using the same feed concentration and TMPs but at two stirring speeds. The SK model fitted the experimental data reasonably well, while the KK model significantly under predicted the flux. Similarly, in Figure 13b, flux over time is plotted at different TMPs. Again, the SK model outperformed the KK model with closer agreement to experimental data. The SK model was also better at predicting the permeate solids concentration based on the TMP. The poorer performance of the KK model is likely due to its coefficients being dependent on concentration itself, while the SK model's coefficients are not dependent on concentration.[103] This independence would allow better predictions of flux and other properties, which are influenced by concentration.

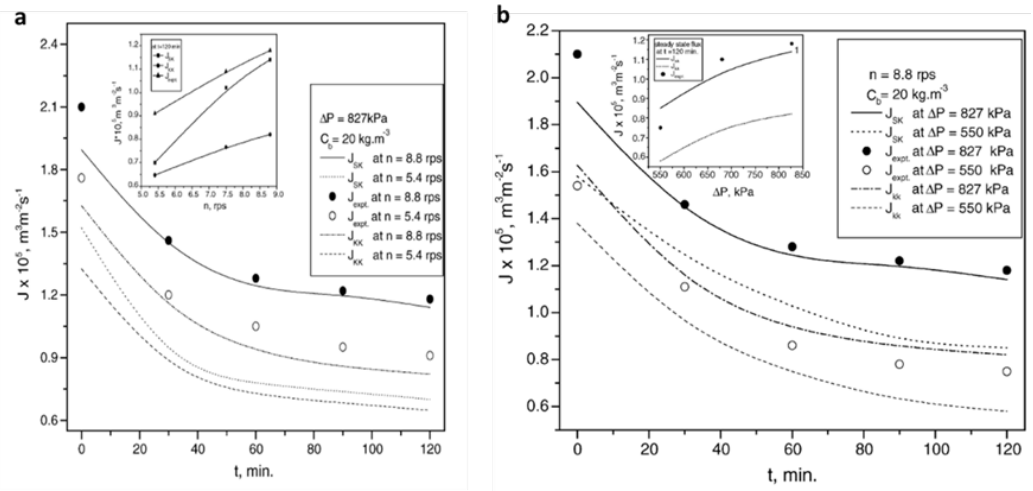

Figure 13: Comparison of the SK and KK models for flux decline over time at: (a) different stirring speeds, and (b) different TMPs. From Ref.[64]

1.8 Concentration Polarization and Fouling in BL Concentration Membranes

One of the challenges in successful application of membrane technology to BL concentration and separation, is that of maintaining high permeate fluxes. After showing initially higher values, the fluxes stabilize at lower levels and then may decline slowly over time. These characteristics result from the contributions of concentration polarization and fouling by gel layer formation or adsorption of solutes inside the membrane pores. Concentration polarization and gel layer formation are reversible, meaning that they can be removed during membrane cleaning and the membrane flux can be restored to its original value.[61] Other types of fouling such as blocked pores may be irreversible. Thus, minimizing these effects (in addition to the development of chemically stable membranes) is important in extending the membrane lifetime.

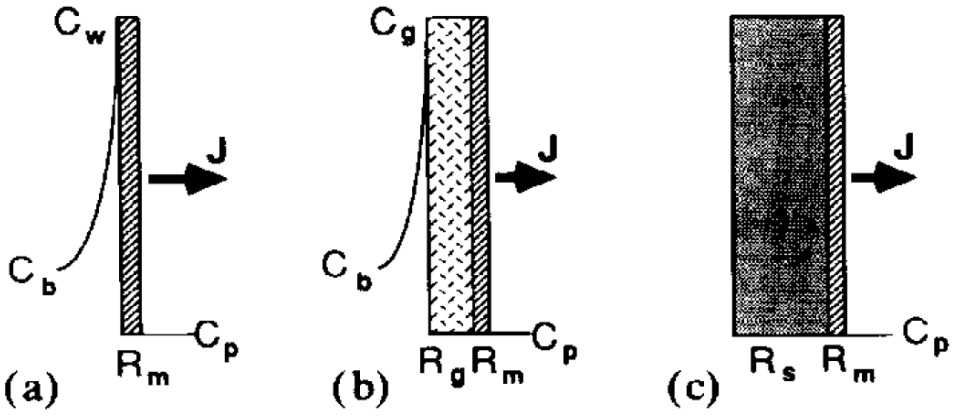

Figure 14: Schematic representation of the different concentration polarization models. (a) osmotic pressure model, (b) gel layer model, and (c) series resistance model. From Ref.[96]

There are three general models that account for concentration polarization/fouling resistances (Figure 14), with the osmotic pressure and resistance models being popular in

BL concentration studies.[65, 96] For most other UF applications, the osmotic effects are negligible.[96] However, this may not always be true in UF concentration of BL and is not true for NF and RO.[27, 54, 91, 96, 104] In this model (Figure 14a), the concentration at the membrane wall is determined by a steady-state mass balance of solute arriving at the wall (due to TMP-driven convection) and solute back-diffusion to the bulk solution (due to the concentration gradient). This condition, combined with a power-law solute concentration dependence of the osmotic pressure and the generalized Equation (4), gives a nonlinear equation for the flux:[96]

$$J = \frac{\Delta P - aC_b^n \exp(nJ/k)}{\mu R_m} \qquad (9)$$

In Equation (9), the osmotic pressure $\Pi = aC_b^n$ (power-law dependence on concentration) and it is assumed that $\sigma \sim 1$, $C_p \sim 0$, and $R_m >> R_g$. As seen in Equation (7), other resistance terms could be added to Equation (9) as appropriate. The osmotic pressure is expected to be the main factor in limiting flux for smaller solutes (10-100 kDa) in BL concentration, compared to gel layer formation in general UF applications.[96, 98] In BL, almost all solutes are below 100 kDa (except a small fraction of lignin in some BLs), so flux decline due to gel formation is less likely. A gel layer (Figure 14b) is proposed to be a collection of accumulated large solutes, and is the equivalent of the concentration polarization layer for small solutes.[54, 56] When a gel layer occurs, the flux becomes independent of TMP (limiting flux scenario) because higher TMPs also increase the gel layer thickness, resulting in an overall unchanged flux.[91] This model has not been widely used to interpret UF membrane data for BL treatment, presumably because of the

uncertainty in estimating the gel layer thickness as well as the smaller size of BL solutes as mentioned above. On the other hand, the resistances-in-series model (Figure 14c) is useful because it is easier to differentiate between the different flux decline factors and it can also predict a TMP-independent limiting flux.[96] Equation (7) may be used. A few works[58, 96] describe experimental means to determine these resistances, based upon either the variation of surface shear (by changing the feed stirring rate) or by variation of the solute concentrations.[58, 96]

Turning to the experimental reports, there are several works describing the flux decline behavior in BL concentration membranes.[4, 7, 9, 33, 72, 73] Dafinov et al. reported that the flux dropped from 0.062 to 0.037 $m^3/(m^2\ h)$ for their 5 kDa ceramic (TiO_2) membrane and from 0.058 to 0.018 $m^3/(m^2\ h)$ for their 15 kDa ceramic (ZrO_2) membrane at 0.5 MPa TMP, within about 100 minutes of operation.[4] This is unexpected, since membranes with higher MWCOs usually have higher fluxes. To explain these results, the authors suggested pore blockage of the membranes by lignin macromolecules (which had sizes similar to the 15 kDa pores). The flux then remained stable, with experimental data measured until almost 10 hr . and 24 hrs. for the 5 kDa and 15 kDa membranes respectively. Cortinas et al. considered the use of a ceramic MF membrane made of alumina (0.2 um pore size, 33% porosity, 99.9 % selectivity) to remove pitch (suspended colloids) from BL.[72, 73] In one set of experiments, they reported a significant drop in flux from the initial ~0.3 $m^3/(m^2\ h)$ to 0.15 or 0.11 $m^3/(m^2\ h)$, depending on TMP (0.32 MPa or 0.15 and 0. 24 MPa) during a stabilization time of up to 600 min.[72] To minimize long-term flux decline, a periodic permeate back-pulsing strategy was investigated. Pulsing for 60 s at variations of 5,15, and 30 minute intervals allowed a reasonably steady flux of

about 0.2 $m^3/(m^2\ h)$ over about 6.7 hr at 0.24 MPa TMP and 7.7 m/s. In another experiment, flux did not drop below 0. 2 $m^3/(m^2\ h)$ from an initial flux of almost 0.4 $m^3/(m^2\ h)$ even after almost 8 days of operation. Flux behavior was similar regardless of the operating conditions. High cross-flow velocities (about 8.5 m/s) were required to stabilize the flux. Both these requirements resulted in quite high energy costs (e.g., pumping was estimated to be about 70% of operating costs).[72, 73]

Wallberg et al. showed that with regular cleaning, ceramic (Al_2O_3–TiO_2) UF membranes maintained flux for over two weeks.[7] It was also found that the flux decline is more pronounced as the retentate becomes more concentrated. This is generally depicted in plots of flux versus VR.[13] For example, in one study the flux declined from 0.12 $m^3/(m^2h)$ to 0.02 $m^3/(m^2h)$ when VR changed from 0 to 0.9.[77] Liu et al. also described similar behavior using ceramic (α-Al_2O_3) MF and polymeric MF & UF membranes (pore sizes/MWCOs: 0.8, 0.2, 0.22 μm for MF and 3, 6, 10, 30, 60 kDa for UF) for lignin removal from wheat straw BL, achieving a lignin retention of 70-80%.[9, 33] The polymeric MF was made of cellulose acetate and the polymeric UF membranes were made from polyacrylonitrile (PAN), polyaryletherketone (PAEK), or polyethersulfone (PES).[9, 33] Periodic cleaning and the use of high cross-flow velocities (to reduce concentration polarization resistance) enabled high fluxes of 0.15-0.24 $m^3/(m^2\ h)$ to be maintained over more than 40 days of operation. For membranes with MWCO < 10 kDa, resistances from pore plugging and gel layer formation dominated whereas at MWCO >10 kDa, concentration polarization was dominant. The intrinsic membrane resistance was not greatly important in both cases. While pore plugging and gel layer formation/surface adsorption probably does occur in both types of membranes, the smaller-pore membranes

are more affected by these phenomena because even slight pore plugging significantly reduces the pore size. Thus, it can be generally assumed that smaller MWCO membranes (e.g., NF and RO) for raw BL concentration applications will be more affected by pore plugging and adsorption resistances, whereas larger MWCO membranes (e.g., UF) will be more affected by concentration polarization. On the other hand, if RO membranes are used to treat NF permeates containing mainly inorganic ions and small organic solutes, the role of concentration polarization can become important in a manner similar to that occurring in desalination RO membranes.

Cleaning of membranes is most commonly carried out using either commercially available alkaline solutions or alkaline NaOH-based solutions. These solutions facilitate cleaning by dissolving the low-MWCO solutes and reversing the precipitation of residual lignin.[41] For example, Ultrasil 11 is a popular industrial membrane cleaning agent. While its exact formulation is proprietary, Ultrasil 11 contains NaOH (30–60%), ethylenediamine tetraacetate (30–60%), $NaCO_3$ (10-30%), triphosphoric acid, a pentasodium salt (5-10 %) and dodecylbenzenesulfonic acid sodium salt (1-5%). It is highly alkaline, with a 1 wt.% solution having a pH of 12.8. The manufacturer recommends passing the Ultrasil 11 solution through the membrane module for 20 minutes at 49–71°C. Literature reports on BL concentration membranes generally used 0.1-0.75 wt.% Ultrasil solution followed by rinsing with water.[7, 16, 67, 73, 76, 78, 79, 91] Actual cleaning times used could be much longer than 20 minutes. For example, Wallberg et al. found that a ceramic UF membrane module needed to be cleaned between 1-16 hours every week, such that a pilot plant was successfully operated for 8 months without fouling issues to extract lignin directly from the digester.[7] Some researchers have also

used their own alkaline solutions. The primary component of these solutions is 0.1-0.5 M NaOH, although surfactants, phosphates, and sequestering agents may be added.[4, 9, 12, 15, 41, 96]

1.9 Membrane Operation Modes in BL Concentration Studies

BL concentration has been studied in a variety of operational modes (modules) to characterize the membrane performance . These modules include dead-end filtration (operated without stirring, stirred, and/or by rotating the module itself), and cross-flow filtration. Cross-flow filtration modules include the industrially relevant tubular modules as well as rectangular and axial modules. Highlighted here are examples and mathematical models for each operational mode.

1.9.1 Dead-End Filtration

A dead-end cell (Figure 15a) is the simplest module consisting of one input for the feed and one input for the permeate. Dead-end modules are useful for performing initial measurements to characterize rejection values and stability of the membrane, but show rapid decline of flux due to concentration polarization from the built-up solutes. To mitigate this issue, a stirring mechanism can be added to minimize fouling and achieve higher flux. Less commonly, there are attempts to generate high shear on the membrane surface (thus reducing concentration polarization from greater surface turbulence) by rotating the membrane itself (with or without stirring).[62, 63] These cells produce more uniform TMP over the membrane surface.[62] However, dead-end modules are not suited

for scale-up of BL concentration membranes due to their high costs and fouling difficulties.[62, 96]

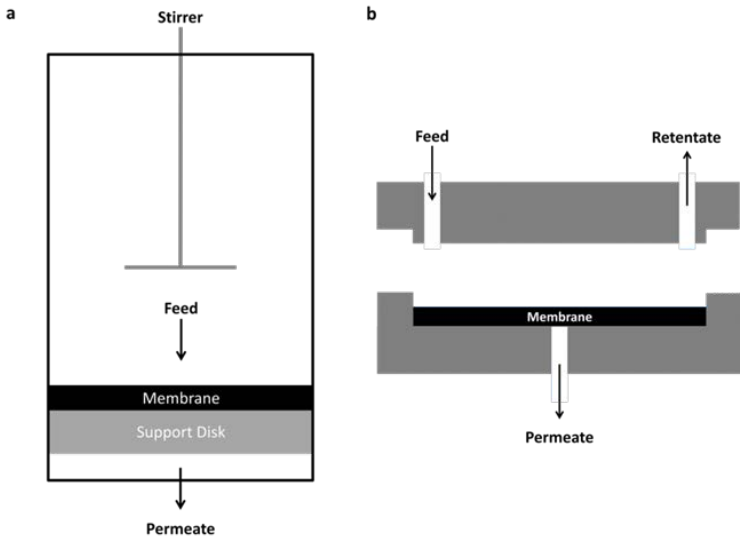

Figure 15: Schematics of (a) a simple stirred cell, and (b) Schematic of a rectangular cross-flow module. Adapted from Ref.[65]

One way to express the level of concentration polarization in a stirred cell is using the concentration polarization modulus, defined in Equation (10). Here, C_m is the concentration at membrane wall, C_b is the bulk retentate concentration, R_{obs} is the observed rejection coefficient, k is the solute mass-transfer coefficient and J is the observed water flux.[57]

$$\frac{C_m}{C_b} = \frac{\exp(J/k)}{R_{obs} + (1 - R_{obs}) * \exp(J/k)} \qquad (10)$$

The solute mass-transfer coefficient can be estimated using Equation (11), where *D* is the solute diffusion coefficient, ω is the angular velocity, υ is the kinematic velocity, and *r* is the radius of the membrane.[58, 105]

$$k = 0.0443 * (\frac{D}{r}) * (\frac{\nu}{D})^{0.333} * (\frac{\omega r^2}{\nu})^{0.8} \qquad (11)$$

1.9.2 Cross-Flow Filtration

Cross-flow filtration consists of an input feed stream and two output streams: permeate and retentate. It is more practically relevant due to lower fouling from the high Re as well as easier scalability, particularly for the tubular modules. Many laboratory studies have been done on flat-sheet cross-flow systems, typically operated in a rectangular module (Figure 15b). Less commonly used are radial cross-flow cells (wherein the feed enters at the center and flows in the radial direction), and spiral-cross-flow cells (wherein the feed is introduced tangentially and flows in a spiral pattern on the surface) which can be used for measuring small disc samples.[106] Higher cross-flow velocities are desirable because they remove or minimize the concentration polarization layer, allowing the greatest permeate flux to occur. However, as the feed BL becomes more concentrated, filtration becomes more difficult and the energy costs increase. Using a tubular ceramic module, Nordin et al. showed that beyond a TS concentration of 31-35 wt.%, the (pump) energy costs drastically increase (e.g. by 400% from 35 to 44 wt.% at velocity of 2 m/s) and the permeate flux significantly decreases (e.g. by 86% from 31 to 44 wt.%) at 2 m/s) (Figure 5).[79] Further concentration would require the traditional reboilers.

1.10 Economics and Energy Requirements

Owing to the significant industrial interest in membrane-based BL concentration, several technoeconomic analysis studies on this subject have been published since the 1980s. Table 4 summarizes the main findings of these works. In an early work on membrane filtration of BL, Uloth et al. (1989) compared economic feasibility of lignin removal by acid precipitation and an unspecified UF membrane .[24, 25] Acid precipitation performed better than UF, being about half as expensive as UF and having better lignin recovery. UF had at best 54% recovery, while acidification could remove up to 95% of the lignin in BL at pH 4. Additionally, the capital (operating) costs for UF were about 1.7 (2.2) times greater. This is initially surprising, since a large amount of acid must be added to precipitate lignin However, the membrane replacement cost and steam usage were found to be much higher than the chemical cost of precipitation, hence the greater overall cost. Thus, membrane filtration of BL was considered to be very expensive in the late 1980s.

Table 4: Summary of technoeconomic data on membrane-based BL concentration. Cost values calculated in the cited works are adjusted in this work to 2015 US dollars.

Reference #	[24, 25]	[72, 73]	[78]	[16]
Year	1989	2002	2008	2014
Inlet solids concentration(wt.% TS/TDS)	32.5	14-14.8	17	183 g/L TDS
BL feed rate	800 tons pulp/day	8 m/s	180, 200 m^3/hr	100 m^3/hr
Feed Lignin (kg/m^3)	X	X	59 (UF), 54 (NF)	74 (ceramic NF), 63 (polymeric NF)
Retentate Lignin (kg/m^3)	X	X	90 (UF), 165 (NF)	252 (ceramic NF), 282 (polymeric NF)
Membrane Details	UF (unspecified material, 6-60 kDa)	MF (alumina, 0.2 µm)	UF (Al_2O_3-TiO_2, 15 kDa); NF (Polymer, 1 kDa)	UF (Al_2O_3-TiO_2,20 kDa), NF (TiO_2, 1 kDa), NF (polymer composite, 1 kDa)
Permeate flux (m^3/m^2 h)	0.070, 0.090	0.144	0.082, 0.110	0.088, 0.17
Lignin Rejection (%)	X	X	~52-60 max	80 (ceramic NF), 90 (polymeric NF)
Membrane Area (m^2)	X	355	1200, 2300, 4200	X
Membrane Lifetime (yrs)	1	10	1.5, 6	1.5, 6
Operating Time (hrs/yr)	8000	X	8000	8000
Capital Cost (k$/yr)	12000	860	260, 840, 1500	X
Operating Cost (k$/yr)	2500	850	470, 1200, 2400	2800, 3000, 3500, 4400
Total Cost (k$/yr)	X	1700	740, 2040, 3940	X
Lignin Produced (ton/yr)	24000	300000 (ton pulp/yr)	72000,78000,108000	8300,30000, 41000, 68000
Lignin Production Cost ($/ton lignin)	99	3 ($/ton pulp)	10, 26, 36	46, 68, 120, 430

Since then, advances in membrane technology have improved the economics of membrane-based BL concentration due to higher water fluxes and solute rejections. Table 4 shows that the economic potential has improved significantly since 1989. In 2002, Cortinas et al. performed an economic analysis using α-Al_2O_3 MF membrane (0.2 um pore size) for the rejection of pitch (colloidal particles, 99.2% rejection).[72, 73] The final cost to reject almost all of the pitch from going through the membrane was 2.8 $/ton of bleached pulp (2015 equivalent value). Back-pulsing (to reduce fouling) was very expensive (about 7 % of the total operating cost). Another high cost included the pumping energy required to maintain high cross-flow velocities which are needed for stable fluxes. This pumping cost was 70% of the operating cost. The membrane lifetime was estimated as 10 years, owing to the use of a ceramic (alumina) membrane.

There have been more recent studies comparing the usage of UF and NF combinations versus NF or UF alone, as well as comparisons of polymeric and inorganic membranes for these processes. Jonsson et al. analyzed the economics of removing lignin from various parts of the digesting process.[78] A ceramic (Al_2O_3–TiO_2) membranes (15 kDa MWCO) was used for UF and a polymeric membrane (unspecified material) was used for NF (1kDa MWCO).[78] Three scenarios were considered: (A) treating BL directly from the digester with UF, (B) same as (A) but adding a NF step, and (C) using the traditional evaporators to concentrate BL to 31% TDS and then sending that stream to UF. Though the cost (36 $/ton of lignin; adjusted to 2015 value) of the UF/NF combination (B) was about the same as that of using evaporators followed by UF (C), the UF/NF combination resulted both in the greatest lignin concentration and also the greatest purity. UF alone (A) at 26 $/ton (adjusted to 2015 value) of lignin was the

cheapest, but its low lignin rejection (~8.5%) is not sufficient for industrial use. It is noteworthy that even with inefficient UF membranes, the UF/NF combination was a comparable alternative to the evaporators, thus demonstrating the value of replacing some of the evaporation steps with membranes.

Of final note in Table 4 is the 2014 study by Arkell et al., which used laboratory-scale NF membranes with high lignin rejection (~90% for a polymeric membrane and ~80% for a ceramic membrane, both with MWCOs of ~1 kDa). The laboratory-scale experimental results were used to estimate the economics of an industrial-scale process with a feed flow rate of 100 m^3/h and a retentate lignin concentration of 230 kg/m^3 (i.e., more than 23 wt.% solids if one adds the contributions of other BL components such as inorganics) [16]. Both the polymeric and the ceramic membranes had a MWCO of 1 kDa. Based on their estimates, the total cost of removing lignin with NF only was 46 (68) $ton of lignin (2015 values) for the ceramic (polymeric) membranes respectively. In comparison, a combination of UF and NF was much more expensive, at 120 (430) $/ton of lignin (2015 values) for the ceramic (polymeric) membranes.[16] It is apparent that regardless of the membrane material, NF alone achieved greater recovery at a much lower capital cost and that the polymeric membrane was considered more economical due to its lower fabrication cost despite its much shorter lifetime (1.5 years compared to 6 years for the ceramic membrane).

Overall, the following technoeconomic conclusions can be drawn. If simple concentration of BL to higher TDS content is desired at a lower cost than traditional evaporators, direct NF appears to be the most desirable option but it requires long-lived (i.e., non-polymeric) membranes. Furthermore, these membranes must have lower cost

than current ceramic NF membranes and also have higher lignin rejections (> 80%). There is a significant challenge in developing membranes that satisfy these requirements. If more detailed separation of the solids into different MW fractions (lignin, other organics like hemicellulose, and inorganics) is desired, then a combination of carbonation/acidification, UF and NF membranes would be necessary. Neither of the above scenarios addresses the recovery of inorganics, which would be recovered conventionally by combustion of the further concentrated SBL stream. On the other hand, the addition of an RO membrane downstream of the NF membrane could be beneficial in producing pure water and further concentrating the inorganics and low-MWs. In this case, significant challenges also exist in developing robust RO membranes. The third and most conceptually simple scenario is direct RO for raw BL concentration (retaining all the suspended and dissolved components and permeate water). This scenario will likely remain unfeasible in the foreseeable future due to the very high TMPs required for RO of raw BL and the prohibitively large amount of fouling that would occur with a raw BL feed.

1.11 Carbon Molecular Sieves (CMSs)

Carbon molecular seieve membranes (CMSs) are very stable, selective, and permeable.[107] CMSs are graphite-like (many graphite layer) whose pores ultimately form during the pyrolyis step, though unlike graphite, the overall struture is amorphous.[107] During pyrolysis, a polymer precursor is transformed into a carbon membrane under vacuum or inert gas conditions at high temperatures (typically 500-1000 °C), with some shrinkage of polymer occuring.[107] A good polymer precursor is thermosetting and

temperature resistant (i.e. not softening or liquefying during pyrolysis).[107] Though brittle and generally requiring supports (e.g. metal oxides), CMSs are advantageous because they are rigid and can withstand high pressures.[107, 108] Compared to typical costs of polymeric membranes ($10-20 per m^2), CMSs are more expensive at $50-100 per m^2.[108] However, this cost is counterbalanced by the greater selectivity of CMSs and, in the case of BL, their excellent stability at the high pHs and temperatures of real BL. CMS membranes can be characterized using gas permeation and sorption (which can provide pore size, density, and volume information), wide angle x-ray diffraction (WAXD), elemental analysis, thermogravimetric analysis (TGA) coupled with fourier transform infrared spectroscopy (FTIR), SEM and optical imaging, as well as determination of pore size via probe molecules and rejetions by MWCO of test molecules (for liquid applications).[108]

There are five key steps in the process of making CMS membranes, with step (4), pyrolysis, being the most important.[107]

1. Select (precursor) polymer
2. Prepare the polymer membrane
3. Pretreat the (precursor) polymer (if needed)
4. Pyrolize (most important step)
5. Post-treat pyrolized product (if needed)

Small changes in pyrolysis conditions can significantly affect final product.[107] Key pyrolysis variables include the final pyrolysis temperature, heating (ramp) rate, inert gas flow rate or vacuum conditions (pyrolysis atmosphere, concentraiton of the inert gas

and oxygen present in the system, inert gas pressure or final vacuum reached, and the total soak time at both intermeditate and final pyrolysis temperatures.[107] Increases in the pyrolysis temperature results in increased gas selectivity from smaller pores (increased rejection of solutes in liquid streams), decreased permeability (reduced flux in liquid systems), a thinner (more compact) membrane that is more crystalline and dense in structure with smaller distances between graphite layers.[107] Increasing temperature also results in increase in turborstraticy (layers are more haphazard and less in line with each other).[107] Allowing periodic soaking at intermediate tempreratures increases selectivity.[107] Slower heating (ramp) rates increase crystallinity and selectivity by decreasing the pore size.[107] However, if the heating rate is overly rapid, then cracks will form, resulting in defective membranes.[107] Inert or vacuum atmoshpere conditions prevent the combustion and other chemical damage of the polymer.[107] Under vacuum, selectivity increases while permeability decreases (i.e. smaller pores) while under inert gas conditions (e.g. Ar), increasing the flow rate increases the permeability (flux) while keeping the selectivity constant.[107] If needed, various post-treatments can repair some of the CMS defects and slighty adjust some of its properties.[107] For example, post-oxidation increases pore sizes, and chemical vapor deposition an increase selectivity.[107] However, from an industrial point of view, it is best if there are no (or at least minimum) post-treatments since extra process steps add to manufacturing costs.

CMSs are effective at efficient gas separation because of their molecular sieve pore-structure which allows the rejection of target species while maintianing high permeabilities (fluxes). CMSs have two distributions of pore sizes: ultramicropores and micropores. Ultramicropores (< 10 Å) are the smallest pores in the CMSs and give the

sieving (selectivity) behavior of the CMSs. Micropores (6-20 Å) are larger and give higher fluxes.[107, 108] The resultant selectivity depeds on the ratio of these two pore types; higher number of ultrmicropores give higher selectivities due to the smaller effective pore size of the CMS. Table 5 below shows a summary of the expected gas permeability for Matrimid® from the literature on a free-standing thin films, the gas permeation of several gasses through Matrimid-based CMS and the CO_2/N_2 selectivies obtained.[109, 110]

Table 5: Matrimid Gas and Matrimid-based CMS Permeabilities and CO_2/N_2 selectivities at 35°C.

Sample	**O_2**	**CH_4**	**N_2**	**CO_2**	**CO_2/N_2**	**Ref**
Matrimid	1.46	0.21	0.22	7.29	33.14	[109]
CMS: 550 °C, 2 hr vacuum	435	20	50	1250	25	[110]
CMS: 550 °C, 8 hr vacuum	166	4.2	18.2	375	20.6	[110]
CMS: 800 °C, 2 hr vacuum	24	0.21	1.8	43.5	24	[110]

CHAPTER 2

EXPERIMENTAL METHODS

As discussed in Chapter 1, there is considerable potential for membranes to replace 1-2 multiple effect evaporators for the concentration of Kraft black liquor, resulting in significant energy savings, as well as scale reduction and possibility of value-added products. Many commercial modules have been studied. Polymeric membranes have been used most often because their low cost and smaller pore-sizes. However, they are unstable in BL and most studies lower the temperature and/or pH to compensate for this. This adds additional unit operations and increases the costs of the membrane technology (most studies focus just on the economics of the separation, not combining the costs with the additional unit operations required to lower temperature and/or pH). Therefore, ceramic membranes are more advantageous because BL can be directly used without temperature and pH adjustments. However, the direct membrane cost is higher compared to using polymeric membranes (typically after temperature and/or pH adjustment), partially due to the larger pore sizes of ceramic membranes. Specifically, only three ceramic materials (metal oxides) based either on alumina, zirconia, or titanium. Clearly, there is room not only to improve the existing ceramic technologies, but to apply material science and engineering knowledge to design membranes from novel materials that can address these limitations. This has been the focus of this thesis.

First, an attempt was made to use zeolites and carbon molecular sieves (CMSs). As shown in the results section, zeolites were unstable but CMSs were promising. These

required ceramic supports. In the ceramic work, an attempt was made not only to achieve the right coating for a defect-free CMS membrane, but also to improve the ceramic performance as a prefilter (i.e. at or beyond the current state-of-the-art in commercial modules). It should be noted that the author is not aware of any prior work using CMS for liquid filtration, let alone for a difficult fluid such as BL. The challenges resulted in obtaining defect-free membranes that could not be improved by the thesis defense date. Thus, work was also taken to improve the ceramic performance, both as a pre-filter and as preparation for more successful CMS coatings on top of these improved ceramic supports.

2.1 Initial Work with Disc Supports

For industrially relevant usage of membranes, the filtration configuration needs to be cross-flow to minimize surface area requirements and fouling/concentration polarization. Due to the numerous fouling species and the increasing viscosity of concentrated BL, tubular modules are the most industrially relevant configuration for BL due to their high surface area to volume ratios (up to 200 m^2/m^3)[49] and adequate space for fluid flow. In light of these considerations, the initial CMS synthesis protocol was chosen from a paper[111] using α-alumina tubes.

However, initial lab-scale work was done in discs instead with plans to later switch to tubes. Lab-scale tubular modules were not commercially available and even a smaller, custom design by Swagelok would require larger membrane surface areas then we could initially make. Furthermore, dead-end cells were commercially available that

could withstand the high pressures get use very small surface areas to characterize the initial membranes and work-out any defects. The plan was to switch to tubular modules once the synthesis protocol had been optimized and the membranes were shown to be defect-free with the proper solute rejections on the much smaller and easier to test disc dead-end modules.

2.2 Stability Tests of Four Target Materials

As mentioned in the introduction and literature sections, BL is a very corrosive fluid. Not many materials remain stable in the hot caustic solution. Therefore, it was important to choose membrane supports and membrane materials that can survive these rough conditions.

Based on group experience, zeolite and CMS membranes were initially considered since these were known to be stable at higher pHs. However, both of these unsupported membrane types cannot handle the high TMPs necessary for BL work (ranging from 20-70 bar or higher). Therefore, these membranes must be placed on supports. These supports had to be very porous (to allow easy passage of permeate), with a proper pore size to prevent infiltration (and thus pore blockage) of the membrane precursor coating and be stable in BL. Literature has already used inorganic (ceramic) materials for MF and UF and even NF, albeit with low lignin and salts rejections due to the large pore sizes compared to the polymeric membranes. However, these ceramic materials are stable in BL and make excellent supports. One common ceramic is α-alumina. It was chosen not only because of its stability and strength once fired properly,

but also because it is readily and cheaply commercially available in a variety of particle sizes (both as commercial discs and as powders for in-house synthesis/coating).

In the beginning of the project, actual BL from our sponsors was not yet available; thus the project began with examining candidate materials for stability first in model BL (key salts only), and then in actual BL itself (once we received samples). Four materials were examined: a Matrimid-based CMS disc and three zeolites: FAU, MFI, and SAPO. Stability was analyzed by looking at XRD spectra (PANalytical X'Pert Pro; PANalytical, The Netherlands). If the material was stable in model BL and/or real BL, then its peaks before and after exposure should remain unchanged. Note that for the model BL, the pH was varied by changing the NaOH concentration to determine the effect of pH and to determine at which pH, if any, the four materials became unstable.

2.2.1 Formulation of the Model BL

The model BL consisted only of salt-species only to avoid issues with fouling from the organic species and lignin precipitation at lower pHs. The model BL (Table 6) was based on average values found in literature for softwood (pine) BL because the real BL used in this work came from sponsor companies primarily use softwoods as their pulp source.

Table 6: TDS Inorganic Composition of Model BL. Adapted from Refs.[31, 32]

Percent of TDS in weak BL	Component
1.3	NaOH
3.7	Na_2S
7.0	Na_2CO_3
2.6	Na_2SO_4
3.1	$Na_2S_2O_3$
1.5	Na_2SO_3

The basis for how much to add of each inorganic salt was weak BL at 14.5 wt.% TDS How much of each inorganic to add was determined as follows: A desired mass (or volume) of overall solution was chosen (e.g. 800 g or 800 mL). 14.5 % of that was TDS mass (113. 7g). Of that TDS mass, 1.3% was NaOH (1.5 g), 3.7 % was Na_2S (4.2 g), and the like. The remaining mass was made up of DI water (taken either as the difference between the desired mass and the total mass of the inorganics or, if a desired volume is needed, then based on a BL density correlation from the literature[112]). Additional NaOH was be added as needed to increase the pH (if needed). Likewise, for stability tests, acid (e.g. sulfuric or hydrochloric acids) was used to lower the pH.

2.2.2 Zeolite and CMS Stability Tests

In collaboration with Dr. Ketki Sharma, pH stability tests were performed on three types of zeolite membranes (MFI, FAU, and SAPO-34) and on a Matrimid-based CMS membrane using a simulated BL composition that only contained the inorganic components. Matrimid was used as a precursor to the CMS because of its low-cost and ease of commercial availability.

The pH was varied from 7 to 12 and stability tests were performed in Teflon-lined Parr bomb vessels. Teflon was chosen because it is inert and stable in many fluids, including BL. Parr vessels were chosen because of their ability to hold liquids under pressure (samples were placed in these Teflon-lined Parr bombs, sealed, and heated in an oven. During heating, the vapor pressure increased. The Parr vessels ensured a safe way to maintain that pressure without losing BL from evaporation of water).

FAU, MIF, and SAPO zeolites samples and a Matrimid-based CMS sample were tested for stability using XRD, where the peaks before and after exposure to model and real BL should remain the same if the sample is stable. Zeolite samples were kept in the model BL at 90 °C for 2 days and one additional day was used for cooling the samples (still in model BL) to room temperature (RT). Similar conditions were used for CMS with actual BL(15 wt.% TS).

2.2.3 Use of Matrimid as a CMS Precursor

A number of polymers (such as 6FDA-DAM, 6FDA:BPDA-DAM, polyamic acids and many others)[108, 113] have been used in the literature for the CMS precursor. Choice of precursor depends on the desired CMS properties (some precursors, even at the same pyrolysis conditions, give more/less permeable and more/less selective CMSs), as well as ease of synthesis/purchase and cost. Matrimid® 5218 (Huntsman Advanced Materials, The Woodlands, Texas) was chosen because it was a readily available, low-cost commercial polymer that had undergone many past studies for gas permeation (e.g.[107, 108, 114]) and pervaporation (e.g. [111, 115, 116]), but had not been used yet for liquid filtration, let alone for BL.

2.3 Membrane Fabrication Protocols

Commercial discs (ADS-96R, 15-20% porosity; CoorsTek, Grand Junction, Colorado) were chosen because of the rapid availability of hundreds of discs for membrane fabrication experiments, while pressing in-house discs would have taken considerably longer. However, as subsequent sections will show, some in-house discs were necessary due to difficulties encountered with the CoorsTek samples. As discussed in the results section (Chapter 3), the support pore sizes were too large for adequate coating (polymer infiltrated into pores and created abnormally low gas permeations). Discs of 1mm and 0.63 mm thicknesses were tried, with 1 mm samples used for most of the work due to their stronger mechanical strength. Several batches were used, but were mostly the same except one batch, which had a significant number of impermeable discs. Once the problem was identified, all remaining discs within that batch were tested with N_2 gas permeation to ensure that the discs were not impermeable. Mercury porosimetery (AutoPore IV 9500; Micromeritics Instrument Corporation, Norcross, Georgia) was used to analyze the pore size distribution of the bare supports and ImageJ software[117] was used to provide estimates of the pore sizes of alumina-coated supports based on SEM images.

2.3.1 Disc Polishing

To increase the quality of the eventual CMS membrane, the coating of its Matrimid precursor must be defect-free as any defects are carried over to the CMS. To do this, both the coating technique and the support surface are important. The Matrimid coating and pyrolysis methods will be discussed later, while the focus here will be on the alumina support.

The support surface should be as smooth as possible.[118] The literature supports this, as shown in Figure 16 below, showing the difference between a polymer coat on an rough (top image) surface and a smooth (bottom image) surface. As can be seen, the smooth surface resulted in a defect-free coat, while there was insufficient polymer to completely cover all of the rough peaks and troughs in the top image.

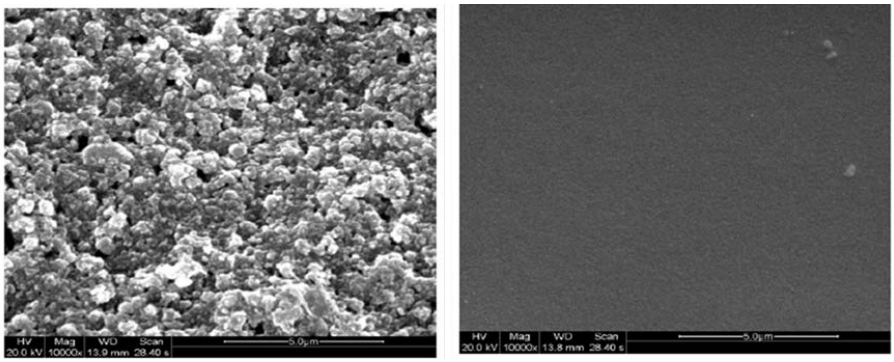

Figure 16: Polymer coat on a rough (left) and smooth (right) supports. From Ref.[118]

In this work, all discs were polished for one minute at 150 RPM using silicon carbide 600 grit paper on a polishing machine, both from Buehler (Petrolap Lapping system with a Petrographic Abrasive Dispenser; Lake Bluff, IL USA). Discs were held by hand onto the rotating polishing paper. A few samples were also polished at 60 RPM, but no noticeable difference in quality was observed between the different speeds. The fire alumina discs are very hard and quickly wear-out the Buehler polishing film, requiring frequent replacement. Also, for a longer-lasting polishing paper and a finer polish, diamond lapping paper (1 μm Diamond Lapping Film Discs, 12" from Precision Surfaces International, Houston, Texas) was used in the later stages of the work (after

first polishing with the Buehler paper). However, the quality of the surface did appear to improve significantly from using the diamond film.

To ensure adequate and even polishing, discs were initially polished for one minute, then rotated by 90°, polished again for one minute. This was done for each of the 90° directions (four minutes total). Towards the later part of the work, the time was optimized and, at 150 RPM and with firm pressing of the disc against the Bueher polishing paper, each direction could be held for ~15-20 seconds without affecting the quality of the polish (it was observed that during the initial seconds, most of the alumina was removed to achieve a polished surface). After polishing, the membrane-side was no longer touched. Discs were then sonicated (Model 75T from VWR, Radnor, Pennsylvania) for 30 minutes and then vacuum-dried for~ 24 hours at 100 °C. To avoid any damage to the discs (and more importantly, for the subsequent Matrimid and CMS coatings), vacuum was slowly applied and released.

2.3.2 Dip and Spin-Coating of Matrimid

It is important to create a thin membrane layer to increase the flux and thus minimize surface area requirements. Two methods were employed in applying thin membrane coatings: dip/tangential coating and spin-coating. For both, it was important to have a smooth surface and a clean surface. To minimize contamination of the surface from dust and other particles in the air, discs were stored in closed containers and gently air-blown prior to coating. Most dip and spin-coated samples were based on the

formulation from our reference paper:[111] 12 wt.% Matrimid in 1-Methyl-2-pyrrolidinone (NMP) (ReagentPlus®, 99%; Sigma-Aldrich, St. Louis, Missouri) was used.

Initially, dip-coating was done by holding the 25 mm disc in tweezers and inserting the membrane side into a short plate/crucible lid until the disc came into contact with the fluid. The disc was then be rapidly and tangentially pulled away and held in a vertical position (Figure 17). A Kimwipe was then used to absorb the drop of solution at the very edge and the disc would be then placed top-side up for drying. This technique suffered from poor reproducibility and was improved (though dip-coating is still more variable than spin-coating).

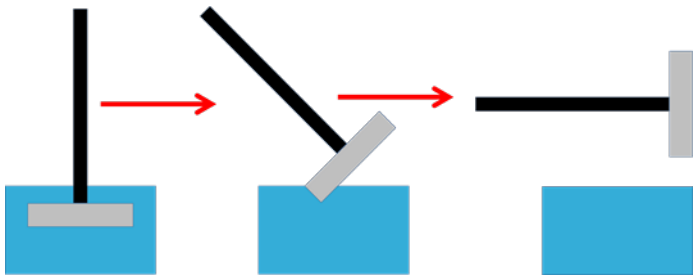

Figure 17: Dip-coating schematic. Adapted from Ref.[119]

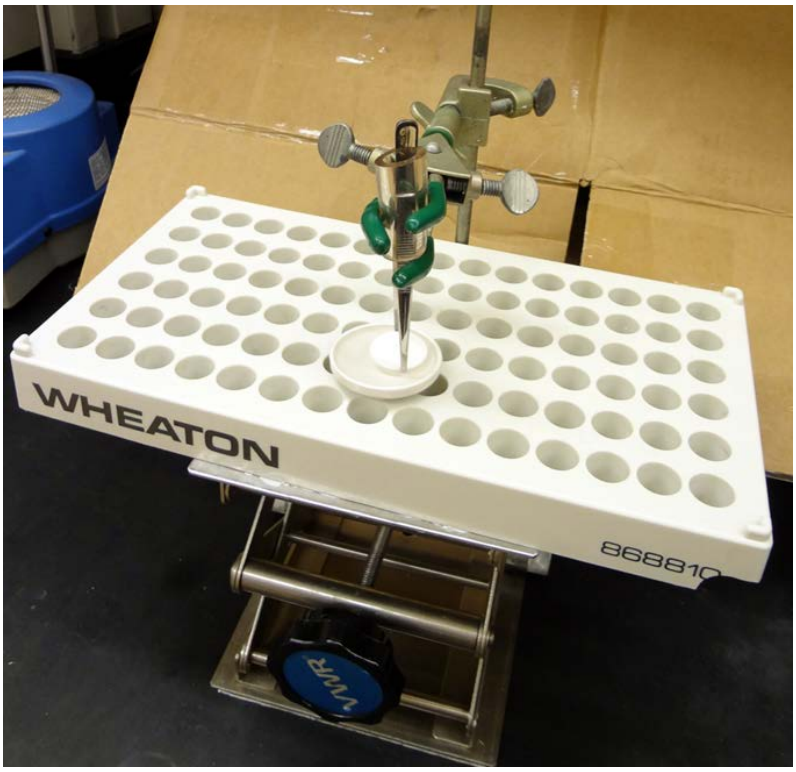

Figure 18: Improved dip-coating setup

The improved version of the dip-coating is shown in Figure 18. Discs were still held in tweezers (membrane-side facing the solution), but the tweezers were held by a clamp. The thin solution container/crucible lid was placed onto a larger support which rested on a scissor ramp that could be adjusted by turning the screw. The ramp was moved up until the disc was in contact with solution, held for a set period of time with the aid of a timer, and then tangentially pulled away into a vertical position. Again, a Kimwipe was used to remove drops from the bottom of the disc. Depending on the coating substance, the disc was kept in this vertical position for drying until it was placed support-side down for further drying steps. For the later alumina coatings, the disc was quickly transferred from the vertical position and place flat (membrane-side up) and

briefly dried in a 110 °C oven (to minimize aggregation from water evaporation by more rapidly removing the water).

One challenge with dip-coating was the thin but still relatively thick films produced when dip-coating Matrimid (alumina coatings were fine in the dip-coating method). During the initial work (in collaboration with another lab member) in pyrolyzing the Matrimid into CMS, the polymer/CMS film cracked, resulting in a defective CMS membrane. All further CMS work focused on spin-coating, which gave thinner films that did not crack during pyrolysis. Note that is still possible to dip-coat and successfully pyrolyze Matrimid films, as one of my colleagues showed. However, this was harder to reproducibly achieve and involved reducing the viscosity of the Matrimid solution (by reducing the concentration) and by applying multiple dip-coats prior to pyrolysis to sufficiently cover uncoated areas. The membranes were still thicker than those from the spin-coating method. Spin-coating (Model WS-650MZ-23NPP using Laurell controller; Laurell Technologies, North Wales, Pennsylvania) was more reproducible and gave significantly thinner films (on order of microns and tens of microns).

Initially, a number spin-coating formulations were tried to see which ones gave better coats. These formulation settings were based on the advice of Dr. Reichmanis' group (who have extensive experience in spin-coating). The settings were slightly modified to help achieve a more optimum coating. The formulation settings are shown below, where the RPMS are both the final spin speed and the acceleration settings:

1. 1200 RPM, 1 minute, 6 wt.%,
2. 1200 RPM, 30 seconds, 12 wt.%
3. 900 RPM, 30 seconds, 12 wt.%
4. 900 RPM, 1 minute, 12 wt.%

After preliminary work, only formulation (2) was used because of better quality of coat and potentially promising permeation results.

Spin-coating was done statically. The disc was first placed onto the spin-coater, vacuum was applied, and the 12 wt.% Matrimid solution was poured onto the disc until the entire surface was covered. Then the spinning began, removing most of the solution except for a very thin layer.

2.3.3 Drying Matrimid

The formulation of our paper[111] of reference was initially followed to dry the Matrimid coats. The initial drying protocol (Protocol 1) was simple, since little details were given in the paper. Dried was first done by placing the coated Matrimid discs into a vacuum oven at 250 °C and applying vacuum or in the pyrolysis setup by first applying vacuum and then heating to 250 °C at ~10 °C/min. Samples were dried ~12-24 hours.

Protocol 1 was not successful and was modified to include gentler drying conditions (Protocol 2). It was hypothesized that pin-holes were created during the drying of polymer films. Rapid evaporation of solvent was thought to break up the polymer chains, creating pin-holes. These pin-holes carry through the carbonization process, resulting in defective CMS membrane with low rejections. Thus, subsequent drying

protocols attempted to dry the films as carefully as possible to avoid pin-hole formation. Care was taken during the transition near the boiling point of the NMP (202 °C) to avoid any evaporation stresses.

Protocol 2 first applied vacuum in the pyrolysis unit (from this point on, all drying protocols used the pyrolysis unit), but this time very slowly and monitored via an O_2 Sensor (Cambridge Sensotec Ltd., Rapidox 2100 series; Cambridge, England) to ensure that the rate of increase/decrease was not overly rapid. Next, the temperature was increased at 1 °C/min up to 120 °C and then allowed to cool naturally to RT. Both the vacuum steps and the first drying step did not yield any visible changes in the Matrimid coating to the visible eye. Once this was assured, the sample was again heated (still under vacuum) at 1/°C/min to 120 °C, then 1/°C/min to 180 °C and cooled. Again, the sample was checked visually for any pin-holes visible to the naked eye. The entire procedure was then repeated again by finally heating up to 210 °C at the same heating rate and cooling naturally to RT.

Despite seeing no visible changes along the heating path in Protocol 2, pin-holes were still observed under microscope. Thus, Protocol 3 was tested. First, the Matrimid sample was air dried to 150 °C at 0.5 °C/min and allowed to soak at that temperature for 1 hour before naturally cooling down to RT. Afterwards, vacuum was slowly applied. Next, the sample was dried to 150 °C at 0.5 °C/min and then (no soaking) died to 210 °C (1 hour soak before cooling naturally to RT) at 0.1 °C/min. This worked well and has been the drying protocol using for the rest of this work.

2.3.4 Polymer Infiltration and PEG/Isooctane filler

Though the reference paper[111] used PEG as an intermediate layer (between the alumina support and the Matrimid coat), coating directly onto the support was first tried to see how much effect it would have. As discussed in the results section, a good layer was achieved but it showed infiltration and was almost impermeable. This was not surprising since literature is aware of possible polymer infiltration and thus either changes the support and/or polymer solution properties to prevent or minimize infiltration or adds an intermediate layer (which may or may not be removed in subsequent processing steps) to achieve the same objective.[111, 113, 120-122]

Based on the reference paper, [111] PEG 4000 (BioUltra, 4,000; Sigma Aldrish, St. Louis, Missouri) (5 wt.% in MeOH) was used because according to the literature TGA data in Figure 19 below, the PEG fully decomposed by 522 °C during pyrolysis (thus avoiding its carbonization), creating a CMS layer directly on the alumina support. In this work, pyrolysis conditions were kept at or above 525 °C to ensure that PEG was fully decomposed. As discussed in Chapter 3, this strategy was later abandoned due to inability to remove PEG on our commercial supports. A filler of isooctane was tried to fill the pores with isooctane and then remove isooctane during drying (isooctane's boiling point is lower than NMP's), but that was not successful. Other fillers such as waxes[123] were discarded as not feasible (e.g. our current pyrolysis setup could not remove the hot wax, potentially damaging to the vacuum pump and clogging vacuum tubing lines once the wax cooled down)

Since temporary fillers were not successful and the polymer film infiltrated the support pores, the next strategy was to add aluminum oxide layers on top of the existing

supports (or making in-house supports) that had smaller pores, eliminating or minimizing Matrimid infiltration.

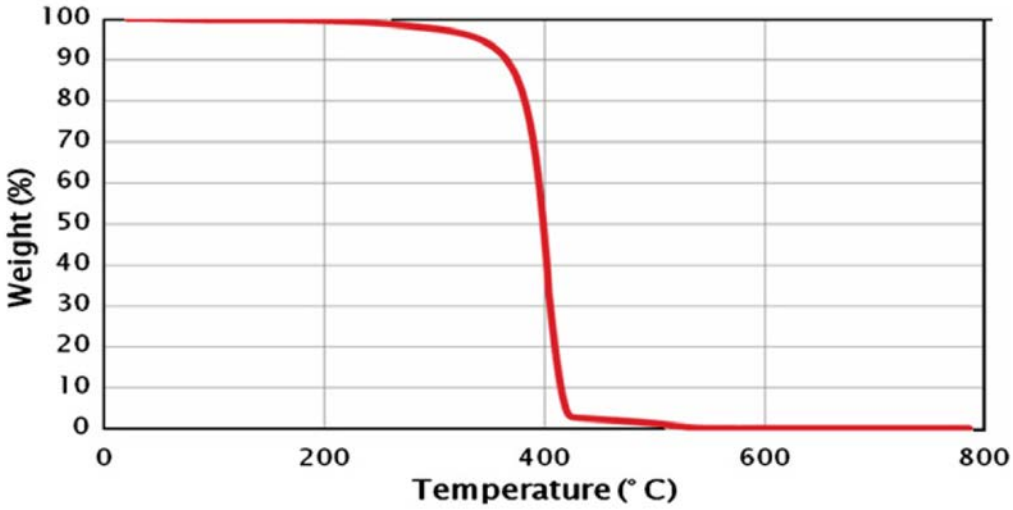

Figure 19: TGA Showing PEG Decomposition. From Ref.[111]

2.3.5 Alumina Coating

Several papers have explored adding alumina layers onto alumina supports. The protocol of Benito et. al.[119] was followed here. The paper used German-based chemicals; thus, the very first batch of coats explored the results using some of the German-based samples (courtesy of Zschimmer & Schwarz, Lahnstein, Germany) as well as very similar alternatives available here in the US. Both solutions used alumina oxide powder (A16SG from Alcoa, New York, New York) with a rated average particle size of ~ 0.25 μm.[124] Actual average particle size was 0.45 ±0.18 μm based on SEM images of dilute particles).

Based on the paper by Benito et. al.[119] the expected pore sizes from a good coat was expected to be ~0.1-0.2 μm and the coated layer was expected to be ~6-10 μm thick. All coatings were performed on the CoorsTek alpha-alumina supports.

The procedure mixed together 8 wt.% of the α-alumina powder, 1 wt.% of a low viscosity binder (Polycol 5 for the German batch, carboxymethylcellulose sodium [low viscosity, CA193 from Spectrum Chemical, New Brunswick, New Jersey] for the US batch), 0.75 wt.% Deflocculant (Dolapix CE 64 for the German batch, 4,5 Imidazoledicarboxylic acid [Sigma Aldrich, St. Louis, Missouri] for US batch) along with the remaining wt.% of DI water. The solution was then mixed for an hour in a Ball mill, sonicated for at least 30 min. Prior to dip-coating, the solution was also shaken up and usually briefly sonicated. Dip-coating was the same as in the improved dip-coating method (still on Buehler polished supports), but with a total dipping time at 60 seconds for each sample. After dip-coating, samples were taken directly to a furnace to dry and sinter by heating to 1100 °C at 200 °C/hr, soaking for 2 hours at that temperature, and then allowing the samples to cool naturally to RT. It should be noted that for this first batch, there were difficulties with reaching and maintaining the 1100 °C temperature (later resolved by using a different furnace when it became available). Thus in this first batch, 1100 °C was never actually reached; the actual maximum temperature was, at most, 995 °C.

This coating (1st batch) was then used to coat and pyrolyze Matrimid. However, the CMS film delaminated, likely from the rough surface morphology of the coatings. This resulted in improved coating protocols that attempted to avoid aggregation of alumina (thus giving smoother coats) so that performance could be characterized both

with and without CMS. Polishing the coated supports was briefly considered and tried, but abandoned because the thin coated layers were prone to be completely removed even with the gentlest polishing.

The second coating protocol (batch 2) attempted to keep particles from agglomerating while avoiding the use of binders and defloculants, since these create larger pores when they are decomposed during sintering. Because alumina powder is slightly basic, consuming H^+ ions in water, literature suggested using an acidic solution to maintain similar charge and thus discouraging significant aggregation.[125] The second protocol used HCl in water (pH ~5.3) and tested the effects of both the 0.25 um particle size from Alcoa (batch 2A) as well as a 5.8 nm alpha-alumina (batch 2B) powder (Aluminum oxide, activated, neutral, Brockmann Grade I; Alfa Aesar, United Kingdom). Particle size measurement by SEM was unable to see very small particles. The smallest seen were 0.14 ±0.07 μm. Both powders composed 1 wt. % of the pH 5.3 solution (the dilution was an another attempt to minimize particle aggregation). This time, a better furnace was used (Barnstead Thermolyne 1400; Thermo Fisher Scientific, Waltham, Massachusetts) that reached 1100 °C and was soaked at that temperature for 2 hours. The furnace did not have a ramp rate control, however, it was observed that the total time taken to increase the temperature from RT (~25 °C) until 1100 °C was 1 hour, with the initial ramp rate quicker and then slowing down as the target temperature was approached. It should also be noted that post dip-coating, samples were quickly dried with a Kimwipe while in the vertical position and then placed horizontally (coated side up) in a 110 °C oven to increase the rate at which water was removed and minimize aggregation from shrinkage caused by slower drying of water.

As discussed in the results section, this second protocol yielded some rejections (comparable to the pressed discs for the 0.25 μm powder). But it was thought that results could be improved, particularly with the 5.8 nm powder (since it was so small that it could easily have infiltrated the powers and thus didn't have enough particles on top of the support to create a defect-free coat). Coating protocol 3 consisted of either coating (in pH 5.3 solution) 3 wt.% of 0.25 μm alumina powder, firing as in protocol 2, and then coating and firing again a 8 wt.% of 5.8 nm (batch 3B) or coating (in pH 5.3 solution) 1 wt.% of 0.25 μm alumina powder (same concentration as in Protocol 2, for comparison), firing as in protocol 2, and then coating and firing again a 8 wt.% of 5.8 nm (batch 3A). Enough discs were made that a second coating of 5.8 nm powder was applied to both batches in this protocol.

Protocol 3 yielded low lignin rejections and two further coating strategies were tried. First, because the 5.8 nm particles were small, it was hypothesized that even 8 wt.% was too low to ensure adequate surface coverage due to loss of particles from infiltration. Guided by the literature, the concentration of 5.8 nm particles was increased to 40 wt.% in pH 2.14 (using HCl) to minimize aggregation.[119, 126, 127] Coating and firing was done as before (no diamond lapping film since by this time, it was shown to be ineffective), though the 40 wt.% solution was mechanically stirred prior to coating and dried in air for at least half a day prior to firing.

Second, it is known that compared to α-alumina, γ-alumina can result in smoother surfaces and small pore sizes (1-5 nm, with smaller pore sizes can be achieved by lowering the firing temperature) as well as provide thinner CMS layers.[128-130] Here, the procedure of Chen et al. was followed with minor adaptations:[128]

Three mL of ethanol and ~25.5 mL of Al-tri-sec-butoxide (97%, Sigma Aldrich, St. Louis, Missouri) were manually mixed by violently shaking the 40 mL vial to form a homogeneous solution. This was then added to 425 mL of 80 °C DI water, heated to 90 °C and stirred under reflux for 1 hour. Next, 4 mL of acetic acid (Sigma Aldrich) was added and the solution continued to stir at 90 °C for 1 hour under reflux. Then, 0.5 ml glycerol (Sigma Aldrich) was added with the same stirring and reflux at 90 °C for one more hour. The heat was then turned off and the solution was allowed to cool and age for at least 12 hours (still stirring and under reflux). The aged, RT solution was then dip-coated for 60 s, dried at RT for ~12 hrs, dried in a 110 °C oven for ~12 hrs, and then fired at 3 C°/min to 600 °C (2 hour soak time). Note that in the only batch to be made for this thesis, the furnace used had difficulties reaching 600 °C and thus the total soak time was a bit above 12 hours.

2.3.6 In-house Alumina Pressed Discs

Due to the limitations of the commercial CoorsTek support (e.g. Matrimid infiltration), attempts were also made to make in-house supports with smaller pore-sizes to prevent infiltration and improve the water flux properties. The 0.25 μm powder was used to make the discs in a 25 mm X.R.F. die (max load of 30 tons) and pressed using a mechanical press (carver 50,000 pound Press). The die consisted of a bottom support, a top piece, two 25 mm discs (one side was polished and shiny-this is the side that was in contact with the alumina powder), and a pressing rod.

The first Protocol was based on the literature formulation and pressing conditions.[131, 132] The literature suggested adding either water[131, 132] to the alumina powder, or a binder (e.g. polyvinyl alcohol [PVA]).[119, 133]Also, a former group member shared his own formulation and that was considered as well. Because of the slight variance between the formulations and pressing protocols, four different types of overall protocols were tested and one of them (ConC) was ultimately chosen as the method to use due to better performance (i.e. disc was less prone to cracking between the pressing and firing steps). These four methods are discussed below. Note that for the 0.25 μm powder ~1 g in the 25 mm cell corresponded to a thickness of ~ 1mm. Initially, discs were made somewhat thicker (~2 mm) but once the final protocol was chosen, almost all discs were pressed to yield ~ 1 mm discs (1 mm was the maximum thickness that could be used in our standard dead-end cell).

The first method (ConA) was based on the formulation of our former group member. In ConA, 2.1g of α-alumina was mixed with 0.3138g DI water using a mortar and pestle. This mixture was then pressed for 2,500 lbs for 5 seconds followed by 5,000 lbs for 120 seconds.

The second method (ConB) was based on reference 131.[131] 2.1g of α-alumina was mixed with 0.0875g DI water using a mortar and pestle. This mixture was then pressed for 5,000 lbs for 5 seconds followed by 15,000 lbs for 120 seconds.

The third method (ConC) was based on reference 132.[132] 2.1g of α-alumina was mixed with 0.1826g DI water using a mortar and pestle. This mixture was then pressed for 1,300 lbs for 30 seconds followed by 5,000 lbs for 120 seconds.

The fourth method (ConD) was based on reference 133.[133] Instead of water, a 10 wt.% polyvinyl alcohol (~89-98 kDa, from Sigma Aldrich) in water solution was used. Thus, 2.1g of α-alumina was mixed with 0.1826 g PVA solution using a mortar and pestle. This mixture was then pressed for 15,700 lbs for 5 seconds followed by 20,200 lbs for 120 seconds.

After pressing, all discs (regardless of method or protocol) were fired in the same way. Initial attempts to fire at 982 °C for ~36 hr and 1100 °C for ~2 hrs yielded discs that broke upon light pressure. Thus, the final firing conditions that were used were 1300 °C for 2 hours with natural cooling to RT. The ramp rate was ~3-5 °C/minute using a bottom loading Keith furnace (1600 °C maximum temperature with $MoSi_2$ heading elements). Note that shrinkage occurs during firing. At a firing temperature of 1300 °C, the shrinkage was ~ 1 mm (i.e. final discs were ~24 mm in diameter).

2.3.7 CMS Pyrolysis Protocol

Matrimid films coated unto α-alumina supports were pyrolized using the equipment shown in Figure 20 below. An Edwards vacuum pump (Model RV3) is connected to a glass quartz tube (GE Type 214 Quartz Tubing 55.00 mm x 59.00 mm x 4 ft. from National Scientific Company, Quakertown, Pennsylvania) that sits inside a furnace (XST-3-0-24-3C three-zone furnace from Thermcraft, Winston Salem, North Carolina). Inside the quartz tube is a quartz plate (52 mm x 500 mm x 4 mm thick slotted plate with 10 slots, each 2 mm x 2 mm, from United Silica Products; Franklin, New Jersey) on top of which samples are placed. Also connected is an oxygen sensor

(Cambridge Sensotec Ltd., Rapidox 2100Z, Cambridge, England) to ensure adequate oxygen removal by the pump and to ensure that the vacuum is applied and released slowly, as well as a pressure transducer (MKS Baratron Type 727/728A). Not used in this work but also available is a line for inert gas (e.g. Ar) hook-up. In this work, all pyrolysis occurred in a vacuum, with all pressures less than 5 mTorr and with oxygen concentrations below 10^{-20} ppm.

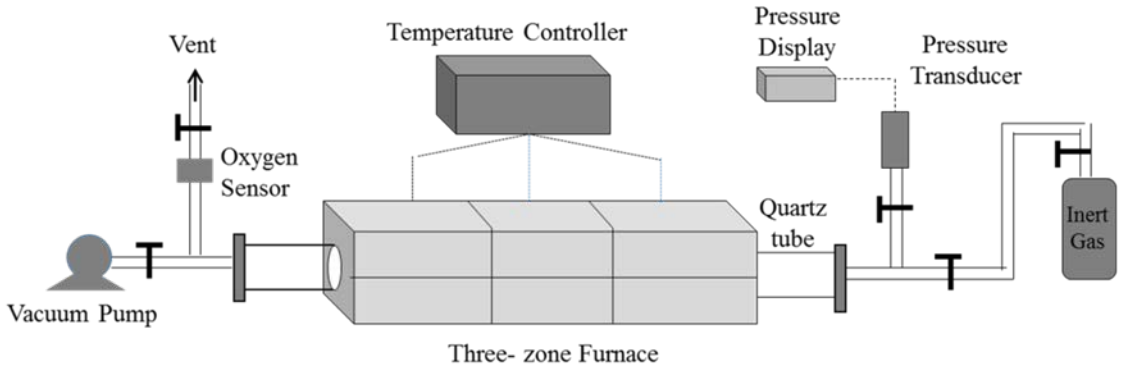

Figure 20: Schematic of the pyrolysis setup

Early work was based on the ramp rates of our reference paper[111]. The heating protocol there is shown in Figure 21 below.

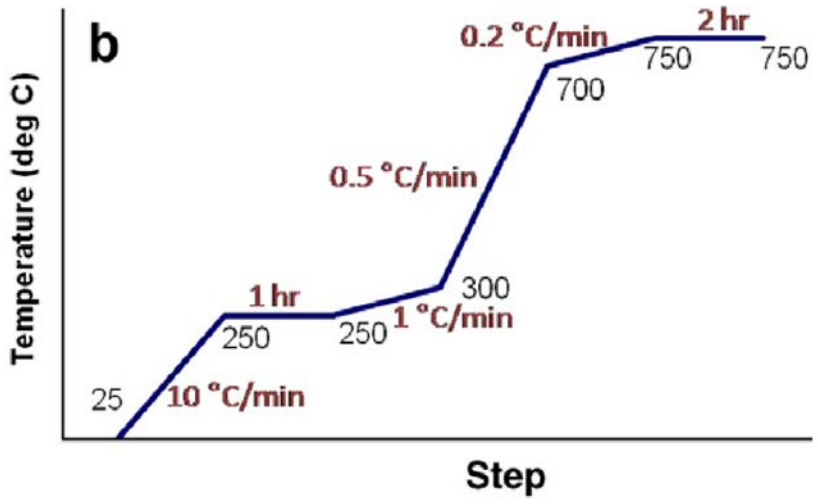

Figure 21: Initial Pyrolysis Protocol. From Ref.[111]

Because of the lack of significant gas and liquid permeation in initial samples, this pyrolysis protocol was replaced by one from the Rungta Thesis,[108] where the pyrolysis temperature was lower (525 °C). The lower temperature was chosen to increase the pore size and thus permeability of both gas and liquid. The protocol is:

1. RT (~25°C)→250°C at a ramp rate of 13.3°C/min
2. 250°C →510°C at a ramp rate of 3.8°C/min
3. 510°C → 525°C at a ramp rate of 0.2°C/min
4. Soak for 2 hours at 525 °C

2.4 Membrane Characterization

2.4.1 Optical and SEM Imaging

Optical microscope (Olympus BX51, TH4-100) and SEM (LEO 1530 FE-SEM) images were used to examine if there were any visible defects on the Matrimid and/or CMS films (top surface), to obtain the thicknesses of coated layers (both alumina and Matrimid and/or CMS), as well as to examine the quality of the alumina coatings. SEM images and ImageJ were used to estimate the pore size (liquid porosimetery was not yet available)

2.4.2 Gas Permeation

An in-house gas permeation system was used to access the quality of the Matrimid and CMS coats in comparison to literature gas permeance, permeability, and selectivity values. Figure 22 below shows the setup. Vacuum was applied until the pressure in both the feed and permeate sides was 0 psig. Then, either N_2 or CO_2 gas (and sometimes SF_6) was allowed to flow through at ~52 psia and the rate of change of the permeate pressure with time was measured. Its initial slope is linear and that slope was used to calculate the gas permeability.

Figure 22: Gas Permeation Setup

2.4.3 Liquid Permeation

A BL dead-end filtration system was designed and assembled to study the flux and rejection of membranes under BL, model black liquor, water, and salt solutions. Figure 23 shows the schematic of the setup.

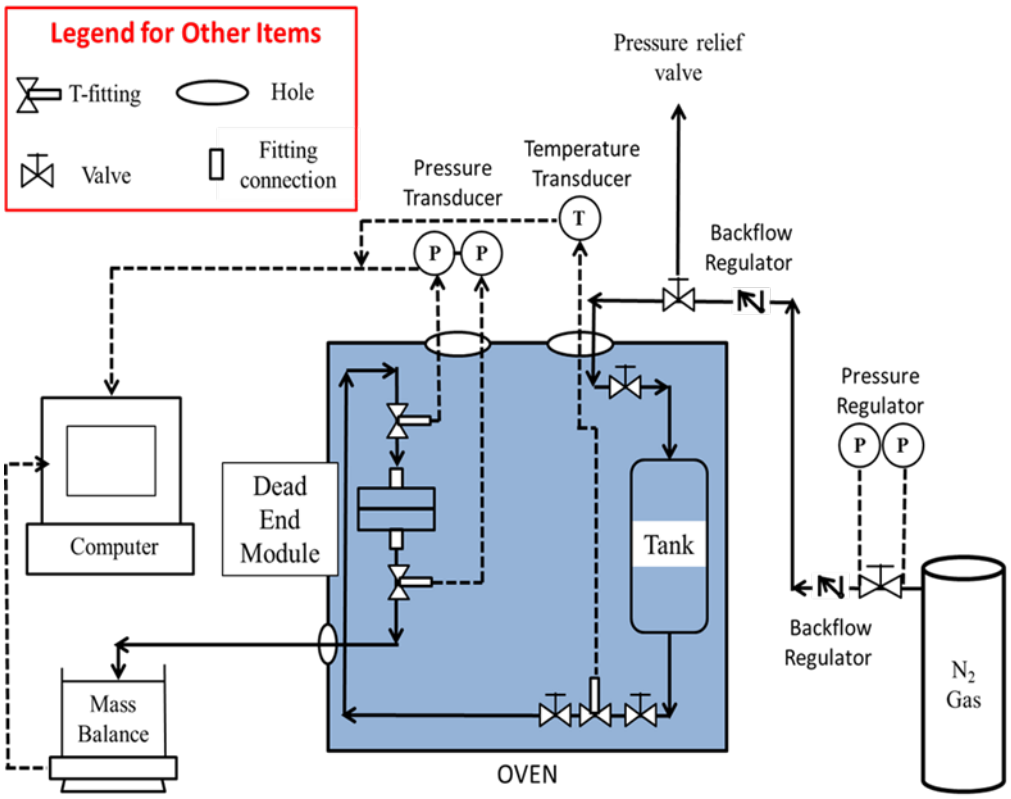

Figure 23: BL filtration system

The system is capable of high temperatures (90-100 °C for black liquor studies and up to 200 °C based on oven's max setting). There is a nitrogen gas (N_2) cylinder that has a high-pressure gauge capable of delivering up to 137 bar of pressure. N_2 is an excellent choice because it is chemically inert and avoids the corrosion concerns if a pump was used. However, the system is limited by the maximum pressure rating of its weakest link, which in the current configuration is the feed tank. The tank's maximum pressure limit is 120 bar at room temperature and 93.7 bar at 93 °C. There is an automatic relief valve to avoid over-pressurization. It should be set at least several bars below the system's lowest maximum pressure rated component at the highest operating

temperature. There is also a manual relief valve to depressurize pressure system manually, particularly when releasing pressure post a membrane filtration experiment.

The filtration parts are shown in Figure 24, which includes a 1 L feed tank (A), temperature (B) and pressure transducers (C), and the dead-end (non-stirred) module (D).

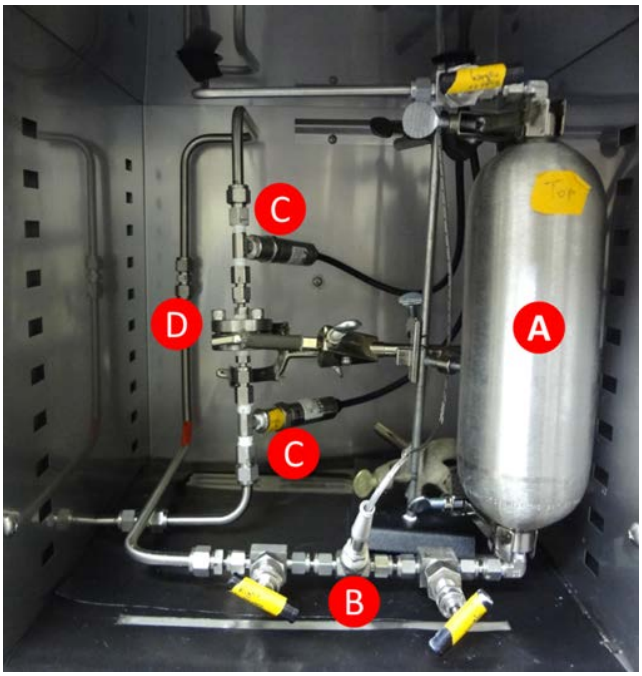

Figure 24: Schematic of Gas-Driven Membrane Separation System

The membrane module (D) is a non-stirred, a dead-end filtration module from Millipore (high-pressure SS filter holder, 25 mm; EMD Millipore Corporation, Billerica, Massachusetts) (max 350 bar room temperature [RT] rating), shown in Figure 25. In the schematic, (I) is the bottom piece, (II) is the top piece, (III) is the support disc that goes into the bottom piece (small mesh size side facing user), (IV) are the screws that hold the

top and bottom pieces together, (V) is the screwdriver needed to tighten the screws, and (VI) is an optional, but helpful screwdriver for getting the support disc out and for helping to remove the membrane from the module. This cell does have flux limitations due to the build-up of foulants (i.e. increase in concentration polarization and osmotic pressure), but is useful for quick rejection studies.

Figure 25: Millipore Dead-end filtration model, including the support disc, screws, and helpful screwdrivers

The dead-end cell accepts in discs 1” (24 mm) diameter. For stability in BL, the inner O-ring used was either EPDM, Teflon, or Silicone. After initial work with EPDM showed a stickiness of it to the membrane post an experiment, silicone was used instead (it stuck less often to the membrane, making it easier to remove). All O-rings were purchased from McMaster Carr (Atlanta, GA) (e.g. Silicone: Super-Resilient High-

Temperature Silcone O-Ring, 1/16 Fractional Width, Dash Number 018) A torque wrench was later used to ensure that all screws consistently receive the same torque and are not overtightened (~40 in-lbs).

The default module had only O-ring, creating a seal on the feed side (the permeate side did not have an O-ring, which caused leaks). Thus, an EPDM outer-O-ring was added to seal the permeate side. It was purchased from McMaster Carr (Steam-Resistant EPDM O-Ring, 1/16 Fractional Width, Dash Number 022, Catalog # 9557K118). It was 1" in inner diameter, 1 1/8" outer diameter; making it just the right fit (if it was too thick/bigger, it would get in the way of the screws).

The module required further modifications. First, since the module was designed for thin films and not 1 mm discs, the initial seal created by the outer O-ring was not enough to prevent leakage. Also, the inner O-ring did not protrude sufficiently from the groove in the module, giving very little O-ring for a seal of the feed side and increasing the chances of metal-to disc contact, which cracks the disc. The issue was addressed by machining 0.010" off the top O-ring wall.

Also, since with 1 mm discs, there is some gap when the module is fully clamped, it was thought that a 1 mm deeper groove would help. So a second module was bought and its permeate size was made 1 mm deeper. Surprisingly, this actually caused discs to break even upon finger tightening of the screws. Consequently, that module was not used except for the few 2 and 3 mm pressed discs, since the normal module could not handle such thick discs without easily breaking or leaking from the permeate side.

As mentioned previously, this dead-end cell has several limitations. The chief one is significant fouling from strong concentration polarization and even possible gel-layer formation. Ideally, a Sterilitech module (HP4750X Stirred Cell, for Operation up to 2500 psig, 172 bar max at RT, 49 mm disc diameter [47-50 mm range] would be used because the stirring would approximate a cross-flow cell and minimize the fouling, allowing realistic and not days-slow fluxes to be achieved. However, this was not done in the early work because of the large disc diameter required (2”). At the time, we could not coat such larger discs and were not confident that a mask would be strong enough at the high pressures, pHs, and temperatures used in BL. Since that time, we have gained the ability to begin coating larger discs and, if needed, masking smaller ones. The Sterlitech module will be used in all future work.

Flux data was collected using the mass-balance (Ohaus Pioneer Model PA313; OHAUS Corporation, Parsippany, NJ). Because permeate volumes are low for high-quality discs, a closed 3-decimal point accuracy mass balance (max mass 350 g) was used to monitor permeate flux. It was connected to LabVIEW using a serial port and had neoprene liners to prevent damage to MB components

Real-time data collection of mass, temperature and pressure was done using LabVIEW. The outside box is a CompactDAQ Chassis (National Instruments Corporation, Austin, Texas) and it connects to the computer via a USB cord. Many devices, such as the pressure and temperature transducers, are connected to a NI 9219 4 Ch-Ch Isolated, 24-bit, ±60V,100S/s Universal AI Module that fits inside the Chassis.

To make a liquid filtration run successful, several factors had to be considered: (1) Proper module clamping, (2) slow increase in pressure and (3) sufficient soak times at low pressures.

The module must be clamped tight enough on the membrane disc to ensure adequate pressure on the O-ring, preventing leaks from both the feed and permeate sides. However, too much tightening (too much torque) will apply too much pressure on the disc and crack it. A torque wrench is recommended (20 in-lbs for the Millipore cell) to ensure that the module is not over-tightened. Also, it is necessary to tighten the screws in a “star” pattern, where screws are not tightened in order but in alternates and across from each other. Screws should be tightened as evenly as possible to ensure even pressure distribution from clamping.

A slow initial increase in pressure is vital. Sudden application of high pressures will crack the discs. In this work, initial pressures were increased by 1-2 psi every several seconds until pressure reached about 3.5 bar. After that point, pressure was increased 0.1-0.2 bars per several seconds. There was also periodic soaking. Typical times required to go from 0 to 3.5 bars was between 30-60 min. As mentioned previously, the mass-balance data was used to calculate flux. UV-Vis (280 nm) was used to calculate the lignin rejections in a quartz cuvette using an Agilent 8510 Spectrophotometer. A conductivity meter (Oakton CON 150 conductivity/TDS handheld meter; OAKTON Instruments. Vernon Hills, Illinois) was used as a quick measurement of the inorganic rejection.

CHAPTER 3

RESULTS & DISCUSSION

3.1 Stability tests of four target materials

The XRD patterns of FAU, MFI, and SAPO zeolite materials before and after model BL exposure are shown in Figures 26-28, where the peaks before and after exposure to model and real BL should remain the same if the sample is stable. As seen in Figure 26, the FAU peaks were lost by pH 12.2, indicating that it would not be stable in real BL, whose pH is ≥12. This was confirmed with real BL (data not shown). MFI also did not survive past pH 12.2 (Figure 27) and was rejected as a possible membrane candidate. The SAPO material was the unstable even under pH 8.5 (Figure 28) and was also eliminated as a membrane possibility. It is known that some zeolites become unstable at sufficiently high pHs, losing their crystalline structures.[134, 135] This is likely because the silicate/aluminosilicate/silicoaluminophosphate frameworks are susceptible to base-catalyzed hydrolysis at high pHs, although the explicit tests were required in order to determine whether this degradation mechanism occurred specifically at the pH levels relevant to BL streams for the three zeolites tested.

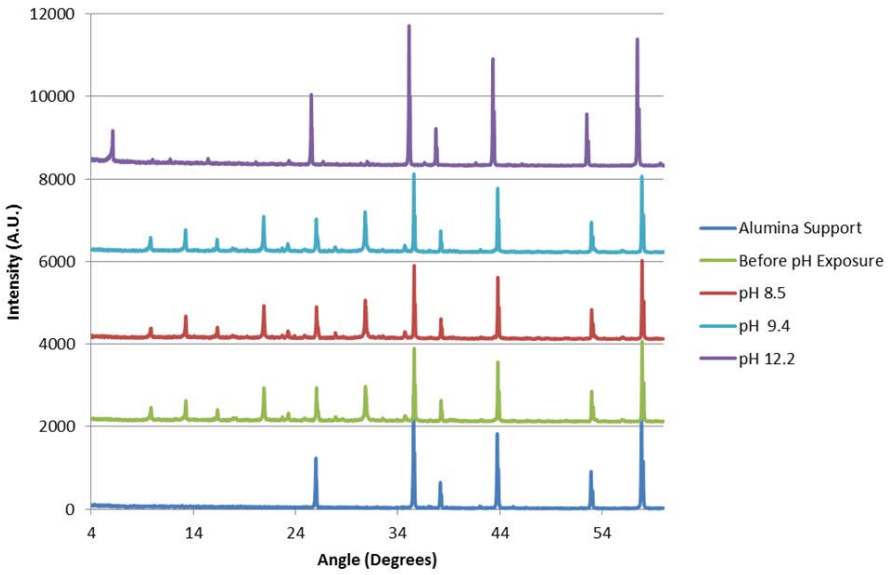

Figure 26: XRD patterns of zeolite FAU before and after exposure to model BL at different adjusted pHs. The XRD pattern of the α-alumina support is also shown in order to identify the peaks from the alumina support which are also seen in the membrane samples.

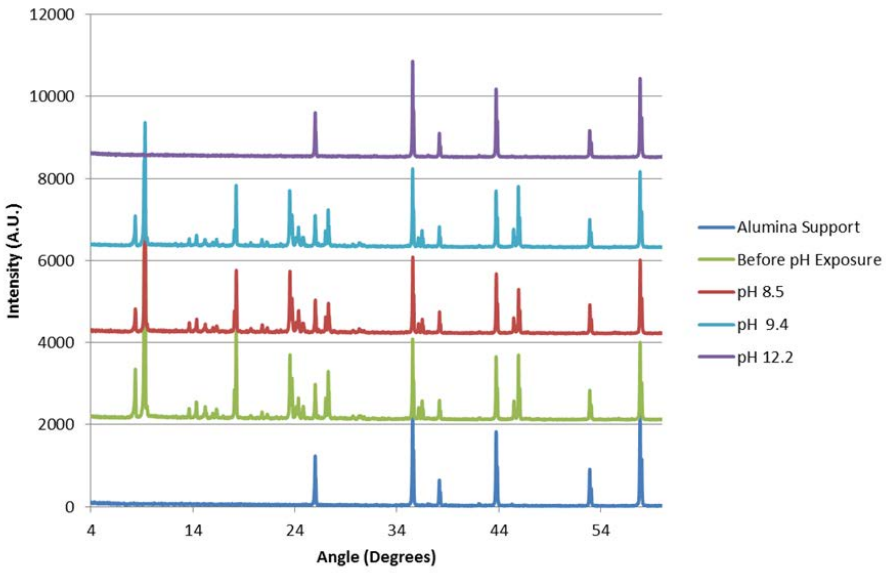

Figure 27: XRD patterns of zeolite MFI before and after exposure to model BL at different adjusted pHs. The XRD pattern of the α-alumina support is also shown in order to identify the peaks from the alumina support which are also seen in the membrane samples.

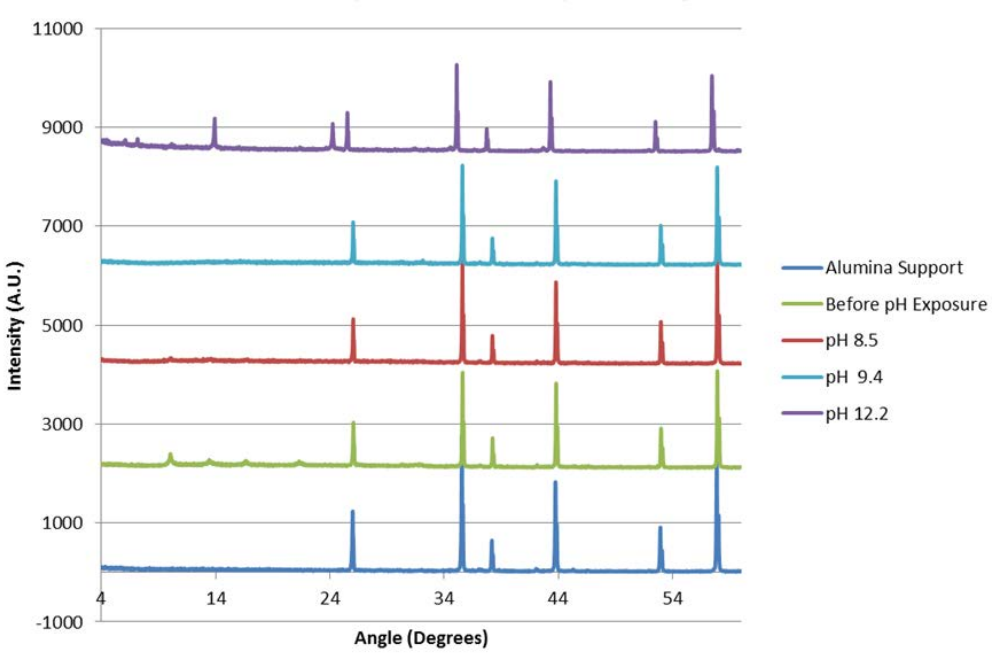

Figure 28: XRD patterns of zeolite SAPO before and after exposure to model BL at different adjusted pHs. The XRD pattern of the α-alumina support is also shown in order to identify the peaks from the alumina support which are also seen in the membrane samples

On the other hand, CMS proved stable in both model and real BL, as shown in Figure 29 below before and after exposure to real BL. The CMS sample shows the broad XRD pattern characteristic of its amorphous structure based upon "turbostratic" arrangement of graphitic layers.[108] From this point on, CMS membranes were chosen for further development.

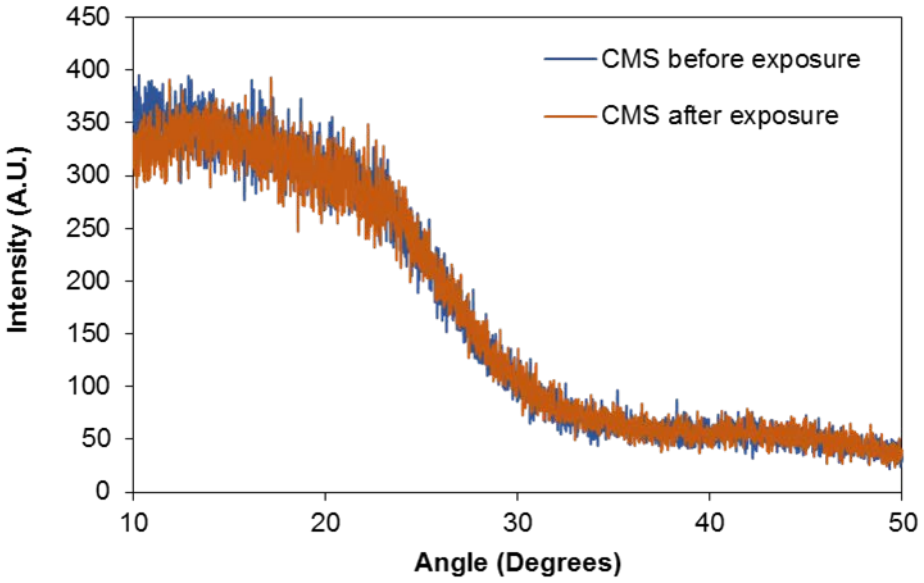

Figure 29: XRD of CMS (750 °C vacuum pyrolysis) before and after real BL exposure. Courtesy of Dr. Sharma

3.2 Investigation of membrane processing parameters

3.2.1 Disc polishing

As mentioned Chapter 2, the smoothness of the support significantly affects the quality of subsequent membrane coats. Consequently, the CoorsTek α-alumina discs were polished prior to use to ensure a smooth coating surface. Sample SEM images of the polished support is shown in Figures 30-31. The polished surface is much smoother and does not contain bumps that could negatively affect polymer coating.

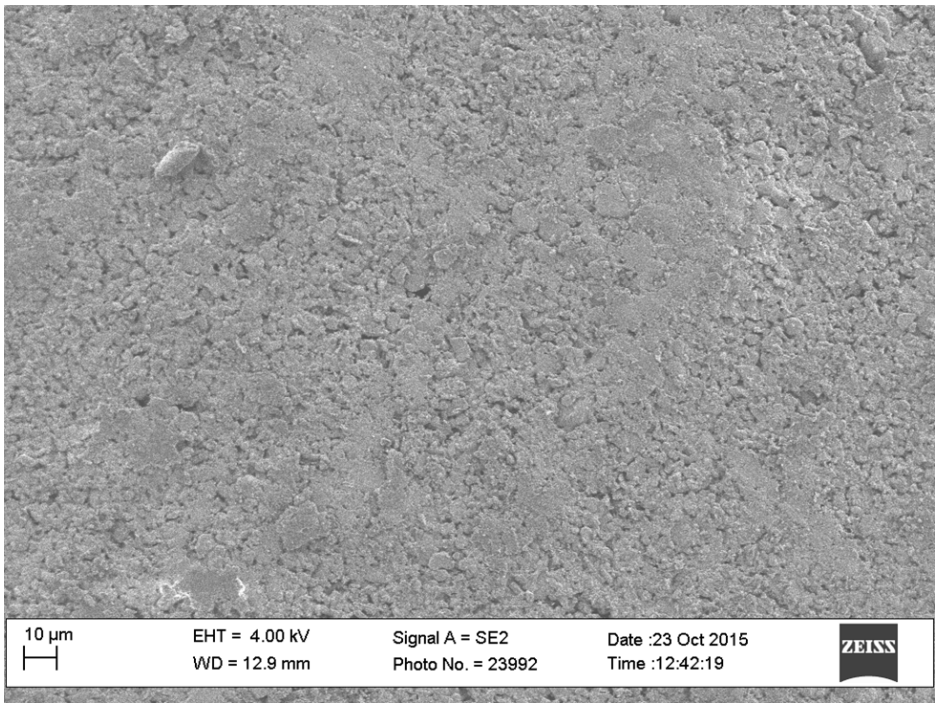

Figure 30: Top surface of non-polished CoorsTek alumina disc

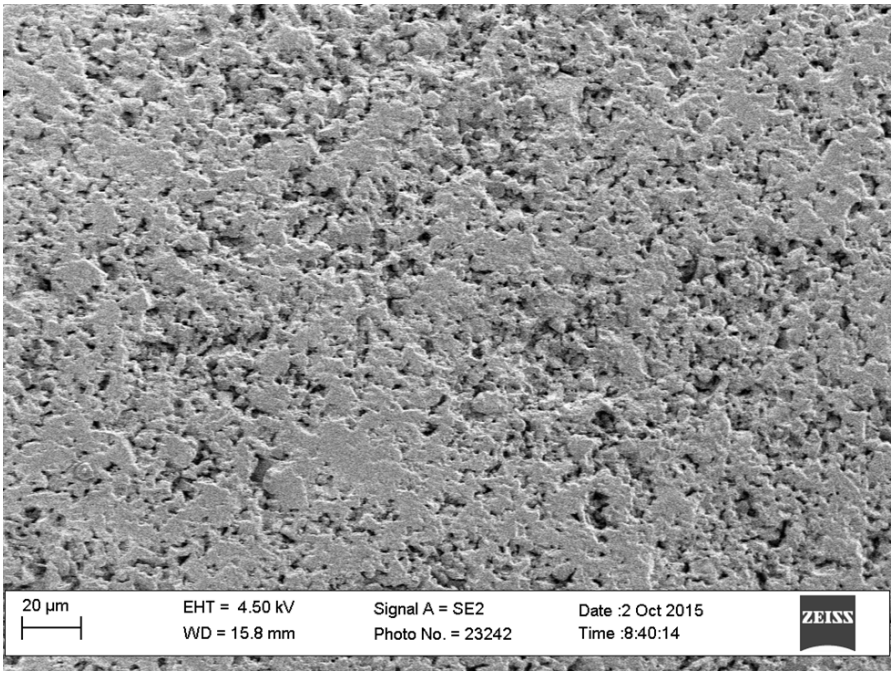

Figure 31: Top surface of polished CoorsTek alumina disc

Figure 32 shows the pore size distribution of the polished CoorsTek alumina disc from Hg porosimetery data. Most of the pores are approximately 0.43 μm in diameter, though a small portion of pores are 5-9 μm in diameter.

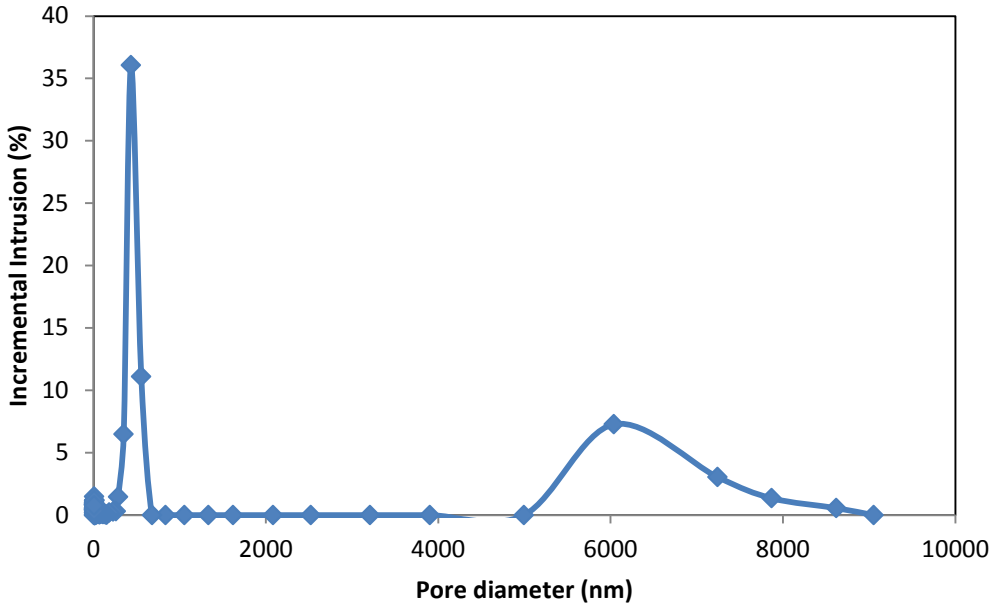

Figure 32: Pore size distribution of polished CoorsTek alumina disc

3.2.2 Dip and spin-coating Matrimid

As mentioned in Chapter 2, the spin-coating settings were initially varied to determine an optimum coat. Again, the formulations were:

5. 1200 RPM, 1 minute, 6 wt.%,
6. 1200 RPM, 30 seconds, 12 wt.%
7. 900 RPM, 30 seconds, 12 wt.%
8. 900 RPM, 1 minute, 12 wt.%

As seen in Figure 33, 6 wt.% was too dilute and (3)-(4) had somewhat lower-quality coats compared to (2). Thus, formulation (2) was used for the remainder of this work, unless otherwise noted.

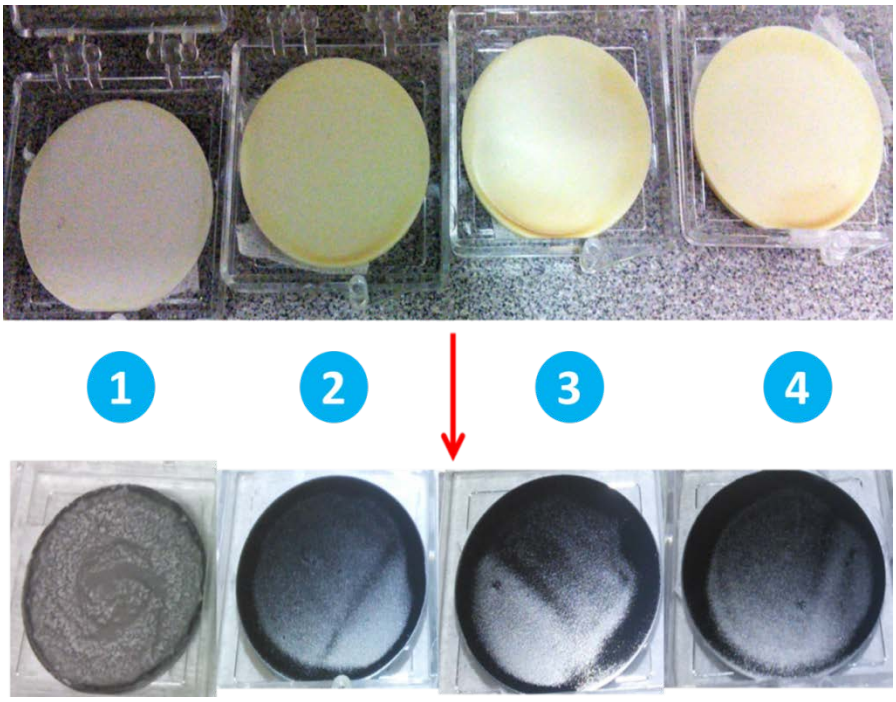

Figure 33: Initial Spin-Coating Results Using different Formulations

3.2.3 Drying Matrimid

Drying the Matrimid film by Protocol 1 led to a highly defective membrane. The resultant Matrimid film had a large number of holes visible to the naked eye (Figure 34). Optical microscope observation (e.g. Figure 35) showed that these holes were mostly 10-25 µm in diameter, with a few smaller holes (4 µm) also visible as well (more precise analysis was not done since the actual size of the pin-holes was not important; what was

important if there were holes or not). A second coat was also applied, but it did not fill these defects.

Figure 34: Matrimid Coat after Protocol 1 Drying; image contrast/brightness slightly adjusted to make the larger pinholes easier to see

Figure 35: Optical image of one of the holes

It should be noted that pin-hole defects transferred to the pyrolyzed CMS membranes, as seen in Figure 36 below. These pin-holes (12-35 μm) explain why the rejections of lignin by the initial CMS membrane discs were almost the same as that of bare alumina supports.

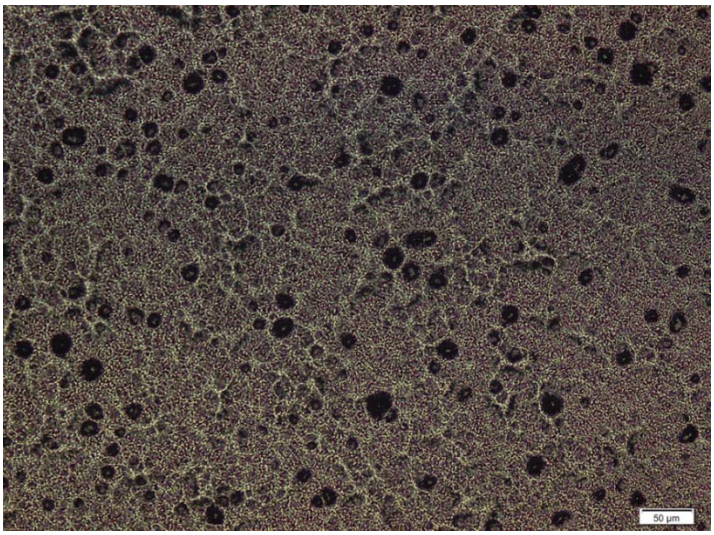

Figure 36: Pinholes in a CMS sample, from optical microscope

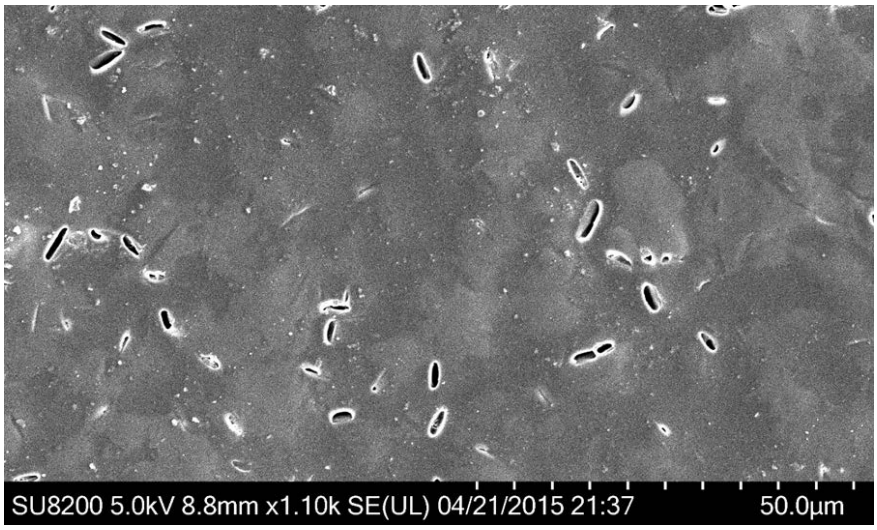

Figure 37: Pin-Holes Visible in SEM: (courtesy of Dr. Rashidi)

When drying by Protocol 2, it was observed that the top solvent layer quickly evaporated in air post spin-coating. Upon the application of vacuum, the sample again looked wet for a few minutes until the vacuum pulled out additional solvent from the Matrimid coat. Again, pin-holes were detected, likely from the rapid removal of the solvent by the vacuum. Even when both eye and optical microscope examination showed no pin-holes, they were still visible under SEM, as shown in Figure 37. The drying protocol was thus improved in Protocol 3 by first preheating the sample in air to more slowly and gently remove NMP and only then applying vacuum to assist in the removal of any remaining solvent still trapped in the Matrimid coat. Protocol 3 finally yielded Matrimid and CMS coats that had no visible pin-holes, even under SEM, as shown in Figure 38.

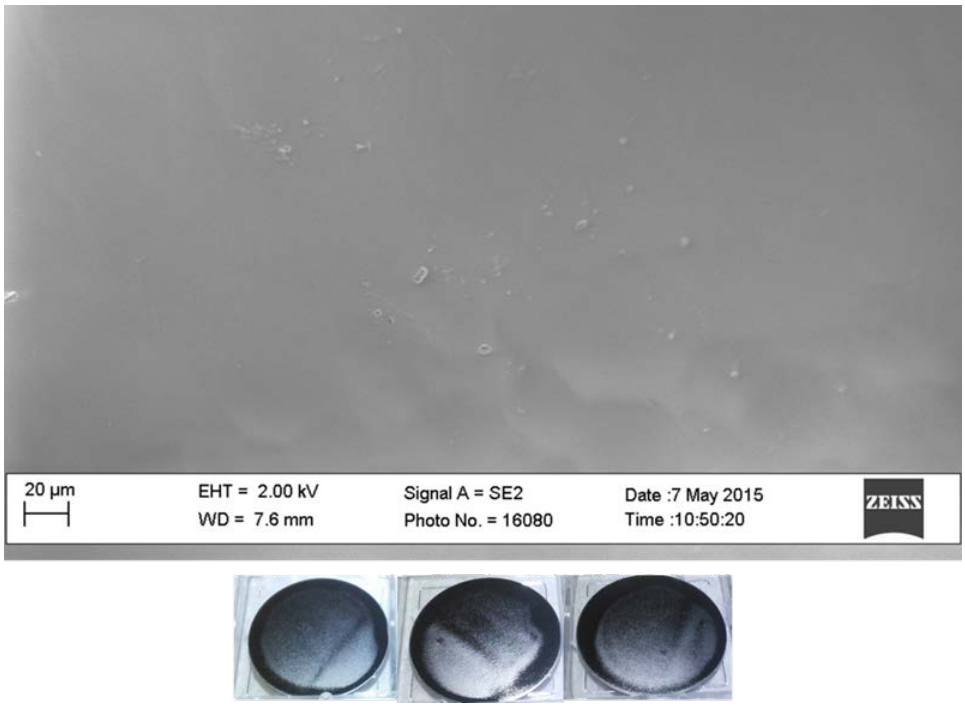

Figure 38: Top: SEM image of top surface of pinhole-free CMS membrane; Bottom: Photographs of defect-free membranes.

3.2.4 Polymer Infiltration and PEG/Isooctane filler

When discs were coated with Matrimid without a PEG layer, the samples were almost impermeable to N_2 and CO_2, suggesting infiltration of the polymer into the support pores, as confirmed by Figure 39 wherein ~30 µm of penetration is visible.

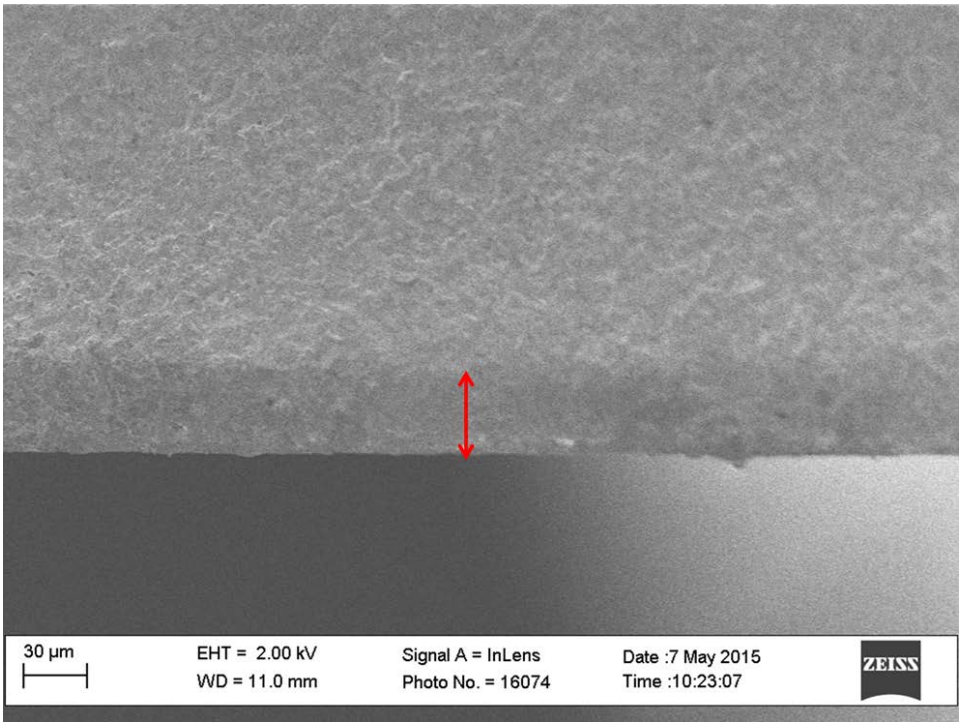

Figure 39: SEM Showing Infilration of Matrimid-based CMS into Alumina Disc

To reduce or eliminate infiltration of Matrimid polymer, PEG was dip-coated onto supports and then the Matrimid coating was applied, dried, and pyrolyzed. Initial pyrolysis temperature was 750 ° C, as in the reference paper.[111] However, both gas and water permeation showed that the discs were virtually impermeable. In the case of water, the discs broke prior to achieving any flux. To increase permeability, the pyrolysis temperature was lowered to 525 °C (just above the PEG decomposition temperature from

the reference paper[111]), since lower temperatures lead to larger pore sizes and thus larger permeabilities.[107, 108] However, this was not found to be effective.

Compared to literature values, even with drying Protocol 3 (i.e. no visible defects under SEM), the permeabilities of both Matrimid and CMSs were orders of magnitude lower than that reported in the literature under similar temperature and atmosphere conditions. For example, one paper reported a CO_2 permeability of ~1210 Barrer for Matrimid pyrolyzed under vacuum at 550 °C and 43.6 Barrer from pyrolysis at 800 °C.[110] In comparison, initial Matrimid-based CMSs were virtually impermeable. Sample permeabilities are shown in Figure 43 later, where the best coatings (at even the lower pyrolysis temperature of 525 °C) were less than 1 Barrer. Even taking into account differences in permeability that might occur because the pyrolysis may occur a bit differently in pores than in thin films, this difference alone is not enough to explain the orders of magnitude in permeability difference. It was later shown that even PEG itself was not decomposed like it should have been but pyrolyzed and yielded a virtually impermeable film.

In addition to the virtual impermeability of PEG-coated samples, PEG also adversely affected the Matrimid coating. If the PEG coating was too thick (or, in the case of the poor reproducibility of the hand-dip-coating method, uneven coats), then the Matrimid film shrank and even delaminated. Attempts to spin-coat PEG were done to minimize this, but some samples were still prone to this shrinking and/or delamination. Figures 40-41 below show examples of shrinkage and delamination of Matrmid on a PEG-coated sample from unfavorable interaction between the two polymers (Sample 1 was better but from other work, did not yield sufficient CMS coverage). Note that by

chance, a small portion of the samples could have just enough PEG to achieve a good coat (though permeability was still not improved)

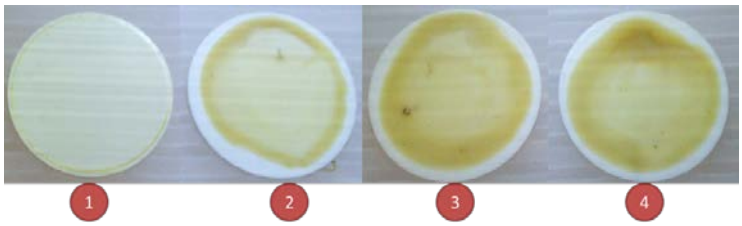

Figure 40: Matrimid shrinkage on Polymer Coats

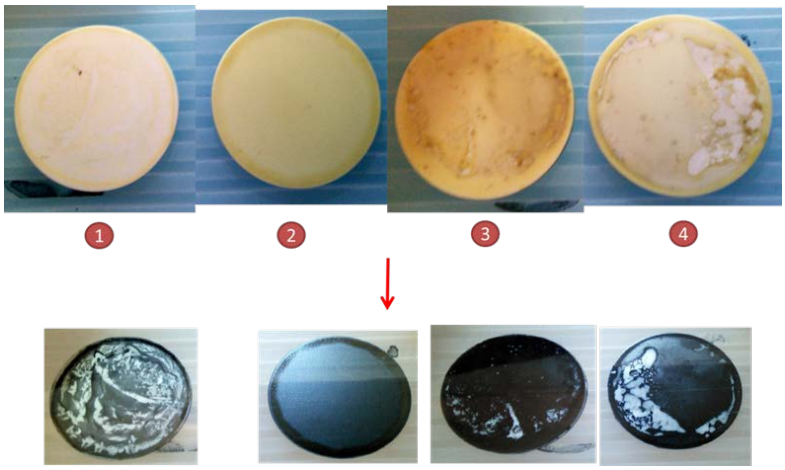

Figure 41: Example of shrinkage and delamination on PEG-coated supports

Where

1. 6 wt.%, 1200 RPM, 1 minute
2. 12 wt.%, 1200 RPM, 30 seconds
3. 12 wt.%, 900 RPM, 30 seconds
4. 12 wt.%, 900 RPM, 1 minute

Figure 42 shows an SEM of a PEG-coated disc. As can be seen, the layer is ~2 µm thick.

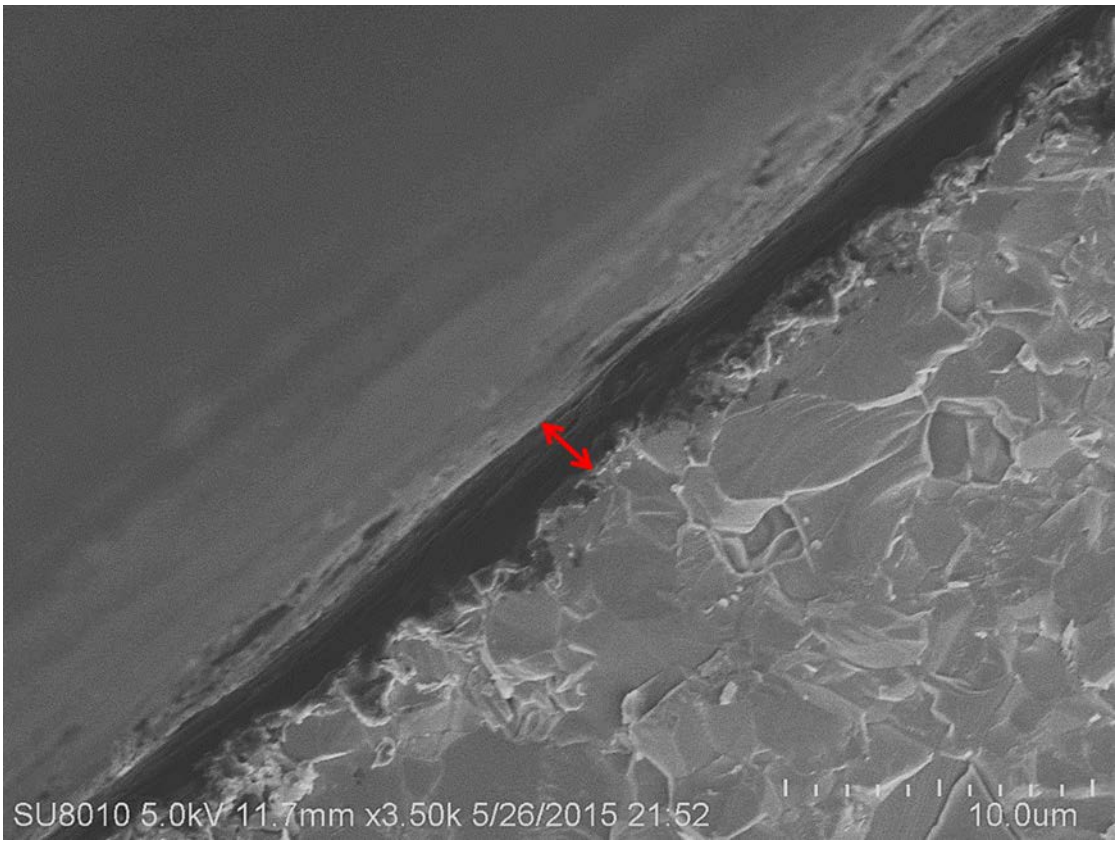

Figure 42: SEM of a PEG-coated disc. Courtesy of Dr. Rashidi

Since a recent paper[111] had reported successful removal of PEG and achieved permeable CMS films, it was surprising that similar results were not observed here. The CO_2 permeation at RT was compared to a blank alumina disc (5.7 x10^6 Barrer), on PEG-coated alumina disc (before and after pyrolysis), along with a CMS on an alumina disc (no PEG) and the best selective (least-defective) CMS sample obtained using a PEG intermediate layer on an alumina support (Figure 43. As shown, PEG exposed to

pyrolysis conditions did not significantly decompose (i.e. the permeability of the blank alumina disc was not restored) and was comparable to the results of directly coating a CMS membrane (which had significant infiltration, as discussed previously). Even the best-selective (least-defective) CMS sample (selectivity of 7.1) still had a permeability under 1 Barrer. Since PEG was soluble in MeOH, a sample was also soaked in MeOH for up to 6 hours but it failed to wash out any PEG. Filling the pores with isooctane (which would evaporate prior to NMP) was tried next, but results were not improved.

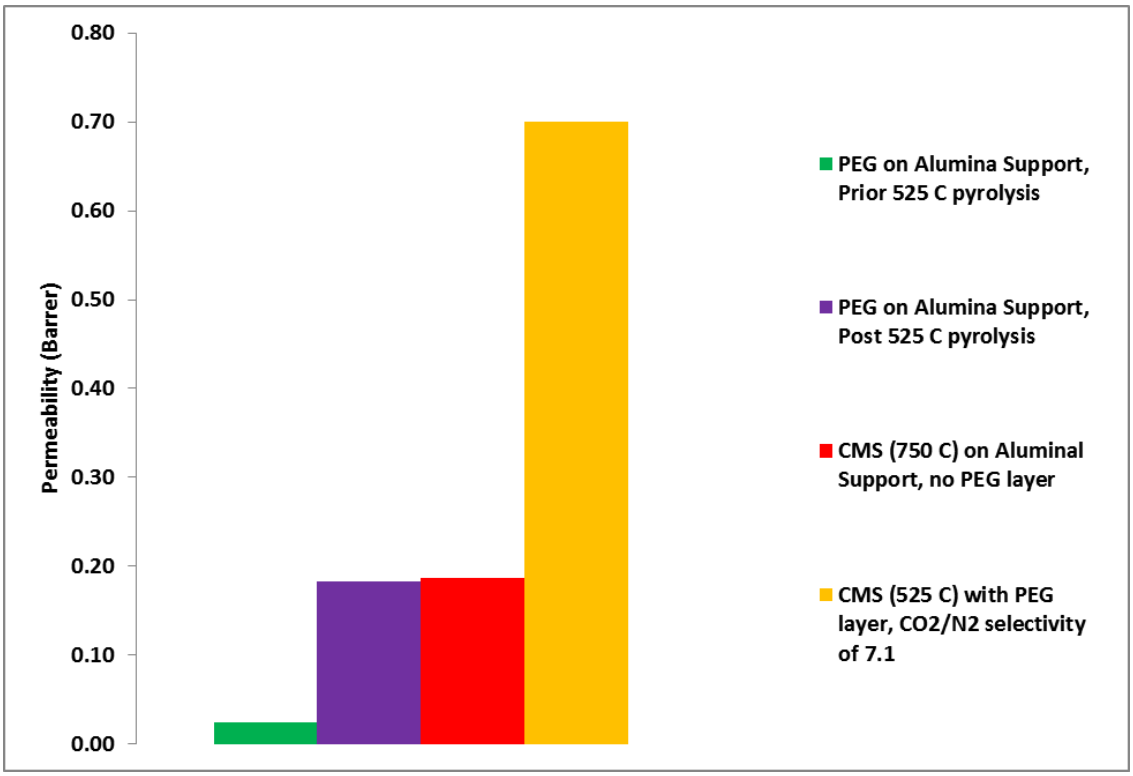

Figure 43: CO_2 Permeability at RT of PEG and CMS with PEG layer on Alumina Supports

Since temporary fillers were not successful and the polymer film infiltrated the support pores, the next strategy was to add aluminum oxide layers on top of the existing

supports (or making in-house support) that had smaller pores, eliminating or minimizing Matrimid infiltration.

3.2.5 Alumina coating

Figure 44 shows the cross-section of a US-sample from the 1st protocol having a thin coat of ~11.5 μm. The coating was too rough for CMS (later section), but was otherwise good, though the pore sizes were still too large, as seen by the lower rejections in Table 7 when compared to the results from the same particle size in protocol 2 and a pressed disc.

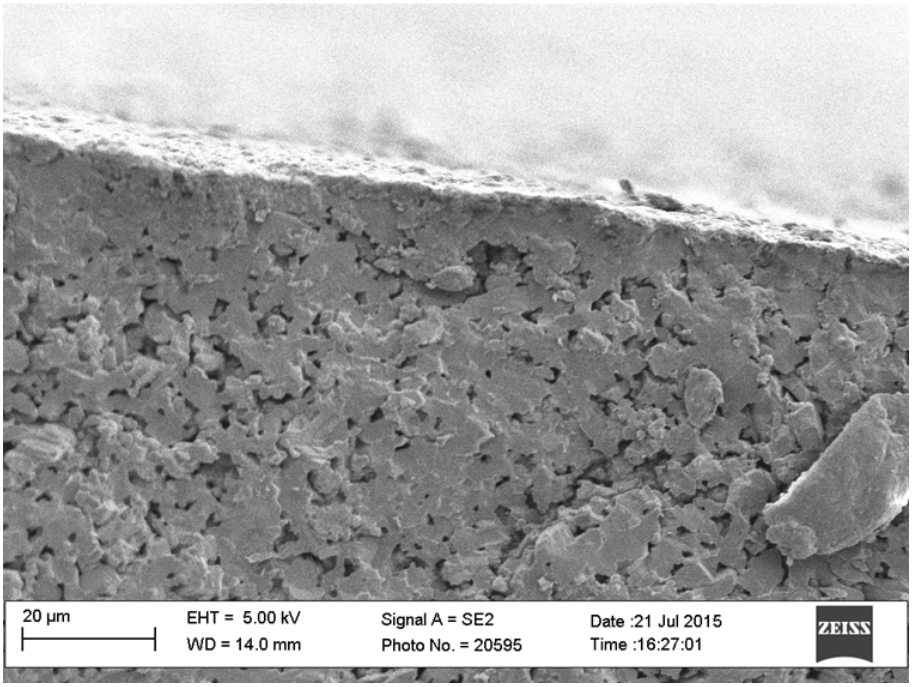

Figure 44: SEM Cross-section of the US batch from Protocol 1

The BL filtration (0.03 wt.%, RT) results are shown in Table 7. Included in the table is the 0.25 μm pressed sample for comparison (i.e. a defect-free 0.25 μm coat should be comparable to the pressed sample, accounting for some variation). Since some of the inorganics, particularly the sodium ions, are associated with lignin at such high pHs,[27] most of the inorganic rejections here are likely those bound to lignin, since the conductivity measurement cannot distinguish between bound and free species. At higher lignin rejections (e.g. NF range of 70-90%), most of the free species would pass through and the difference between the inorganic and lignin rejections should be significant. All of the rejections mentioned here (unless otherwise noted) are observed rejections. Note that there is some variability due to insufficient samples for testing (the initial strategy was to use these ball-park rejections to optimize both a good ceramic coating as a NF pre-filter as well as to use that good coating as a support for the CMS coating. Replicates on those discs was planned in order to obtain an average rejection value with is standard deviation).

Given the SEM images of the 2nd Protocol (Figures 45-46), the 0.25 μm coat (batch 2A) seemed to have incomplete surface coverage, yet surprisingly provided rejections were still comparable to that of the pressed disc. The 5.8 nm coat (batch 2B) had low rejections, likely due to not enough particles on the top surface to achieve desired pore sizes of the low concentration of the coating as well as the large pore sizes of the support (i.e. many particles were lost due to infiltration).

Also in Table 7 are the rejection data from Protocol 3 samples and the results of higher (40 wt.%) 5.8 nm particle coat and that of gamma-alumina. The 5.8 nm coat achieved lower rejection than even the best 0.25 μm coat, suggesting that the 0.25 μm

coating was not successful and that the coating method is not yet reproducible. Further work would focus on improving the reproducibility of first the 0.25 µm particle coat and then the 5.8 nm particle coat, with attention on well-dispersed samples at high-enough concentrations. Both gamma-alumina coats achieved the same lignin rejection of 60 %, likely again due to the poor coating results of alpha-alumina layers. Increases in lignin rejection may be achieved by lowering the sintering temperature to yield smaller pore sizes.

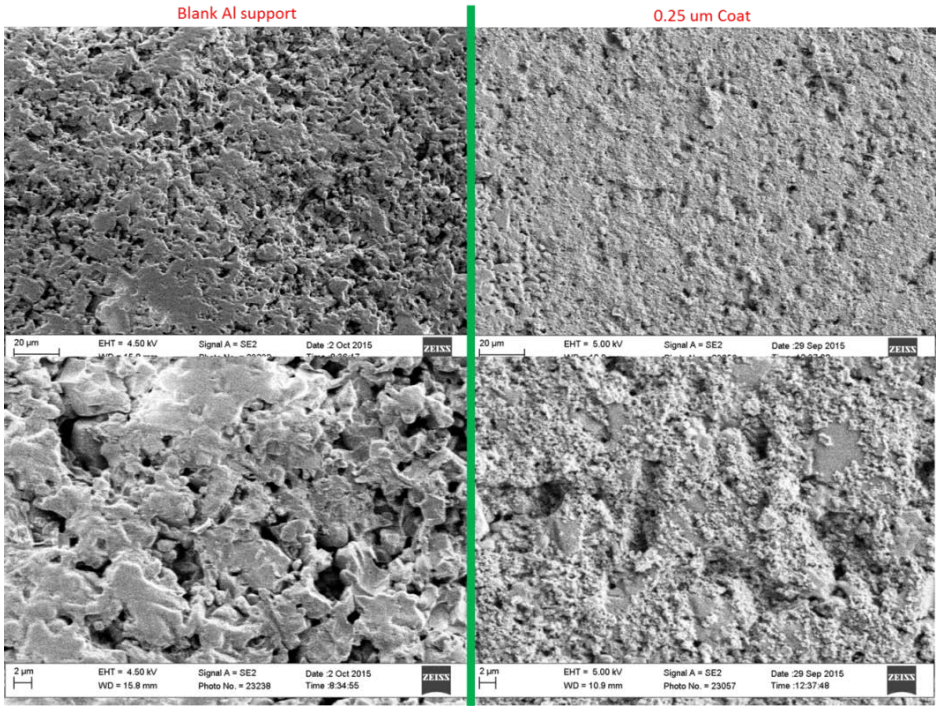

Figure 45: SEM of Batch 2A compared to a blank, polished alumina support

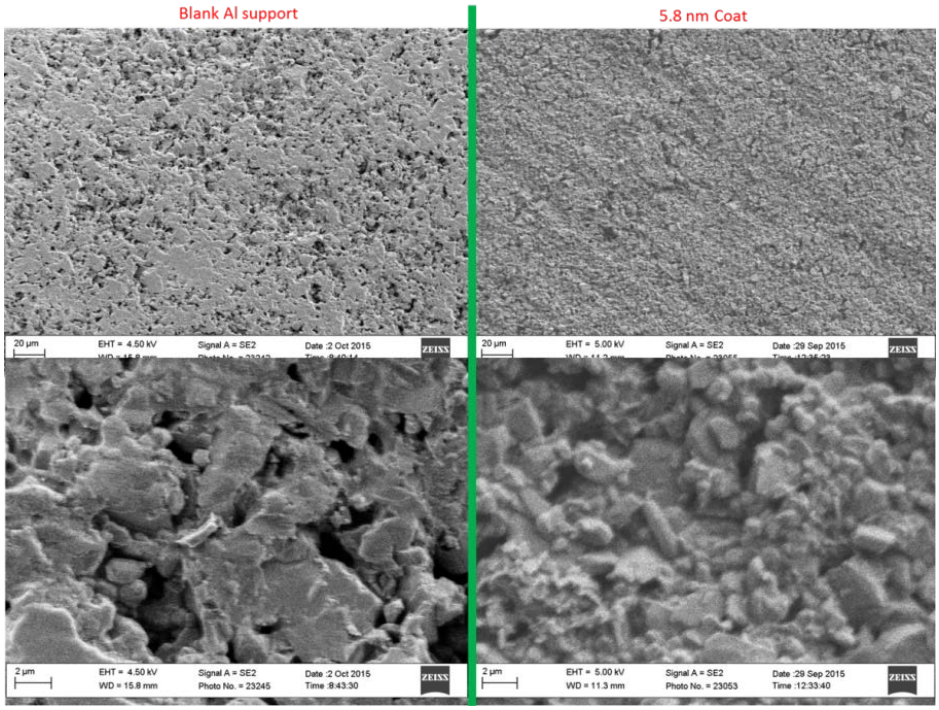

Figure 46: SEM of Batch 2B compared to a blank, polished alumina support

Table 7: Lignin and Inorganics Rejections for different alumina coats/samples and their estimated pore sizes

Sample	Inorganics Rejection (%)	Lignin Rejection (%)
Al blank	4-6	3-9
1st batch 0.25 µm coat	6	16
2nd batch 0.25 µm coat (pH 5.3) (batch 2A)	30	40
0.25 µm pressed	40	35
"2nd batch" 5.8 nm coat (pH 5.3) (batch 2B)	15	18
3rd batch: 1 wt.% 0.25 µm coat, then 8 wt.% 5.8 nm coat	8	5
3rd batch: 3 wt.% 0.25 µm coat, then 8 wt.% 5.8 nm coat	36	-
1 wt.% 0.25 µm, then 2x 5.8 nm coats	9	16
3 wt.% 0.25 µm, then 2x 5.8 nm coats	10	20
40 wt.% 5.8 nm coat on 3 wt% 0.25 µm	11	16
γ-Alumina on Polished Support	-	60
γ-Alumina on 40 wt.% 5.8 nm coated 3 wt.% 0.25 µm coat	-	60

The support layers were thin and their pore size could not be estimated using Hg porosimetery. Instead, ImageJ was used to estimate the pore size. Note that these estimates are likely larger than the actual pore size. For example, though Hg porosimetry for the bare support showed that most of the pores were ~0.4 µm, ImageJ analysis

estimated an average pore size of 1.2 μm. Thus, while the ImageJ estimates cannot be used quantitatively, they provide a qualitative comparisons. For example, though Image J estimated the alumina support's pore size at 1.2 μm, the estimates for the 0.25 μm particle pressed disc was the 0.2 μm pore diameter, an order of magnitude less. This reasonable since such a pore size is in the general range of the trends observed by Benito et. al. for such particle sizes.[119] Note that cross-section images should yield better results in ImageJ, but the coated layers were very thin and difficult to distinguish in SEM. Thus, top-surfaces were used for the majority of these pore estimates.

In a collaboration Dr. Rashidi, 2x Matrimid (6 wt.% in NMP) dip-coating was performed on the 0.25 μm coated commercial bare alumina support. Figure 47 shows the ~ 1.5 μm thick (excluding infiltration) CMS layer on top of the ~1.5 μm thick 0.25 μm particle coat (the white dots in the CMS layer-there was still some infiltration) on top of the alumina support. The top surface roughness is likely from the dip-coated 0.25 μm particles (that surface couldn't be polished). This sample was still defective (no CO_2/N_2 gas selectivity), but its lignin rejection was at 68%. This result is very important. Prior to this point, even though SEM images showed that the CMSs were defective and the gas selectivity was still ~1 (i.e. the quality of the membranes was not better than this one on the 0.25 μm coating), liquid filtration was not successful (discs cracked prior to first water flux, even at pressures as high as 70 bars). Thus, the coatings on commercial supports were too dense/had significant infiltration such that the CMSs broke before water could pass through the defects and the pores. Here, the even with some infiltration into the 0.25 μm layer, the CMS itself was less dense such that water could actually permeate through. Clearly, this is permeation is due to defects (else there would be gas

selectivity and nearly perfect lignin rejection), but it is an encouraging sign. If (a) the coating could be improved and (b) the CMS defects overcome (and likely pore-sizes made larger by sacrificial nanoparticles), then CMSs were promising. In the scope of this work, there was not ample time to improve the CMS pore size and remaining defects, but work was undertaken to improve the alumina coatings to provide better supports for the future, non-defective CMSs. Initial attempts at spin-coating Matrimid onto the 0.25 µm coating and pyrolyzing was unsuccessful; samples delaminated. This further indicated that the coating procedure of the alumina layers had to be improved in order to make further CMS coatings/studies worthwhile.

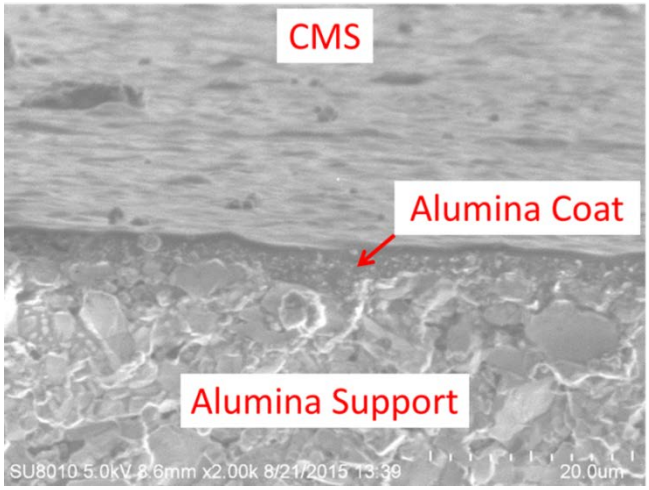

Figure 47: Dip-coated CMS layer on top of the 0.25 µm coat on commercial alumina support, courtesy of Dr. Rashidi.

The BL rejection data was based on 0.03 wt.% BL (which was diluted to this concentration to allow reliable quantification of the rejection and flux without significant influence of concentration polarization and fouling in the non-stirred dead-end cell). Figure 48 below shows the lignin rejection compared to that of a blank alumina and a

0.25 µm coated alumina disc (note: later 0.25 µm coatings could achieve as high as 40% lignin rejections, but could not do better because of the large pore sizes. The CMS was clearly a significant improvement).

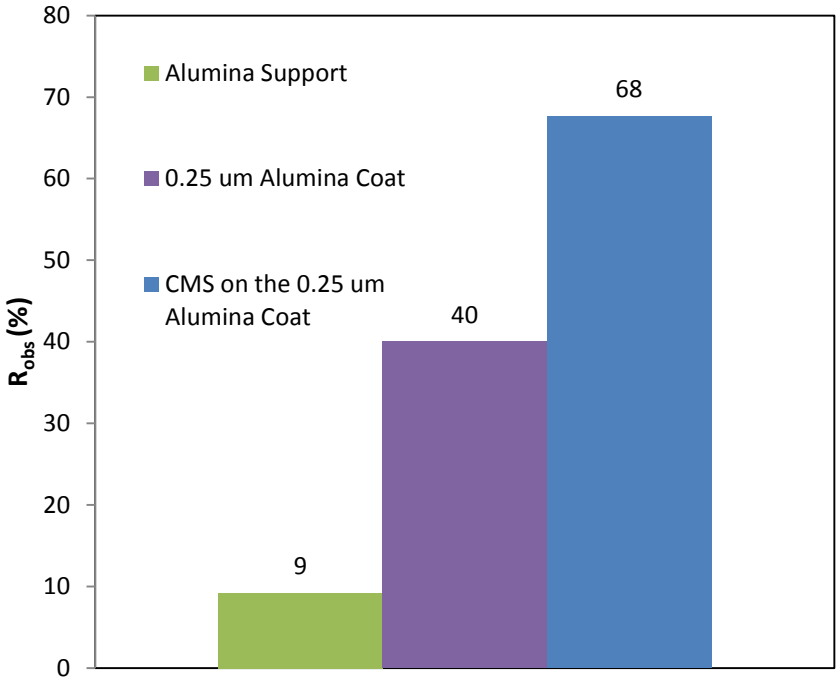

Figure 48: Lignin rejections for bare and modified commercial α-alumina supports.

3.2.6 In-house alumina pressed discs

During initial pressing tests, many discs broke either during pressing or upon contact after firing. This was eventually fixed by using Method ConC (but no water) and a firing temperature of 1300 °C. The lignin and rejection data for the only successfully pressed disc is shown in Table 7 in the previous section (this was for a disc pressed by our former group member). Further pressing at smaller particle sizes was not considered due to the lower flux at the ~0.2 µm pore size (future work could have used a larger

particle size to press the main support following by coating of finer layers). This layer was very smooth and had small pore sizes and performed well when coated with CMS (results will be discussed in the CMS section). As seen in the CMS section, the coated CMS, though of good uniformity and quality as observed in SEM, still did not have the expected rejection characteristics. Otherwise, this is a good support (superior in quality to the CoorsTek commercial discs), but further work was not pursued due to time limitations for the MS thesis (i.e. insufficient time to work out the CMS kinks and make modifications to increase its pore size for good fluid flow). The intermediate strategy was then to coat alumina oxide layers (prior section), but this did not require pressing in-house supports as commercial supports were readily available.

The discs pressed from the 0.25 μm alumina powder were very fragile and only one disc survived (i.e. did not crack at some point along the process) to be spin-coated with Matrmid and pyrolyzed (discussion in the CMS section). However, a pressed disc with the same powder was available from a prior group member 0.03 wt.% BL was filtered through it, achieving 40% inorganics rejection and 35% lignin rejection. These results are useful because they provide the upper bound performance of the 0.25 μm coat (i.e. if my thin layers were good and thick enough, they could not do any better than the 1-3 mm thick pressed dics of the same powder. There is some variability in the data and it is surprising that the inorganic rejections are slightly higher than the lignin and so high. Since conductivity was used as a quick way to measure the overall inorganic content, it is possible that much of the inorganic content that was here rejected was associated with the lignin itself (hence the comparable numbers, given some slight variance). Once current

downside is that the discs are not mechanically strong enough for filtration (i.e. discs may at best survive only one run at the lowest pressures needed to obtain permeation).

Future work would focus on adding binders and increasing the firing temperature to yield stronger discs capable of acting as better supports for CMS coatings. Since pores and porosity decreases at higher firing temperature, a larger alumina particle size may need to be used to improve the performance of the base supports, and then further alumina coatings (with smaller pore sizes) may be required to act as good prefilters and to prevent infiltration of the Matrimid/CMS coat.

3.2.7 CMS pyrolysis results

Initial pyrolysis work was performed by my former colleague, Dr. Ketki Sharma. She was able to obtain dip-coated CMS layers ~9 μm thick (as shown in Figure 49) on commercial CoorsTek α-alumina supports. However, dip-coating suffered from major cracking during pyrolysis and samples were defective (the drying of Matrimid was not yet optimized at this point). In my work, I pursued spin-coating CMS membranes onto the CoorsTek supports, which were thin-enough not to crack during pyrolysis.

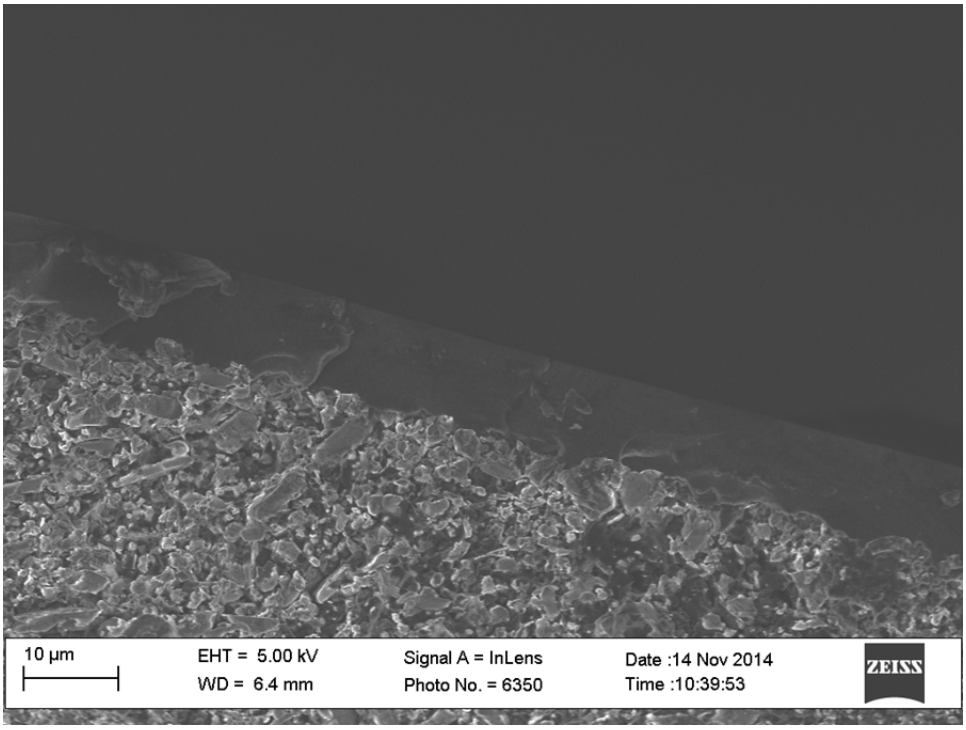

Figure 49: Example of an early dip-coated CMS layer, courtesy of Dr. Ketki Sharma

The early work was with hand-dip coated or even spin-coated PEG. The thickness and uniformity of these layers were highly variable. On occasion, clear layers were seen between the Matrimid and PEG layers, as shown in Figure 50. In Figure 50, the top layer (lighter color) is spin-coated Matrimid (~2 µm thick) and the bottom layer (darker color) is PEG (~1-2 µm thick). As discussed earlier, it was later learned that PEG was not removed prior to pyrolysis but pyrolyzed. This made it impossible to distinguish in SEM the CMS and PEG layers, since both polymers had been carbonized and looked similar.

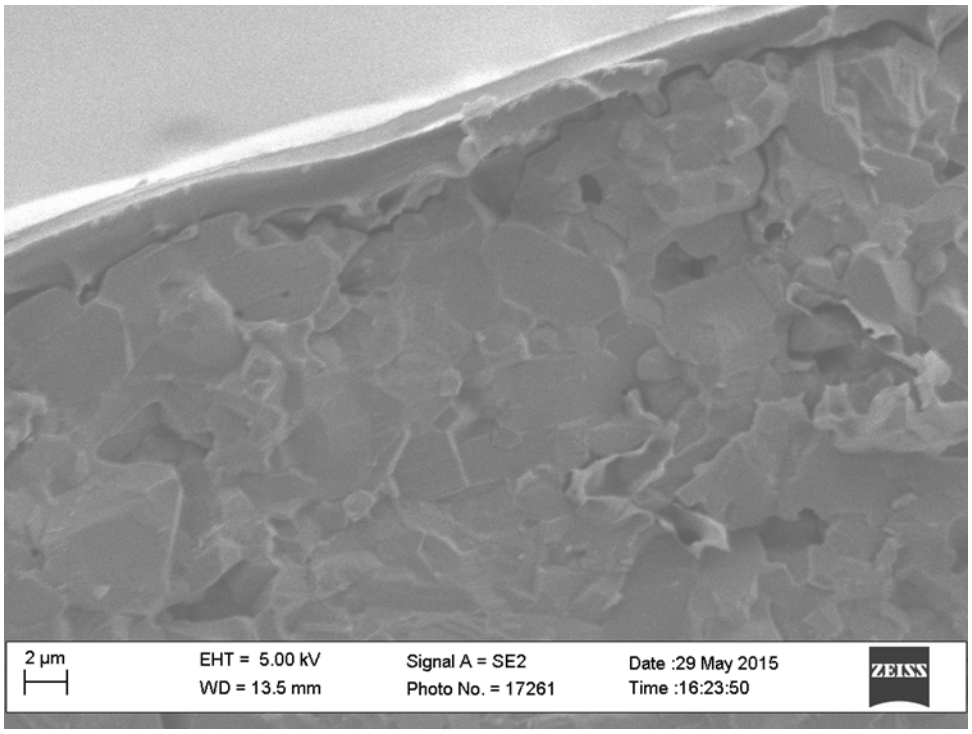

Figure 50: SEM Cross-section of Matrimid, PEG layers

Figure 51 is an example of a defect-free CMS cross-section (spin-coated) after the Matrimid drying was optimized. Here, there was enough PEG coating to prevent infiltration (some samples were significantly infiltrated into the alumina supports and had no distinguishable surface layer). With some confounding due to part of the layer being pyrolyzed PEG, the CMS layer was approximately 1 µm thick.

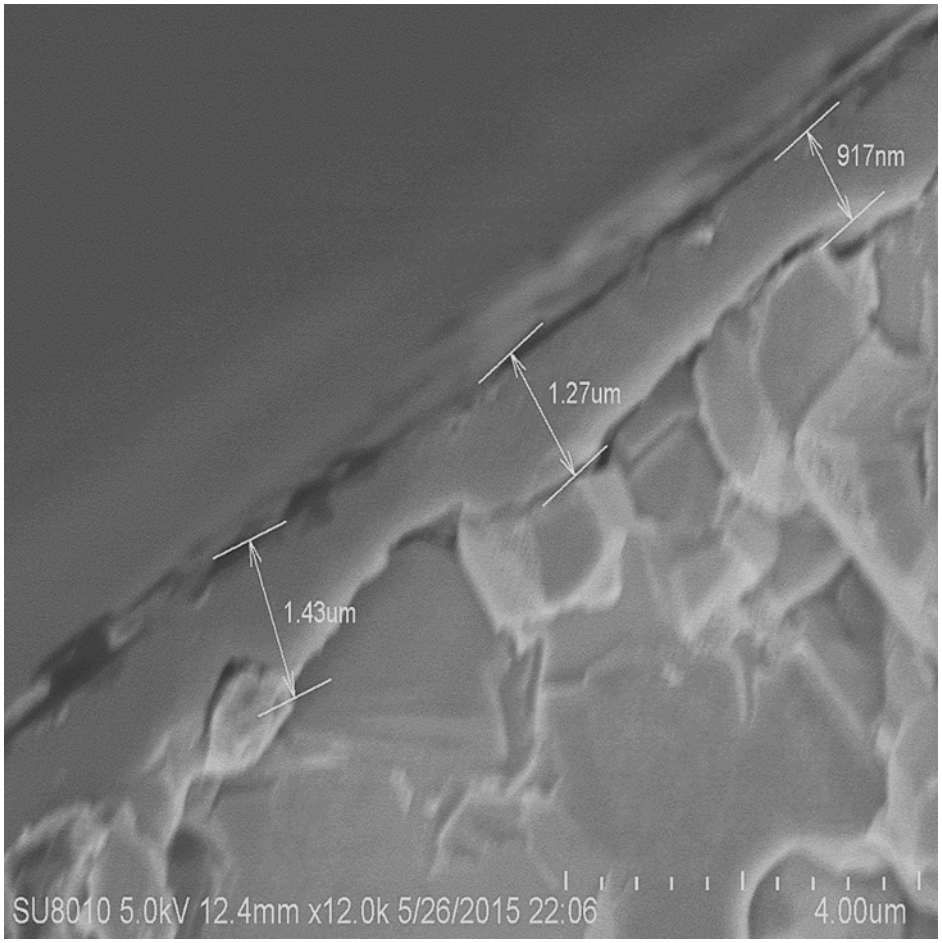

Figure 51: SEM Cross-section of a successful CMS spin-coating. Courtesy of Dr. Fereshteh Rashidi.

The discs pressed from the 0.25 μm alumina powder were very fragile and only one disc survived (i.e. did not crack at some point along the process) to be spin-coated with Matrmid and pyrolyzed. It was not selective for gas permeation (i.e. was defective), but the coating was very shiny. However, broke upon liquid filtration testing due to its smaller size (because of shrinkage) and mechanical weakness. Another CMS sample was coated on a 0.25 μm alumina coat and its lignin rejection was 63%, comparable to the result obtained from a CMS coat on a pressed disc.

No gas permeability data was available for the CMS with the 68% rejection, but a further analysis on a different CMS sample that was also coated a 0.25 μm particle pressed disc shows that the coating surface does play a role. This is seen in Table 8 and Figure 52 below.

Table 8: Gas permeation data on pressed or coated alumina discs

Sample	Gas Permeability (Barrer) (525 °C)	Lignin Rejection (%)	Selectivity	Knudsen Selectivity
CMS on 0.25 μm press, N_2	1227	NA/, but likely >63%	1.63	1.25
CMS on 0.25 μm press, CO_2	2167			
CMS on 0.25 μm particle coat, N_2	3813	63	1.56	1.25
CMS on 0.25 μm particle coat, CO_2	6921			

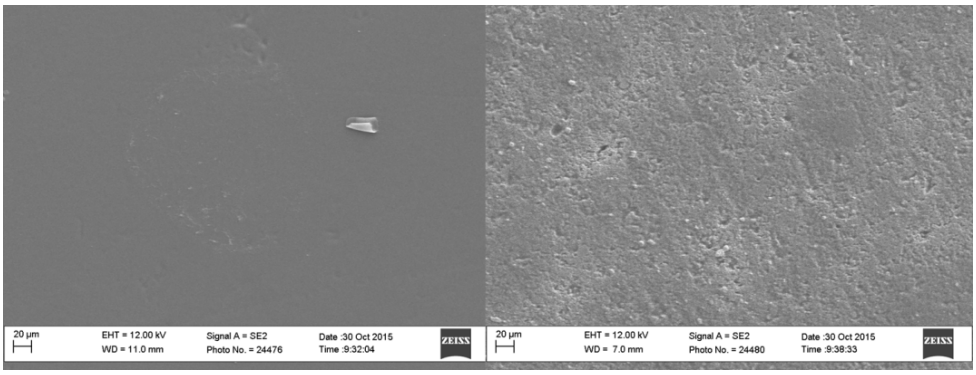

Figure 52: SEM images of CMS on 0.25 µm pressed disc (Left) and on 0.25 µm coat (Right)

As seen from the data, the CMS quality was better on the pressed-disc (which had a smoother surface), resulting in less defects, which was confirmed by the low gas permeation values. Since they are still higher than those in the literature, there are still some defects, but most of these defects are likely less than 20 nm (N_2 free mean path) since the selectivities are slightly above the Knudsen selectivities.

Clearly, further work is needed to both improve the ceramic coats as well as to identify and fix the remaining CMS defects. As discussed previously, alumina particle coatings show promise, but their reproducibility needs to be improved. Gamma-alumina coated supports were made showing high lignin rejections, but CMS tests on those samples were out-of-scope for this thesis due to time constraints. It is expected that CMSs coated on these γ-alumina layers should have better performance. The coated CMSs can then be further improved by reducing the thickness by further optimizing spin-coating (necessary for higher flux), testing a different polymer (e.g. 6FDA:BPDA-DAM) which is known to give more porous CMSs,[108] as well as adding sacrificial nanoparticles

to increase the pore sizes, allowing for high solute rejections while increasing permeate fluxes.

3.3 Liquid Permeation Results

In this work, most consideration was given to the rejection performance, since flux could later be improved once target membrane performance (80% lignin rejection for NF ceramic membranes, 99% lignin rejection by the CMS RO membranes) was achieved. Also, because a stirred-dead-end cell, a tubular module, or a spiral cross-flow module was not yet used, only the water flux data is meaningful for scale-up (i.e. because of increases in osmotic pressure and concentration polarization, flux with anything but water are low and are an unrealistic basis of comparison). The water flux is still useful because it can be seen as the ideal case (i.e. the stirring or cross-flow velocities are sufficiently high such that there is no concentration polarization). Nonetheless, some BL and other non-water flux is presented in a few cases to show the general trends, despite the limitations of the non-stirred dead-end cell. Again, rejection data was given priority in the cases when time-constraints limited the collection of water flux data. It should be noted that initial BLs used were more concentrated (~1wt.%) and then switched to ~0.03 wt.% because of the concentration polarization and osmotic pressure increases in the non-stirred dead-end cell (initial CMS membranes were very defective and could handle higher concentrations of BL).

Initial permeation work was done on the initial spin-coated Matrimid-based CMS samples. It was only later determined that there were large pin-holes in these samples, hence the flux data is abnormally large for these samples. As seen Figure 53, the alumina

support has very high water fluxes, as there is very little resistance to water flow. In the absence of fouling species, flux always increases linearly with pressure (Darcy's law). The 0.25 μm alumina particle pressed disc still has large flux compared to a CMS membrane, but I such lower than the bare alumina support due to its smaller pore size and thickness (3 mm). The 0.25 μm alumina particle coating is comparable to the water flux on the bare support since its coated layer is thin (<10 μm), thus the flux is largely due to the 1 mm support. The flux is slightly higher likely due to some variability between samples and a possible slight increase in pore size of the sample after initial liquid permeation (i.e. pores can slightly increase after an initial liquid run. This sample was tested after an initial liquid run). Fluxes from the gamma coats are high (Figure 54) but lower than those of uncoated supports, as expected.

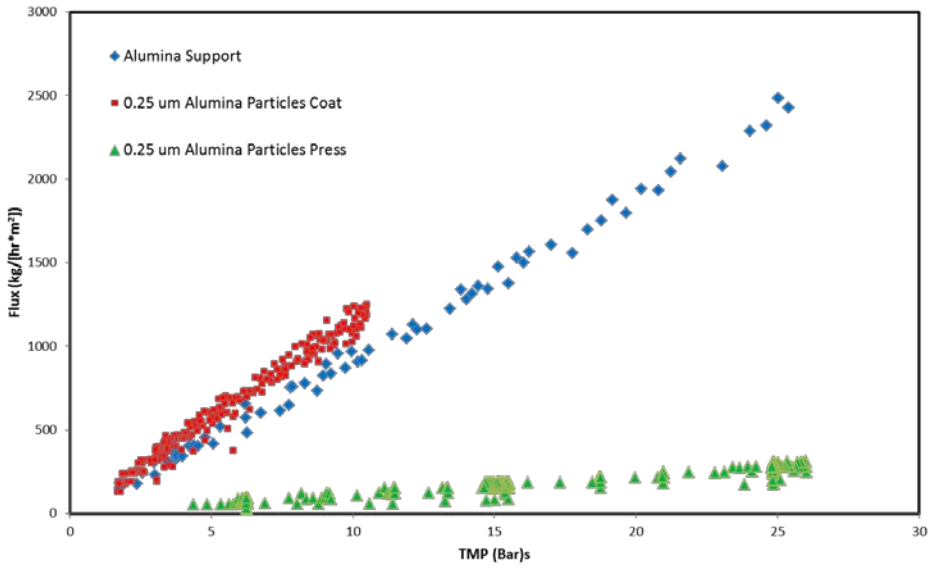

Figure 53: Water flux on alumina support, 0.25 μm alumina particle coating, and 0.25 μm alumina particle pressed disc

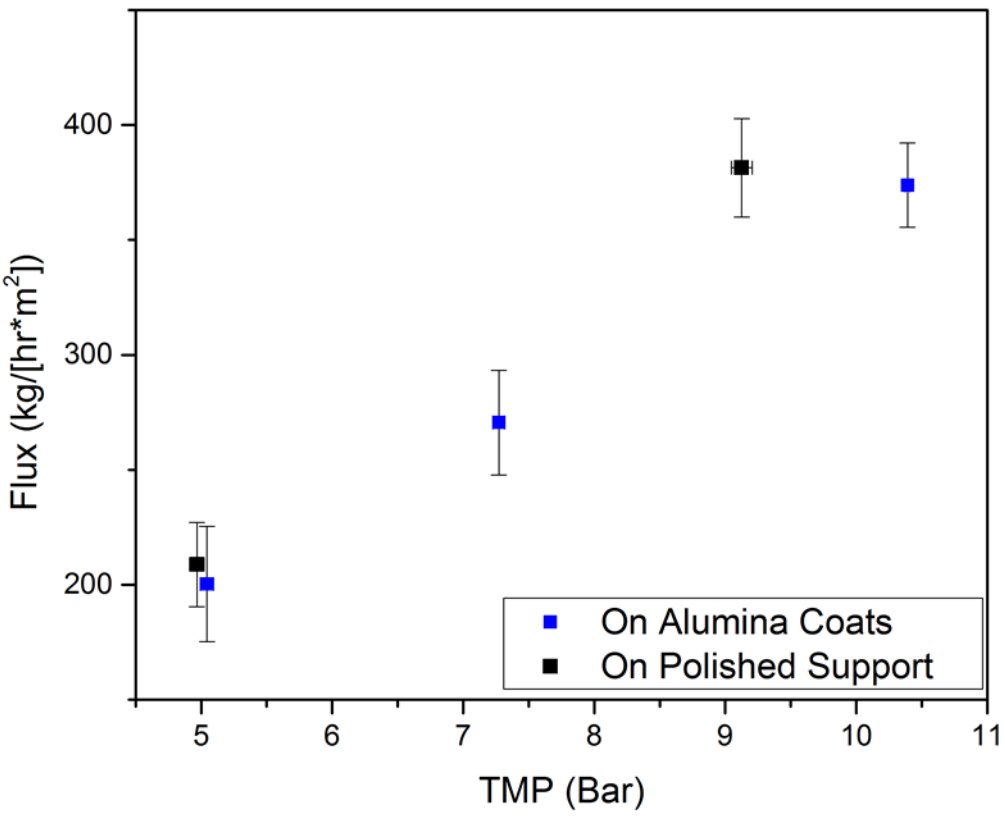

Figure 54: Water flux on from gamma-alumina coat on bare support and on the 5.8 nm-coated 0.25 μm coated supports

Early work used defective CMSs, but the BL studies still were helpful by serving as scoping studies, providing trends of what to expect later with less-defective CMSs. For example, as in Figure 55, there is flux decline over time until a steady-state (SS) is approached. This is normal (some fouling/concentration polarization lowers flux right away), and it is important to estimate the times required for SS to occur in order to properly design and run experiments.

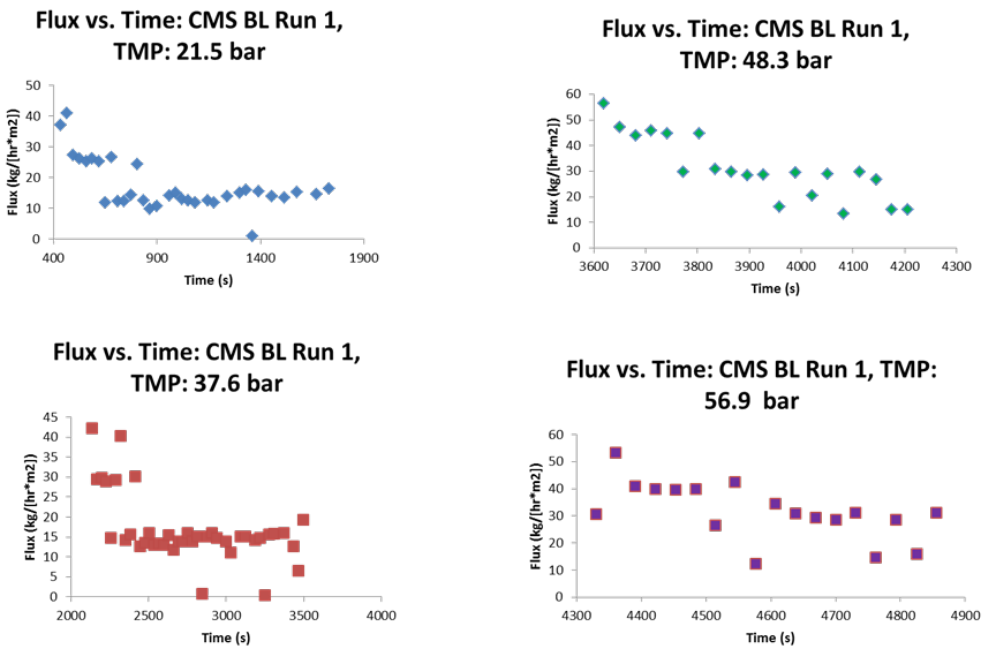

Figure 55: Typical flux decline behavior

3.4 BL concentration membrane scale-up and economic feasibility

Though ideal ceramic or CMS membranes were not fully achieved in this work, we can use a simple mass balance model to demonstrate the value of membranes in BL concentration. Key assumptions in this model include a typical 500 gal/min BL feed, concentration of BL from 15 wt.% to 25 wt.% TS, constant, steady-state flux, and surface area calculation based on 30 kg/(m^2 hr) flux from 1" disc (above this flux, surface area gains are minor, as discussed below), direct concentration by a single membrane tube (no recycle streams, multiple stages, etc.), and tubular membrane with 100 m^2/m^3 average packing density,[49] \$125/m^2 manufacturing cost.[53] Case 1 is RO (CMS targets), with 99% organic (mainly lignin), 95% inorganic rejections, case 2 is NF (minimum alumina target, though some literature has seen as high as 80% lignin rejections) with 68%

organic (mainly lignin), 12% inorganic rejections (values based on only performing CMS, as well as a literature result[78]).

The 30 kg/(m^2 hr) flux was chosen based on Figure 56 using the rejection and BL feed rate assumptions for case 1, since these are the ideal targets for an RO CMS membrane. The liquid permeation tests in this work were largely done on a 1" (25 mm) diameter disc. Based on the feed requirements (500 gal/min), a scaled-up surface area was calculated based on the usable surface area in the 1" diameter disc. The results were then plotted in Figure 56. As seen from the figure, initial flux gains result in drastic surface area savings. However, past ~ 30 kg/(m^2 hr), surface area gains are minor and only an economic analysis would be able to determine if the costs of higher flux are lower than the savings by reduced surface area. If a different BL feed flow-rate is assumed, the surface area values will change (based on scale-up or scale-down), but the overall trend will remain the same, with the same optimum flux of ~30 kg/(m^2 hr).

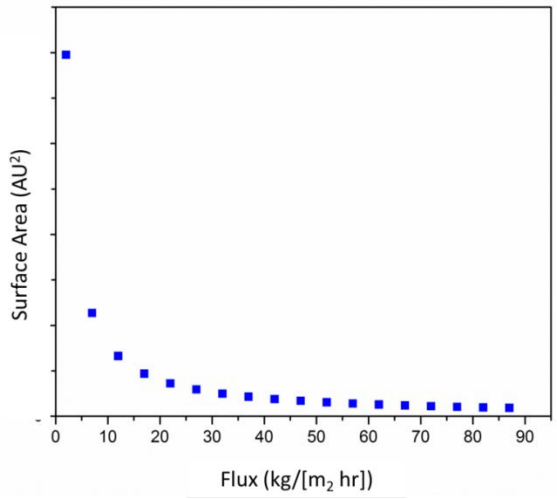

Figure 56: Scaled Surface Area vs. Flux from a 1" diameter disc for Case 1

Figure 57 shows the detailed results of case 1 (RO). It can be seen that for an RO membrane, most of the TS will be rejected, the membrane surface area and manufacturing cost is reasonable, and there is a very pure water permeate which can be used in other parts of the plant.

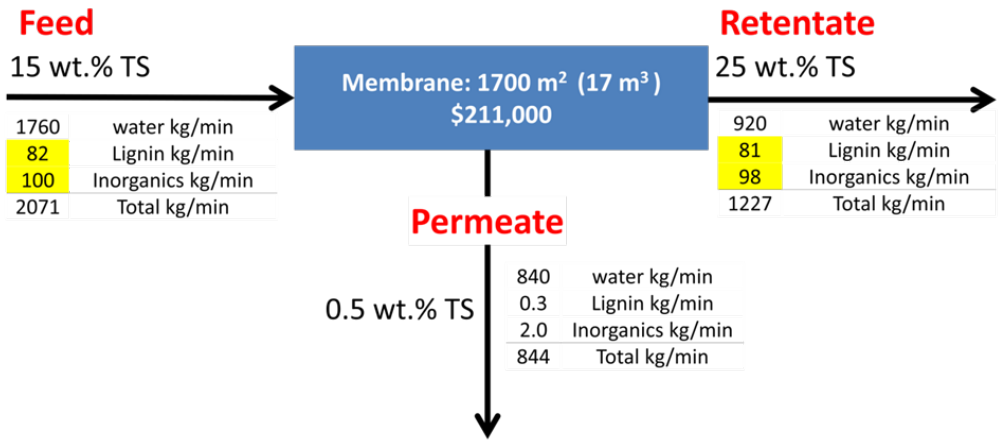

Figure 57: Results of case 1 (RO)

Figure 58 shows the detailed results of case 2 (NF). It can be seen that there is still high recoveries of lignin and inorganics, the membrane requirements are larger, but not unfeasible and the water permeate still has potential to be used in other parts of the plant.

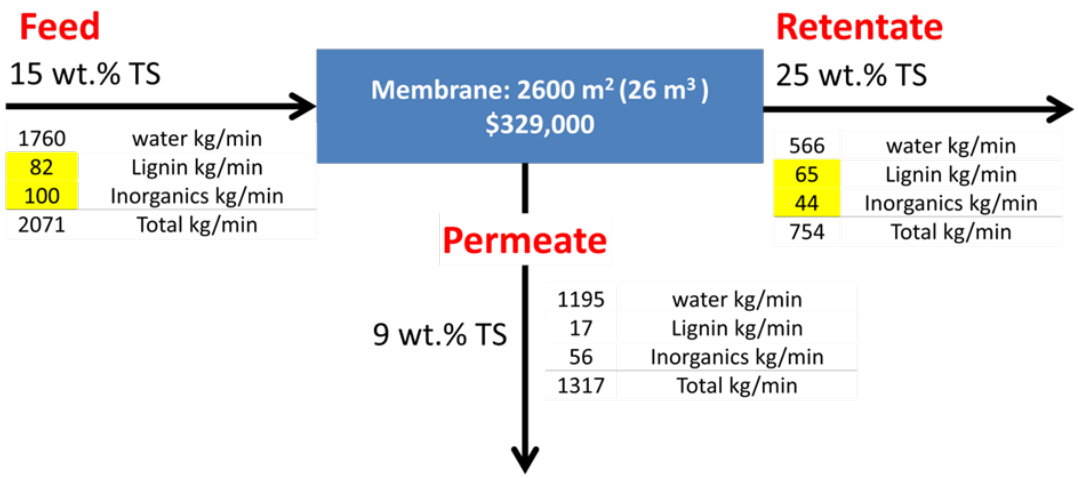

Figure 58: Results of case 2 (NF)

CHAPTER 4

CONCLUSIONS AND FUTURE WORK

Significant reductions in cost from the Kraft process is expected to result from successful development of BL concentration membrane technology. Significant progress has been made in the development and evaluation of membranes for BL concentration. However, polymeric membranes are challenged in BL applications because of their low lifetimes upon exposure to the harsh BL feed conditions. Because of their greater stability, non-polymeric (e.g., ceramic) membranes are expected to play a major role in the concentration of black liquor. However, a major challenge exists in improving their rejection and flux properties to decisively improve the economics of membrane-based BL concentration. Furthermore, to achieve the best possible separation (removal of water and ions), NF and RO membranes are also required. These membranes are still largely polymer-based, and future research will need to focus on the development of robust, lower-cost inorganic NF/RO membranes suited for BL applications.

This thesis work attempted to address these limitations and opportunities by (1) employing a robust and stable material (CMS supported on alumina) to fabricate membranes for BL concentration, and (2) improving the current quality of ceramic (α-alumina) membranes to be uses as prefilters to the NF/RO and as better supports for CMS coats. Results showed that alumina-supported CMS membranes could have high rejections but the membranes were still defective. In liquid permeation, the CMS were very resistant to water flow and the small pore sizes of fully-defect free CMSs do not

make them favorable for direct BL use. Some liquid and rejection data was collected on CMSs, but based on gas permeation results, these CMSs were known to be defective. Thus, the best CMSs achieved were overly dense (too resistant to water permeation) and yet defective (too high flux, no significant selectivity except for one sample with (CO_2/N_2) selectivity of ~7 (which is still low compared to literature). Future work would study and explain the defects as well as adding sacrificial nanoparticles (e.g. silica) that could be etched away, giving small pore sizes for good RO/NF, but larger than the 0.2-0.6 nm of typical defect-free CMSs . Further work would also focus on increasing the porosity (resulting in higher fluxes and making water easier to pass through), using a Sterlitech cell to avoid concentration polarization, and generating thinner layers by further optimizing the spin-coating conditions and by coating one-several graphite layers by techniques different from the multiple graphite layers in CMS.

It should be noted that literature of Matrimid and CMS membranes is typically based upon free-standing films or hollow fibers. There are only a handful of reports on ceramic-supported CMS or Matrimid membranes. Here, the presence of a porous support and infiltration issues (as well as poor quality of most of the support discs) likely contributed to the observed gas permeation defects and dense films for liquid filtration. It is quite possible that drying of Matrimid and pyrolysis occurs differently inside pores. Also, the tortuous pore of the support may have prevented proper drying/pyrolysis products venting (and even PEG removal), leading to abnormal results. Future work would study this issue in greater detail and identify the cause for the unfavorable gas and liquid permeation results.

Given the yet-unresolved challenges encountered with CMS membranes, that were out-of-scope for this MS thesis, the second component of our work focused on improving the ceramic membrane performance, both as a prefilter and as a better coat for CMSs. One strategy examined here consisted of adding smaller, thin ceramic coatings of smaller pore sizes onto existing, readily available, cheap and larger pore-sized alumina supports. Pressed discs from 0.25 μm particle size yielded 35% lignin rejection and the best coat of 0.25 μm particles on an a commercial alumina support achieved a maximum lignin rejection of 40%. Further samples and additional coats with 5.8 nm particles failed to improve or match these rejections. Future work would more carefully study the coating procedure to ensure reproducibility between different batches.

A gamma-alumina coat was also applied to both the bare alumina support as well as on top of the alpha-alumina coats, achieving 60% lignin rejection in both cases. This is still below NF level, but further optimization of the coating protocol as well as lower sintering temperatures should yield smaller pores and increase the lignin rejection to ~90% for NF prefiltration. Moreover, it should yield improved CMS coating layer, since literature has shown that a thinner CMS coating can be obtained due to the smoother gamma-alumina coat. In addition to testing the CMS on the gamma-alumina coat, CMS properties must still be improved to achieve an industrially-acceptable water flux (30 kg/[m^2 hr]). Method to do this include optimizing spin-coating to decrease membrane thickness, changing the polymer precursor to yield a more porous CMS (e.g. 6FDA:BPDA-DAM), and adding sacrificial nanoparticles to increase pore size.

Finally, in addition to using the Sterlitech cell, cross-flow tests on both discs and tubes would be carried out. There is still a possibility that masking would not work for

the 1” discs (the 2” discs may be too thick for the Sterlitech cell) and/or that greater reduction in fouling and concentration would be desired. Thus, two designs are proposed for cross-flow filtration. First, a cross-flow “spiral” design has already been made. Fluid would flow in a spiral fashion. An Isco syringe pump would provide the flowrate at high pressure, while a back-pressure regulator would be used to maintain the desired TMP. Second, the membrane coating procedures would be applied to tubes, which could then be scaled-up for future pilot tests (tubes are the most industrially relevant module for BL filtration due to the fouling considerations). While not built yet, a lab-scale tubular design has been prepared based on commercially available parts from Swagelok.

APPENDIX A

BL PROPERTIES/COMPOSITION SUMMARY TABLES

Table 9: Detailed composition of Black Liquor: General Categories

Lignin (wt. % of dry solids)	Refs		Hemicellulose (wt. % of dry solids)	Refs		TS/TDS (wt. %)	Refs		Organics (wt. % dry basis)	Refs
28.9-43	18, 29, 43, 67, 136		0.11-1.3	29		8.27-52.06	7, 10, 11, 13, 15, 18, 27, 33, 59-61, 64, 65, 74-79, 137		66-68	27, 61, 65, 91
Lignin (g/L)	**Refs**		**Hemicellulose (g/L)**	**Refs**		**Extractives (wt.% of dried solids)**	**Refs**		**Carbohydrates (wt. %)**	**Refs**
26-193	7, 9, 13, 41, 67, 69, 74-79, 91, 138		3.56-30	13, 16, 78, 79		0.3-6.69	8, 19, 29, 139		0.1-4.1	10, 34, 136, 139

Table 9 Continued

Volatile Solids (g/L)	Refs		Inorganics (g/L)	Refs		Extractives (g/L)	Refs		Carbohydrates (g/L)	Refs
38-53	9		35-45	75-77		0.47-2.06	7		5-9	7

Table 10: Detailed composition of Black Liquor: Salts and Elements

$Na_2S_2O_3$ (g/L)	Refs		SiO_2 (g/L)	Refs		Na_2S (g/L)	Refs		Na_2SO_3 (g/L)	Refs
4.7-5.8	140		0.6-4.98	9, 33		0.88-1.11	27, 61, 65		4.1-8.4	140
$Na_2S_2O_3$ (wt.% of dried solids)	Refs		SiO_2 (% of dry solids)	Refs		NaOH (g/L)	Refs		Na_2CO_3 (g/L)	Refs
1.6-4.1	140		0.2-0.7 (wood) 1-30 (grasses)	39, 43		0.14-40	7, 27, 61, 141		2.05-3.5	27, 61, 65
Na_2SO_4 (wt.% of dry solids)	Refs		Na_2CO_3 (wt.% of TDS)	Refs		Mg (mg/L)	Refs		Na (g/L)	Refs
0.9-8.3	29, 39		6.6-12.3	29, 39		6.0-46.2	74, 77, 91		8.42-42.3	7, 9, 16, 59, 60, 64, 74, 77

Table 10 Continued

Ba (mg/L)	Refs	Cu (mg/L)	Refs	Mg (ppm)	Refs	Na (wt.% of dry solids, bound to organics)	Refs
0.8-0.9	91	0.8-1.5	91	140-240	19, 39	8.7-10.3	29
Fe (mg/L)	**Refs**	**Al (mg/L)**	**Refs**	**Mn (mg/L)**	**Refs**	**Na (% of dry solids)**	**Refs**
2.0-3.4	74, 77, 91	9.0-10.5	91	8.1-13.1	74, 77, 91	8.8-26.0	18, 29-31, 39, 43, 137
Fe (ppm)	**Refs**	**Al (ppm)**	**Refs**	**Mn (ppm)**	**Refs**	**C (kg/m3)**	**Refs**
56-120	19, 39	32-300	19, 39	96	39	19.4-50	69
Si (g/mL)	**Refs**	**S (% of dry solids)**	**Refs**	**Ca (mg/L)**	**Refs**	**C (% of dry solids)**	**Refs**
66.5-73.5	91	0.4-7	18, 29-31, 39, 43	9.5-36.7	77, 91	23.7-50.7	18, 30, 31, 43, 59, 60, 64
Si (% of dry solids)	**Refs**	**S (g/L)**	**Refs**	**Ca (ppm)**	**Refs**	**Cl (% of dry solids)**	**Refs**
0.1-3.8	18	4.8-11.2	74, 77, 91	40-1300	19, 39	0.1-4.5	18, 30

Table 10 Continued

K (g/L)	Refs		O (% of dry solids)	Refs		H (% of dry solids)	Refs		N (% of, dry solids)	Refs
3.1-8.6	7, 74, 77, 91		32-39	30		0.08-5.53	18, 30, 31, 43, 59, 60, 64		0-3.6	18, 30, 31, 59, 60, 64
K (wt.% of dry solids)	**Refs**		**B (ppm)**	**Refs**						
0.3-9.2	18, 29-31, 39, 137		202	39						

Table 11: Detailed composition of Black Liquor: Lower MW Organics

Acetic acid (g/L)	Refs		Glycolic acid (g/L)	Refs		Lactic acid (g/L)	Refs		Oxalic acid (g/L)	Refs
6.7	[67]		2-3	[67]		4-5.1	[67]		0.13-0.17	[67]
Acetic acid (wt.% of dry solids)	**Refs**		**Malic acid (g/L)**	**Refs**		**Glyceric acid (g/L)**	**Refs**		**2-Hydroxyadipic acid (g/L)**	**Refs**
2.08-8	[29, 31]		0.16-0.3	[67]		0.11-0.13	[67]		0.24-0.4	[67]
Xyloisosaccharinic acid (g/L)	**Refs**		**Glucoisosaccharinic acid (g/L)**	**Refs**		**Glucoisosaccharinaric acid (g/L)**	**Refs**		**3-Hydroxypropanoic acid (g/L)**	**Refs**
0.5-4.2	[67]		4-9	[67]		0.5-0.7	[67]		0.02-0.19	[67]
2 -C-Methylglyceric acid (g/L)	**Refs**		**3-Deoxyhexonic acid(g/L)**	**Refs**		**2,5-Dihydroxypentanoic acid (g/L)**	**Refs**		**2-Hydroxybutanoic acid (g/L)**	**Refs**
0.1-0.12	[67]		0.3	[67]		1.1	[67]		1.2	[67]
3,6-Dideoxyhexonic acid (g/L)	**Refs**		**2,5-Pihvdroxypentanoic acid (g/L)**	**Refs**		**4-Hydroxybutanoic acid (g/L)**	**Refs**		**2-Hydroxyghitaric acid(g/L)**	**Refs**
0.16-0.6	[67]		0.9-1.5	[67]		0.1-0.19	[67]		0.4-0.5	[67]

Table 11 Continued

Succinic acid (g/L)	Refs		2-Hydroxybutanoic acid (g/L)	Refs		2-Hvdroxypentenoic acid (g/L)	Refs		3,4.Dideoxypentonic acid (g/L)	Refs
0.22	[67]		1-7	[67]		0.15-0.3	[67]		1.2-2.2	[67]
3-Deoxytetronic acid (g/L)	**Refs**		**3-Deoxypentaric acid (g/L)**	**Refs**		**Meihylsuccinic acid (g/L)**	**Refs**		**Anhydroisosaccharinic acid (g/L)**	**Refs**
0.3-0.6	[67]		0.05-0.07	[67]		0.04-0.18	[67]		0.18-0.3	[67]
2-Decoxytetronic acid (g/L)	**Refs**		**2-Hydroxyadipic acid (g/L)**	**Refs**						

APPENDIX B
METHODS FOR DETERMINATION OF BLACK LIQUOR COMPOSITION

Table 12: Methods for determination of black liquor composition

	Organics	Inorganics/Ash	TS/TDS	Lignin
Brief Description	Weigh dried solids, heat them to 500-950 °C, and reweigh. The difference in weight is the organic content.[75]	Overall inorganic content: Heat the dried TDS samples up to ~575-950 °C. Ash content is the remaining weight.[7, 16, 74, 76, 79,] Composition: First pretreat with nitric acid and organics filtered out, then analyze concentration and composition via inductively coupled plasma atomic emission spectroscopy, a flash elemental analyzer or by using a pH metric triple titration method.[27, 75, 142]	For TS: weigh dried samples at 105 °C. For TDS, same as TS first use a filter to remove the suspended solids.[7, 62]	Concentration: UV-Vis (280 nm);[56] Amount of precipitated lignin: acid hydrolysis, then gravimetric analysis or one-minute autoclave, hot filter (no pre-hydrolysis).[139, 142] Lignin MW: size exclusion chromatography; Chemical structure: FTIR analysis;[11] Particle size distribution: droplet and particle sizer[23]
Common Standard(s)	Similar to that in NRL LAP-012.[11]	Overall inorganic content: TAPPI 211, CPPA J.15P, KCL 59:83, TAPPI 625cm-85, KCL 60:64, ISO 1762.[31, 142] Composition: SCANN 38:01, also similar to that in NRL LAP-012.[7, 11]	TAPPI Test T650 om-89, SCAN-N 22:96, ISO 638:2008, NRL LAP-012.[11, 18, 139]	Klason's acid-hydrolysis method (1893), TAPPI T 222 om-02, TAPPI T 249 cm-00, TAPPI UM 250, SCAN-CM 71:09.[139]

Table 12 Continued

	Carbohydrates	**Total Na**	**Heating Value**	**$Na_2S_2O_3$**	**Na_2S**
Brief Description	Ion chromatography.[7]	Conductivity meter, atomic absorption spectroscopy, flame emission spectroscopy.[39, 62, 138]	Heating by complete oxidizing liquor in an adiabatic calorimetric bomb.[18]	HgCl titration via mercury pool electrode.[39]	Potentiometric titration using an ion-selective electrode.[39]
Common Standard(s)	Acid hydrolysis (TAPPI 222 om-02 and SCAN-CM 71:09).[142]	SCAN-N 38, TAPPI T 623cm-83 and 625cm-85, KCL 65:82.[31, 142]	TAPPI Test T684.[18]	TAPPI T 625cm-85 and 699om-87, KCL 70:83.[31]	Sulfide and hydrogen sulfide: TAPPI T 625cm-85 and 699om-87, SCAN-N 31:94, KCL 69:91.[31]
	Na_2SO_4	**Na_2CO_3**	**C**	**H**	**K**
Brief Description	Ion chromatography.[33]	CO_2 evolution.[39]	Combustion of dried liquor in oxygen (>1000 °C) in Elementary Analyzer.[18]	Combustion of dried liquor in oxygen (>1000 °C) in Elementary Analyzer.[18]	Atomic absorption spectroscopy with addition of HCl.[18]
Common Standard(s)	TAPPI T 625cm -85 and 699om87, KC:L 71:81.[31]	Carbonate: TAPPI T 699om-87, KCL 68:91, TAPPI method T 624 os-68.[31, 32, 39]	KCL 62:64.[31]	KCL 62:64.[31]	TAPPI Test T266.[18]

Table 12 Continued

	Active Alkali		**N**		**Inorganic/organic ratio**		**Silica, Fe, Al, Ca, Mg, Mn, K, P**		**S**
Common Standard(s)	SS-EN ISO 9963-1, TAPPI T 625cm-85, CPPA J.15P, KCL 67a:87.[7, 31]		KCL 64:92.[31]		TAPPI T 625cm -85, KCL 61:83.[31]		TAPPI T 625cm-85, CPPA J.15P, KCL 231:92, STFl AH41-l :83, AH41-3:R3, AH41-4:81, AH4-I-7:80. AH41-8:80, and AH42-5:81.[31]		TAPPI T 625cm -85, CPPA J.15P, KCL 72a:84, sulfur: TAPPI T 625cm-85, CPPA J.15P, KCL 63:64 and 63a:84, SCAN N 30:85,ABNT Test MB 106/65.[7, 18, 31]
	NaCl		**Extractives**		**COD**		**BOD**		**Oil/Grease**
Brief Description	Volhard method titration with $AgN0_3$ via indicators or potentiometry.[39]		Extract with petroleum ether, gas chromatography.[7, 35]		Titrate $K_2Cr_2O_7$ against $(NH_4)_2Fe(SO_4)_2$.[62]		Winkler Azide method (measure COD on 1st and 5th day).[62]		Mix sample with n-hexane and shake. Separate the n-hexane from the other phase and evaporate the n-hexane phase to recover the oil and grease.[62]

Table 12 Continued

	Hemicellulose	Volatile Solids	Si or Silica	Cl
Common Standard(s) or Brief Description	First acid hydrolysis, then high-performance anion-exchange chromatography.[16]	Concentration: gravimetrically after drying the sample in an incubator at 550 °C.[9]	Si: gravimetry, colorimetry;[18, 33] Silica: oxidized by aqua regia, heated to boiling with water, filtered, gravimetric measurement after burning at 550 °C.[9]	TAPPI T 699om-87, KCL 73a:84.[31]

APPENDIX C
BL MEMBRANE LIT SUMMARY TABLES

Table 13: Polymeric membranes investigated for black liquor concentration.

Pulp Type	Membrane Material	Membrane Type	MWCO (kDa) or Pore size	Module(s)	Refs
Spruce	Cellulose acetate	UF, RO	Unknown	Plate and frame	[68]
Unknown	Cellulose acetate	UF, NF	10, 20, & 70 kDa	Stirred batch cell	[57]
16 % solids model BL	Polysulfone	UF	10 & 20 kDa	Unstirred batch cell	[14]
Northern & southern hardwood & softwood	MF: nylon UF: polysulfone	MF & UF	MF: 0.5-μm pore size; UF: 6, 20, & 50 kDa	Plate-and-frame	[19]
Maine 70% hardwood-30% softwood liquor mix	Polysulfone	Unknown	50, 100, 200 kDa	Plate-and-frame Hollow fiber	[15]
Unknown	Moist type G05T polyelectrolyte complex membrane	UF	5 kDa	Asymmetric stirred batch cell	[58]
Mixed hardwoods	Cellulose acetate	UF	5 kDa	Stirred batch	[59, 60]

Table 13 Continued

Unknown	Cellulose acetate	(A) Carbonation, UF, NF (B) Carbonation, NF (C) NF	1 (UF) 0.5 (NF) kDa	Flat-sheet cross flow	27
Unknown	Asymmetric cellulose acetate (low rejecting) Thin film composite (high rejecting)	UF	1, 0.5 kDa	Flat-sheet cross flow	65
Pine- but used model BL (acid precipitated lignin in 0.1 M NaOH)	Cellulose & polysulfone	Unknown	1, 10, 30, 100 kDa	Stirred batch cell	56
Unknown	Polyacrylonitrile	UF	3, 20, 80, 110 kDa	Plate & frame	69
Unknown	Cellulose acetate	UF	5 kDa	Radial cross flow	61
Unknown	Cellulose acetate	UF	1 kDa	Rectangular cross flow	61
Unknown	Cellulose acetate	UF	1, 5 and 10 kDa	Stirred dead-end	61
Bleached softwood	Polysulfone and polyethersulfone	Unknown	4,8, 20 kDa	Tubular	76
Wheat straw BL	MF: 2 asymmetric membranes were made of α-alumina, one was made of cellulose acetate. UF membranes were made either from polyacrylonitrile, polyaryl ether ketone, or sulfone	MF, UF	MF: 0.8, 0.2, 0.22 μm; UF: 3, 6, 10, 30 ,60 kDa	MF: 2 of them were tubular, one was flat sheet UF: flat sheet asymmetric membranes, some dead-end batch, stirred	9

Table 13 Continued

Unknown	Cellulose triacetate, polysulfone	Unknown	5, 10, 20, 30, 100 kDa	Flat sheet	66
Rice & jute straw	UF: asymmetric cellulose triacetate MF: polyethersulfone (PES)	MF & UF	UF: 5 kDa; MF: 0.45 µm pore size	Dead-end: different combinations of stirred feed and/or rotating disc	62, 63
Mixed hardwoods	Asymmetric cellulose triacetate	UF	5 kDa	Stirred dead-end	64
Softwood & hardwood cooking liquor; hardwood BL	Ceramic (Al_2O_3–TiO_2) (UF) & polymeric (polyethersulfone, polysulfone, polyvinyldifluoride) (NF)	UF, NF	1-100 (15 for main ceramic UF), 1 (for main polymeric NF). Polyethersulfone: 4 & 6 , polyethersulfone (20), polyvinyldifluoride (100) kDa	Tubular	78
Wheat straw	Polyethersulfone	UF	6 kDa	Hollow fiber	70
Hardwood and softwood	PES	UF, NF	0.4, 1 kDa	Flat sheet	67
Wheat straw	PES	UF	6, 10 kDa	Cup membrane ultrafiltration apparatus	12
Softwood	Polymeric Composite	NF	1 kDa	Tubular	16
Softwood	Polymeric Composite	NF	0.6 kDa	Tubular	16
Softwood	Polymeric Composite	NF	0.2 kDa	Tubular	16
Mostly softwood	PES	UF	1.2 kDa	Cross-rotational Plate & Frame	143

Table 14: Ceramic membranes investigated for black liquor concentration.

Pulp Type	Membrane Material	Membrane Type	MWCO (kDa) or Pore size	Module(s)	Refs
Hardwood	Al_2O_3	MF	0.2 um pore size	Tubular	72, 73
Softwood	Al_2O_3-TiO_2	UF	5 & 15 kDa	Tubular	75
Bleached softwood	Al_2O_3-TiO_2	UF	15 kDa	Tubular	77
Softwood and hardwood	Ceramic membranes coated with ZrO_2	UF & NF	1, 5, 15 kDa	Cross-flow	8
Wheat straw	Al_2O_3	MF	Pore sizes of 0.8 μm, 0.2 μm and 50 nm	Tubular	33
Wheat straw	MF: 2 asymmetric membrane were made of Al_2O_3, one was made of cellulose acetate. UF membranes were made either from polyacrylonitrile, polyaryl ether ketone, or sulfone	MF, UF	MF: 0.8, 0.2, 0.22 μm UF: 3, 6, 10, 30, 60 kDa	MF: 2 of them were tubular, one was flat sheet UF: flat sheet asymmetric membranes, some dead-end batch, stirred	9
Softwood	Al_2O_3–TiO_2	UF	15 kDa	Cross-flow	74
Softwood and hardwood	Al_2O_3– TiO_2 with an active layer of ZrO_2	UF	5, 15 kDa	Crossflow	7
Model BL (NaOH and lignin)	Al_2O_3–TiO_2 active layer on ceramic support and TiO_2 active layer on ceramic support	UF	1, 5, 15 kDa	Tubular	41
				Tubular	78

Table 14 Continued

Hardwood	Al_2O_3- TiO_2	UF	15 kDa	Tubular	[79]
Hardwood	Al_2O_3-TiO_2	UF	15 kDa	Tubular	[13]
Straw	TiO_2	UF	5, 10, 15 kDa	Tubular	[11]
Softwood	Al_2O_3 with a surface layer of TiO_2	UF	20 kDa	Tubular	[16]
Softwood	TiO_2	NF	1 kDa	Tubular	[16]
Hardwood and softwood	UF: TiO_2 & ZrO_2	UF	1 kDa	Cross flow	[142]
Carbonized BL	Ceramic	UF followed by NF	UF (1.5-2 kDa) NF (0.15-0.5 kDa)	Tubular (UF) Spiral-wound (NF)	[28]
Hardwood and softwood	Ceramic	90 µm mesh prefiltration, followed by acidification to pH 9-10 and then MF and UF	90 µm mesh (pre-filter), 0.2 µm (MF), 300 & 15 kDa (UF)	Tubular	[90]

Table 15: Lignin concentration with UF and NF membranes. Symbol X denotes 'Unknown.'

Example Permeate Flux (m^3/m^2 s)	Rejection (Retention) (%)	Recovery (%)	pH	T (°C)	Refs
X	Up to 75 lignin	X	10.2-12.5	21, 25	14
1.39×10^{-6} - 2.64×10^{-5}	Up to 26 lignin	X	12.5-13	75, 80	15
$1.94\text{-}2.50 \times 10^{-5}$	X	54 lignin	X	60	24, 25
~1.15×10^{-5} m/s	X	X	8.8	30	59, 60
$1.28\text{-}4.53 \times 10^{-7}$	81-95 TDS	25-78 inorganics	12	26-31	27
8.5×10^{-6}	Up to 35 TDS	X	11.2-11.95	26-31	65
1.23×10^{-5}	Up to 78.7	X	X	X	69
1.2×10^{-5}	52 TDS	X	X	X	61
Above 5.6×10^{-5}	99.2 pitch	40 pitch	X	90-93	72, 73
1.25×10^{-5}, 2.64×10^{-5}	X	33, 63 lignin	13-14	90	75
5.6×10^{-6}	30-40 lignin	X	13-14	60, 75, 90	77
$1.4\text{-}12.2 \times 10^{-6}$	67-68 lignin	X	X	25-80	8
1.39×10^{-4}	70 lignin; 80 silica; 23-27 TS	X	10.94-12.24	30-60	33
4.2×10^{-5}	80, 90 lignin	X	11	30, 32, 63	9
3.06×10^{-5}, 4.4×10^{-5}	35, 45 lignin	X	X	90	74
7.50×10^{-6}	76 lignin	X	7.5-8.8	30	62, 63
1.39×10^{-5}, 2.78×10^{-5}	20, 30 lignin	X	13-14	135, 145	7

Table 15 Continued

9.17×10^{-6}	15-25 lignin; 75-95 hemicellulose	40-45 lignin	13-14	90	[13]
20, 30 kg/(m^2 h)	78 lignin	82	13.5	X	[67]
5.83×10^{-6}, 1.11×10^{-5}	93, 97 lignin	X	13.4	70	[16]
110 kg/(m^2 h)	~70-75 lignin	21, 24 lignin; 76, 88 organic acids	X	60	[143]
X	15,18,28 lignin	X	9-10	70-85, 120	[90]

APPENDIX D

COPYRIGHT PERMISSIONS

Figure 259: Viscosity of hardwood black liquor as a function of shear rate and solids concentration C_{ss}. Adapted from Ref.[18]

ELSEVIER LICENSE
TERMS AND CONDITIONS
Nov 03, 2015

This is a License Agreement between Nikita Kevlich ("You") and Elsevier ("Elsevier") provided by Copyright Clearance Center ("CCC"). The license consists of your order details, the terms and conditions provided by Elsevier, and the payment terms and conditions.

All payments must be made in full to CCC. For payment instructions, please see information listed at the bottom of this form.

Supplier	Elsevier Limited The Boulevard,Langford Lane Kidlington,Oxford,OX5 1GB,UK
Registered Company Number	1982084
Customer name	Nikita Kevlich
Customer address	1950 Roswell Rd MARIETTA, GA 30068
License number	3761411428786
License date	Dec 03, 2015
Licensed content publisher	Elsevier
Licensed content publication	Fuel
Licensed content title	Chemical composition and physical properties of black liquors and their effects on liquor recovery operation in Brazilian pulp mills
Licensed content author	Marcelo Cardoso,Éder Domingos de Oliveira,Maria Laura Passos
Licensed content date	April 2009
Licensed content volume number	88
Licensed content issue number	4
Number of pages	8

Start Page	756
End Page	763
Type of Use	reuse in a thesis/dissertation
Intended publisher of new work	other
Portion	figures/tables/illustrations
Number of figures/tables/illustrations	1
Format	both print and electronic
Are you the author of this Elsevier article?	No
Will you be translating?	No
Original figure numbers	Figure 8
Title of your thesis/dissertation	CARBON MOLECULAR SIEVE AND CERAMIC MEMBRANES FOR BLACK LIQUOR CONCENTRATION
Expected completion date	Dec 2015
Estimated size (number of pages)	180
Elsevier VAT number	GB 494 6272 12
Permissions price	0.00 USD
VAT/Local Sales Tax	0.00 USD / 0.00 GBP
Total	0.00 USD
Terms and Conditions	

For Figure 7: Normalized flux decline for a polymeric (organic) membrane compared to an inorganic membrane. From Ref. [83]

Supplier	Elsevier Limited The Boulevard,Langford Lane Kidlington,Oxford,OX5 1GB,UK
Registered Company Number	1982084
Customer name	Nikita Kevlich
Customer address	1950 Roswell Rd MARIETTA, GA 30068
License number	3761411293806
License date	Dec 03, 2015
Licensed content publisher	Elsevier

Licensed content publication	Water Research
Licensed content title	Comparison of the filtration characteristics of organic and inorganic membranes in a membrane-coupled anaerobic bioreactor
Licensed content author	In-Joong Kang,Seong-Hoon Yoon,Chung-Hak Lee
Licensed content date	April 2002
Licensed content volume number	36
Licensed content issue number	7
Number of pages	11
Start Page	1803
End Page	1813
Type of Use	reuse in a thesis/dissertation
Intended publisher of new work	other
Portion	figures/tables/illustrations
Number of figures/tables/illustrations	1
Format	both print and electronic
Are you the author of this Elsevier article?	No
Will you be translating?	No
Original figure numbers	Figure 4
Title of your thesis/dissertation	CARBON MOLECULAR SIEVE AND CERAMIC MEMBRANES FOR BLACK LIQUOR CONCENTRATION
Expected completion date	Dec 2015
Estimated size (number of pages)	180
Elsevier VAT number	GB 494 6272 12
Permissions price	0.00 USD
VAT/Local Sales Tax	0.00 USD / 0.00 GBP
Total	0.00 USD
Terms and Conditions	

For Figure 9: MWCO changes because R_{obs} changes as flux (TMP) changes. From Ref.[55]

Supplier	Elsevier Limited The Boulevard,Langford Lane Kidlington,Oxford,OX5 1GB,UK
Registered Company Number	1982084
Customer name	Nikita Kevlich
Customer address	1950 Roswell Rd MARIETTA, GA 30068
License number	3761411174810
License date	Dec 03, 2015
Licensed content publisher	Elsevier
Licensed content publication	Journal of Membrane Science
Licensed content title	Improvement of a method for the characterization of ultrafiltration membranes by measurements of tracers retention
Licensed content author	C. Causserand,S. Rouaix,A. Akbari,P. Aimar
Licensed content date	15 July 2004
Licensed content volume number	238
Licensed content issue number	1-2
Number of pages	14
Start Page	177
End Page	190
Type of Use	reuse in a thesis/dissertation
Intended publisher of new work	other
Portion	figures/tables/illustrations
Number of figures/tables/illustrations	1
Format	both print and electronic
Are you the author of this Elsevier article?	No
Will you be translating?	No
Original figure numbers	Figure 3
Title of your thesis/dissertation	CARBON MOLECULAR SIEVE AND CERAMIC MEMBRANES FOR BLACK LIQUOR CONCENTRATION
Expected completion date	Dec 2015
Estimated size (number of	180

pages)	
Elsevier VAT number	GB 494 6272 12
Permissions price	0.00 USD
VAT/Local Sales Tax	0.00 USD / 0.00 GBP
Total	0.00 USD
Terms and Conditions	

For Figure 1160: Separation process for recovery of hydroxyacids from soda black liquor. From Ref.[17]

Supplier	Elsevier Limited The Boulevard,Langford Lane Kidlington,Oxford,OX5 1GB,UK
Registered Company Number	1982084
Customer name	Nikita Kevlich
Customer address	1950 Roswell Rd MARIETTA, GA 30068
License number	3761411007459
License date	Dec 03, 2015
Licensed content publisher	Elsevier
Licensed content publication	Chemical Engineering Research and Design
Licensed content title	Purification process for recovering hydroxy acids from soda black liquor
Licensed content author	Sanna Hellstén,Jussi Lahti,Jari Heinonen,Mari Kallioinen,Mika Mänttäri,Tuomo Sainio
Licensed content date	December 2013
Licensed content volume number	91
Licensed content issue number	12
Number of pages	10
Start Page	2765
End Page	2774
Type of Use	reuse in a thesis/dissertation
Intended publisher of new work	other
Portion	figures/tables/illustrations
Number of figures/tables/illustrations	1
Format	both print and electronic

Are you the author of this Elsevier article?	No
Will you be translating?	No
Original figure numbers	Figure 1
Title of your thesis/dissertation	CARBON MOLECULAR SIEVE AND CERAMIC MEMBRANES FOR BLACK LIQUOR CONCENTRATION
Expected completion date	Dec 2015
Estimated size (number of pages)	180
Elsevier VAT number	GB 494 6272 12
Permissions price	0.00 USD
VAT/Local Sales Tax	0.00 USD / 0.00 GBP
Total	0.00 USD
Terms and Conditions	

For Figure 14: Schematic representation of the different concentration polarization models. (a) osmotic pressure model, (b) gel layer model, and (c) series resistance model. From Ref.[96]

Supplier	Elsevier Limited The Boulevard,Langford Lane Kidlington,Oxford,OX5 1GB,UK
Registered Company Number	1982084
Customer name	Nikita Kevlich
Customer address	1950 Roswell Rd MARIETTA, GA 30068
License number	3761410788165
License date	Dec 03, 2015
Licensed content publisher	Elsevier
Licensed content publication	Chemical Engineering and Processing
Licensed content title	Fundamental principles of ultrafiltration
Licensed content author	Ann-Sofi Jönsson,Gun Trägårdh
Licensed content date	April 1990
Licensed content volume number	27
Licensed content issue number	2

Number of pages	15
Start Page	67
End Page	81
Type of Use	reuse in a thesis/dissertation
Intended publisher of new work	other
Portion	figures/tables/illustrations
Number of figures/tables/illustrations	1
Format	both print and electronic
Are you the author of this Elsevier article?	No
Will you be translating?	No
Original figure numbers	Figure 1
Title of your thesis/dissertation	CARBON MOLECULAR SIEVE AND CERAMIC MEMBRANES FOR BLACK LIQUOR CONCENTRATION
Expected completion date	Dec 2015
Estimated size (number of pages)	180
Elsevier VAT number	GB 494 6272 12
Permissions price	0.00 USD
VAT/Local Sales Tax	0.00 USD / 0.00 GBP
Total	0.00 USD
Terms and Conditions	

For Figure 1961: TGA Showing PEG Decomposition and **Figure 22**: Initial Pyrolysis Protocol. From Ref.[111]

Supplier	Elsevier Limited The Boulevard,Langford Lane Kidlington,Oxford,OX5 1GB,UK
Registered Company Number	1982084
Customer name	Nikita Kevlich
Customer address	1950 Roswell Rd MARIETTA, GA 30068
License number	3761410344614
License date	Dec 03, 2015
Licensed content publisher	Elsevier

Licensed content publication	Carbon
Licensed content title	Carbon molecular sieve membranes for biofuel separation
Licensed content author	Pei Shi Tin,Huey Yi Lin,Rui Chin Ong,Tai-Shung Chung
Licensed content date	February 2011
Licensed content volume number	49
Licensed content issue number	2
Number of pages	7
Start Page	369
End Page	375
Type of Use	reuse in a thesis/dissertation
Intended publisher of new work	other
Portion	figures/tables/illustrations
Number of figures/tables/illustrations	2
Format	both print and electronic
Are you the author of this Elsevier article?	No
Will you be translating?	No
Original figure numbers	Figures 1-2
Title of your thesis/dissertation	CARBON MOLECULAR SIEVE AND CERAMIC MEMBRANES FOR BLACK LIQUOR CONCENTRATION
Expected completion date	Dec 2015
Estimated size (number of pages)	180
Elsevier VAT number	GB 494 6272 12
Permissions price	0.00 USD
VAT/Local Sales Tax	0.00 USD / 0.00 GBP
Total	0.00 USD
Terms and Conditions	

INTRODUCTION

1. The publisher for this copyrighted material is Elsevier. By clicking "accept" in connection with completing this licensing transaction, you agree that the following terms and conditions apply to this transaction (along with the Billing and Payment terms and conditions established by Copyright Clearance Center, Inc. ("CCC"), at the time that you opened your Rightslink account and that are available at any time at http://myaccount.copyright.com).

GENERAL TERMS

2. Elsevier hereby grants you permission to reproduce the aforementioned material subject to the terms and conditions indicated.

3. Acknowledgement: If any part of the material to be used (for example, figures) has appeared in our publication with credit or acknowledgement to another source, permission must also be sought from that source. If such permission is not obtained then that material may not be included in your publication/copies. Suitable acknowledgement to the source must be made, either as a footnote or in a reference list at the end of your publication, as follows:

"Reprinted from Publication title, Vol /edition number, Author(s), Title of article / title of chapter, Pages No., Copyright (Year), with permission from Elsevier [OR APPLICABLE SOCIETY COPYRIGHT OWNER]." Also Lancet special credit - "Reprinted from The Lancet, Vol. number, Author(s), Title of article, Pages No., Copyright (Year), with permission from Elsevier."

4. Reproduction of this material is confined to the purpose and/or media for which permission is hereby given.

5. Altering/Modifying Material: Not Permitted. However figures and illustrations may be altered/adapted minimally to serve your work. Any other abbreviations, additions, deletions and/or any other alterations shall be made only with prior written authorization of Elsevier Ltd. (Please contact Elsevier at permissions@elsevier.com)

6. If the permission fee for the requested use of our material is waived in this instance, please be advised that your future requests for Elsevier materials may attract a fee.

7. Reservation of Rights: Publisher reserves all rights not specifically granted in the combination of (i) the license details provided by you and accepted in the course of this licensing transaction, (ii) these terms and conditions and (iii) CCC's Billing and Payment terms and conditions.

8. License Contingent Upon Payment: While you may exercise the rights licensed immediately upon issuance of the license at the end of the licensing process for the transaction, provided that you have disclosed complete and accurate details of your proposed use, no license is finally effective unless and until full payment is received from you (either by publisher or by CCC) as provided in CCC's Billing and Payment terms and conditions. If full payment is not received on a timely basis, then any license preliminarily granted shall be deemed automatically revoked and shall be void as if never granted. Further, in the event that you breach any of these terms and conditions or any of CCC's Billing and Payment terms and conditions, the license is automatically revoked and shall be void as if never granted. Use of materials as described in a revoked license, as well as any use of the materials beyond the scope of an unrevoked license, may constitute copyright infringement and publisher reserves the right to take any and all

action to protect its copyright in the materials.

9. Warranties: Publisher makes no representations or warranties with respect to the licensed material.

10. Indemnity: You hereby indemnify and agree to hold harmless publisher and CCC, and their respective officers, directors, employees and agents, from and against any and all claims arising out of your use of the licensed material other than as specifically authorized pursuant to this license.

11. No Transfer of License: This license is personal to you and may not be sublicensed, assigned, or transferred by you to any other person without publisher's written permission.

12. No Amendment Except in Writing: This license may not be amended except in a writing signed by both parties (or, in the case of publisher, by CCC on publisher's behalf).

13. Objection to Contrary Terms: Publisher hereby objects to any terms contained in any purchase order, acknowledgment, check endorsement or other writing prepared by you, which terms are inconsistent with these terms and conditions or CCC's Billing and Payment terms and conditions. These terms and conditions, together with CCC's Billing and Payment terms and conditions (which are incorporated herein), comprise the entire agreement between you and publisher (and CCC) concerning this licensing transaction. In the event of any conflict between your obligations established by these terms and conditions and those established by CCC's Billing and Payment terms and conditions, these terms and conditions shall control.

14. Revocation: Elsevier or Copyright Clearance Center may deny the permissions described in this License at their sole discretion, for any reason or no reason, with a full refund payable to you. Notice of such denial will be made using the contact information provided by you. Failure to receive such notice will not alter or invalidate the denial. In no event will Elsevier or Copyright Clearance Center be responsible or liable for any costs, expenses or damage incurred by you as a result of a denial of your permission request, other than a refund of the amount(s) paid by you to Elsevier and/or Copyright Clearance Center for denied permissions.

LIMITED LICENSE

The following terms and conditions apply only to specific license types:

15. **Translation**: This permission is granted for non-exclusive world **English** rights only unless your license was granted for translation rights. If you licensed translation rights you may only translate this content into the languages you requested. A professional translator must perform all translations and reproduce the content word for word

preserving the integrity of the article.

16. **Posting licensed content on any Website**: The following terms and conditions apply as follows: Licensing material from an Elsevier journal: All content posted to the web site must maintain the copyright information line on the bottom of each image; A hyper-text must be included to the Homepage of the journal from which you are licensing at http://www.sciencedirect.com/science/journal/xxxxx or the Elsevier homepage for books at http://www.elsevier.com; Central Storage: This license does not include permission for a scanned version of the material to be stored in a central repository such as that provided by Heron/XanEdu.

Licensing material from an Elsevier book: A hyper-text link must be included to the Elsevier homepage at http://www.elsevier.com . All content posted to the web site must maintain the copyright information line on the bottom of each image.

Posting licensed content on Electronic reserve: In addition to the above the following clauses are applicable: The web site must be password-protected and made available only to bona fide students registered on a relevant course. This permission is granted for 1 year only. You may obtain a new license for future website posting.

17. **For journal authors:** the following clauses are applicable in addition to the above:

Preprints:

A preprint is an author's own write-up of research results and analysis, it has not been peer-reviewed, nor has it had any other value added to it by a publisher (such as formatting, copyright, technical enhancement etc.).

Authors can share their preprints anywhere at any time. Preprints should not be added to or enhanced in any way in order to appear more like, or to substitute for, the final versions of articles however authors can update their preprints on arXiv or RePEc with their Accepted Author Manuscript (see below).

If accepted for publication, we encourage authors to link from the preprint to their formal publication via its DOI. Millions of researchers have access to the formal publications on ScienceDirect, and so links will help users to find, access, cite and use the best available version. Please note that Cell Press, The Lancet and some society-owned have different preprint policies. Information on these policies is available on the journal homepage.

Accepted Author Manuscripts: An accepted author manuscript is the manuscript of an article that has been accepted for publication and which typically includes author-incorporated changes suggested during submission, peer review and editor-author communications.

Authors can share their accepted author manuscript:

- – immediately
    - via their non-commercial person homepage or blog
    - by updating a preprint in arXiv or RePEc with the accepted manuscript
    - via their research institute or institutional repository for internal institutional uses or as part of an invitation-only research collaboration work-group
    - directly by providing copies to their students or to research collaborators for their personal use
    - for private scholarly sharing as part of an invitation-only work group on commercial sites with which Elsevier has an agreement
- – after the embargo period
    - via non-commercial hosting platforms such as their institutional repository
    - via commercial sites with which Elsevier has an agreement

In all cases accepted manuscripts should:

- – link to the formal publication via its DOI
- – bear a CC-BY-NC-ND license - this is easy to do
- – if aggregated with other manuscripts, for example in a repository or other site, be shared in alignment with our hosting policy not be added to or enhanced in any way to appear more like, or to substitute for, the published journal article.

Published journal article (JPA): A published journal article (PJA) is the definitive final record of published research that appears or will appear in the journal and embodies all value-adding publishing activities including peer review co-ordination, copy-editing, formatting, (if relevant) pagination and online enrichment.

Policies for sharing publishing journal articles differ for subscription and gold open access articles:

Subscription Articles: If you are an author, please share a link to your article rather than the full-text. Millions of researchers have access to the formal publications on ScienceDirect, and so links will help your users to find, access, cite, and use the best available version.

Theses and dissertations which contain embedded PJAs as part of the formal submission can be posted publicly by the awarding institution with DOI links back to the formal publications on ScienceDirect.

If you are affiliated with a library that subscribes to ScienceDirect you have additional private sharing rights for others' research accessed under that agreement. This includes use for classroom teaching and internal training at the institution (including use in course

packs and courseware programs), and inclusion of the article for grant funding purposes.

Gold Open Access Articles: May be shared according to the author-selected end-user license and should contain a CrossMark logo, the end user license, and a DOI link to the formal publication on ScienceDirect.

Please refer to Elsevier's posting policy for further information.

18. **For book authors** the following clauses are applicable in addition to the above: Authors are permitted to place a brief summary of their work online only. You are not allowed to download and post the published electronic version of your chapter, nor may you scan the printed edition to create an electronic version. **Posting to a repository:** Authors are permitted to post a summary of their chapter only in their institution's repository.

19. **Thesis/Dissertation**: If your license is for use in a thesis/dissertation your thesis may be submitted to your institution in either print or electronic form. Should your thesis be published commercially, please reapply for permission. These requirements include permission for the Library and Archives of Canada to supply single copies, on demand, of the complete thesis and include permission for Proquest/UMI to supply single copies, on demand, of the complete thesis. Should your thesis be published commercially, please reapply for permission. Theses and dissertations which contain embedded PJAs as part of the formal submission can be posted publicly by the awarding institution with DOI links back to the formal publications on ScienceDirect.

Elsevier Open Access Terms and Conditions

You can publish open access with Elsevier in hundreds of open access journals or in nearly 2000 established subscription journals that support open access publishing. Permitted third party re-use of these open access articles is defined by the author's choice of Creative Commons user license. See our open access license policy for more information.

Terms & Conditions applicable to all Open Access articles published with Elsevier:

Any reuse of the article must not represent the author as endorsing the adaptation of the article nor should the article be modified in such a way as to damage the author's honour or reputation. If any changes have been made, such changes must be clearly indicated.

The author(s) must be appropriately credited and we ask that you include the end user license and a DOI link to the formal publication on ScienceDirect.

If any part of the material to be used (for example, figures) has appeared in our publication with credit or acknowledgement to another source it is the responsibility of

the user to ensure their reuse complies with the terms and conditions determined by the rights holder.

Additional Terms & Conditions applicable to each Creative Commons user license:

CC BY: The CC-BY license allows users to copy, to create extracts, abstracts and new works from the Article, to alter and revise the Article and to make commercial use of the Article (including reuse and/or resale of the Article by commercial entities), provided the user gives appropriate credit (with a link to the formal publication through the relevant DOI), provides a link to the license, indicates if changes were made and the licensor is not represented as endorsing the use made of the work. The full details of the license are available at http://creativecommons.org/licenses/by/4.0.

CC BY NC SA: The CC BY-NC-SA license allows users to copy, to create extracts, abstracts and new works from the Article, to alter and revise the Article, provided this is not done for commercial purposes, and that the user gives appropriate credit (with a link to the formal publication through the relevant DOI), provides a link to the license, indicates if changes were made and the licensor is not represented as endorsing the use made of the work. Further, any new works must be made available on the same conditions. The full details of the license are available at http://creativecommons.org/licenses/by-nc-sa/4.0.

CC BY NC ND: The CC BY-NC-ND license allows users to copy and distribute the Article, provided this is not done for commercial purposes and further does not permit distribution of the Article if it is changed or edited in any way, and provided the user gives appropriate credit (with a link to the formal publication through the relevant DOI), provides a link to the license, and that the licensor is not represented as endorsing the use made of the work. The full details of the license are available at http://creativecommons.org/licenses/by-nc-nd/4.0. Any commercial reuse of Open Access articles published with a CC BY NC SA or CC BY NC ND license requires permission from Elsevier and will be subject to a fee.

Commercial reuse includes:

- – Associating advertising with the full text of the Article
- – Charging fees for document delivery or access
- – Article aggregation
- – Systematic distribution via e-mail lists or share buttons

Posting or linking by commercial companies for use by customers of those companies.

20. **Other Conditions**:

v1.8

Questions? customercare@copyright.com or +1-855-239-3415 (toll free in the US) or +1-978-646-2777.

For Figure 16: Polymer coat on a rough (left) and smooth (right) supports. From Ref.[118]

JOHN WILEY AND SONS LICENSE
TERMS AND CONDITIONS
Dec 03, 2015

This Agreement between Nikita Kevlich ("You") and John Wiley and Sons ("John Wiley and Sons") consists of your license details and the terms and conditions provided by John Wiley and Sons and Copyright Clearance Center.

License Number	3761401469880
License date	Dec 03, 2015
Licensed Content Publisher	John Wiley and Sons
Licensed Content Publication	AIChE Journal
Licensed Content Title	Interfacial adhesion between polymer separation layer and ceramic support for composite membrane
Licensed Content Author	Wang Wei,Shanshan Xia,Gongping Liu,Xuehong Gu,Wanqin Jin,Nanping Xu
Licensed Content Date	Oct 20, 2009
Pages	9
Type of use	Dissertation/Thesis
Requestor type	University/Academic
Format	Print and electronic
Portion	Figure/table
Number of figures/tables	1
Original Wiley figure/table number(s)	Figure 2
Will you be translating?	No
Title of your thesis / dissertation	CARBON MOLECULAR SIEVE AND CERAMIC MEMBRANES FOR BLACK LIQUOR CONCENTRATION
Expected completion date	Dec 2015
Expected size (number of pages)	180
Requestor Location	Nikita Kevlich 1950 Roswell Rd Apt. 19-B5 MARIETTA, GA 30068 United States Attn: Nikita Kevlich

Billing Type	Invoice
Billing Address	Nikita Kevlich 1950 Roswell Rd Apt. 19-B5 MARIETTA, GA 30068 United States Attn: Nikita Kevlich
Total	0.00 USD

Terms and Conditions

TERMS AND CONDITIONS

This copyrighted material is owned by or exclusively licensed to John Wiley & Sons, Inc. or one of its group companies (each a"Wiley Company") or handled on behalf of a society with which a Wiley Company has exclusive publishing rights in relation to a particular work (collectively "WILEY"). By clicking "accept" in connection with completing this licensing transaction, you agree that the following terms and conditions apply to this transaction (along with the billing and payment terms and conditions established by the Copyright Clearance Center Inc., ("CCC's Billing and Payment terms and conditions"), at the time that you opened your RightsLink account (these are available at any time at http://myaccount.copyright.com).

Terms and Conditions

- The materials you have requested permission to reproduce or reuse (the "Wiley Materials") are protected by copyright.

- You are hereby granted a personal, non-exclusive, non-sub licensable (on a stand-alone basis), non-transferable, worldwide, limited license to reproduce the Wiley Materials for the purpose specified in the licensing process. This license, **and any CONTENT (PDF or image file) purchased as part of your order,** is for a one-time use only and limited to any maximum distribution number specified in the license. The first instance of republication or reuse granted by this license must be completed within two years of the date of the grant of this license (although copies prepared before the end date may be distributed thereafter). The Wiley Materials shall not be used in any other manner or for any other purpose, beyond what is granted in the license. Permission is granted subject to an appropriate acknowledgement given to the author, title of the material/book/journal and the publisher. You shall also duplicate the copyright notice that appears in the Wiley publication in your use of the Wiley Material. Permission is also granted on the understanding that nowhere in the text is a previously published source acknowledged for all or part of this Wiley Material. Any third party content is expressly excluded from this permission.

- With respect to the Wiley Materials, all rights are reserved. Except as expressly granted by the terms of the license, no part of the Wiley Materials may be copied, modified, adapted (except for minor reformatting required by the new Publication), translated, reproduced,

transferred or distributed, in any form or by any means, and no derivative works may be made based on the Wiley Materials without the prior permission of the respective copyright owner. **For STM Signatory Publishers clearing permission under the terms of the STM Permissions Guidelines only, the terms of the license are extended to include subsequent editions and for editions in other languages, provided such editions are for the work as a whole in situ and does not involve the separate exploitation of the permitted figures or extracts,** You may not alter, remove or suppress in any manner any copyright, trademark or other notices displayed by the Wiley Materials. You may not license, rent, sell, loan, lease, pledge, offer as security, transfer or assign the Wiley Materials on a stand-alone basis, or any of the rights granted to you hereunder to any other person.

- The Wiley Materials and all of the intellectual property rights therein shall at all times remain the exclusive property of John Wiley & Sons Inc, the Wiley Companies, or their respective licensors, and your interest therein is only that of having possession of and the right to reproduce the Wiley Materials pursuant to Section 2 herein during the continuance of this Agreement. You agree that you own no right, title or interest in or to the Wiley Materials or any of the intellectual property rights therein. You shall have no rights hereunder other than the license as provided for above in Section 2. No right, license or interest to any trademark, trade name, service mark or other branding ("Marks") of WILEY or its licensors is granted hereunder, and you agree that you shall not assert any such right, license or interest with respect thereto

- NEITHER WILEY NOR ITS LICENSORS MAKES ANY WARRANTY OR REPRESENTATION OF ANY KIND TO YOU OR ANY THIRD PARTY, EXPRESS, IMPLIED OR STATUTORY, WITH RESPECT TO THE MATERIALS OR THE ACCURACY OF ANY INFORMATION CONTAINED IN THE MATERIALS, INCLUDING, WITHOUT LIMITATION, ANY IMPLIED WARRANTY OF MERCHANTABILITY, ACCURACY, SATISFACTORY QUALITY, FITNESS FOR A PARTICULAR PURPOSE, USABILITY, INTEGRATION OR NON-INFRINGEMENT AND ALL SUCH WARRANTIES ARE HEREBY EXCLUDED BY WILEY AND ITS LICENSORS AND WAIVED BY YOU.

- WILEY shall have the right to terminate this Agreement immediately upon breach of this Agreement by you.

- You shall indemnify, defend and hold harmless WILEY, its Licensors and their respective directors, officers, agents and employees, from and against any actual or threatened claims, demands, causes of action or proceedings arising from any breach of this Agreement by you.

- IN NO EVENT SHALL WILEY OR ITS LICENSORS BE LIABLE TO YOU OR ANY OTHER PARTY OR ANY OTHER PERSON OR ENTITY FOR ANY SPECIAL, CONSEQUENTIAL, INCIDENTAL, INDIRECT, EXEMPLARY OR PUNITIVE DAMAGES, HOWEVER CAUSED, ARISING OUT OF OR IN CONNECTION WITH THE DOWNLOADING, PROVISIONING, VIEWING OR USE OF THE MATERIALS REGARDLESS OF THE FORM OF ACTION, WHETHER FOR BREACH OF CONTRACT, BREACH OF WARRANTY, TORT, NEGLIGENCE, INFRINGEMENT OR OTHERWISE (INCLUDING, WITHOUT LIMITATION, DAMAGES BASED ON LOSS OF PROFITS, DATA, FILES, USE, BUSINESS OPPORTUNITY OR CLAIMS OF THIRD PARTIES), AND WHETHER OR NOT THE PARTY HAS BEEN ADVISED OF THE POSSIBILITY OF SUCH DAMAGES. THIS LIMITATION SHALL APPLY NOTWITHSTANDING ANY FAILURE OF ESSENTIAL PURPOSE OF ANY LIMITED REMEDY PROVIDED HEREIN.

- Should any provision of this Agreement be held by a court of competent jurisdiction to be illegal, invalid, or unenforceable, that provision shall be deemed amended to achieve as nearly as possible the same economic effect as the original provision, and the legality, validity and enforceability of the remaining provisions of this Agreement shall not be affected or impaired thereby.

- The failure of either party to enforce any term or condition of this Agreement shall not constitute a waiver of either party's right to enforce each and every term and condition of this Agreement. No breach under this agreement shall be deemed waived or excused by either party unless such waiver or consent is in writing signed by the party granting such waiver or consent. The waiver by or consent of a party to a breach of any provision of this Agreement shall not operate or be construed as a waiver of or consent to any other or subsequent breach by such other party.

- This Agreement may not be assigned (including by operation of law or otherwise) by you without WILEY's prior written consent.

- Any fee required for this permission shall be non-refundable after thirty (30) days from receipt by the CCC.

- These terms and conditions together with CCC's Billing and Payment terms and conditions (which are incorporated herein) form the entire agreement between you and WILEY concerning this licensing transaction and (in the absence of fraud) supersedes all prior agreements and representations of the parties, oral or written. This Agreement may not be amended except in writing signed by both parties. This Agreement shall be binding upon and inure to the benefit of the parties' successors, legal representatives, and authorized assigns.

- In the event of any conflict between your obligations established by these terms and conditions and those established by CCC's Billing and Payment terms and conditions, these terms and conditions shall prevail.

- WILEY expressly reserves all rights not specifically granted in the combination of (i) the license details provided by you and accepted in the course of this licensing transaction, (ii) these terms and conditions and (iii) CCC's Billing and Payment terms and conditions.

- This Agreement will be void if the Type of Use, Format, Circulation, or Requestor Type was misrepresented during the licensing process.

- This Agreement shall be governed by and construed in accordance with the laws of the State of New York, USA, without regards to such state's conflict of law rules. Any legal action, suit or proceeding arising out of or relating to these Terms and Conditions or the breach thereof shall be instituted in a court of competent jurisdiction in New York County in the State of New York in the United States of America and each party hereby consents and submits to the personal jurisdiction of such court, waives any objection to venue in such court and consents to service of process by registered or certified mail, return receipt requested, at the last known address of such party.

WILEY OPEN ACCESS TERMS AND CONDITIONS

Wiley Publishes Open Access Articles in fully Open Access Journals and in Subscription journals offering Online Open. Although most of the fully Open Access journals publish open access articles under the terms of the Creative Commons Attribution (CC BY) License only, the subscription journals and a few of the Open Access Journals offer a choice of Creative Commons Licenses. The license type is clearly identified on the article.

The Creative Commons Attribution License

The Creative Commons Attribution License (CC-BY) allows users to copy, distribute and transmit an article, adapt the article and make commercial use of the article. The CC-BY license permits commercial and non-

Creative Commons Attribution Non-Commercial License

The Creative Commons Attribution Non-Commercial (CC-BY-NC)License permits use, distribution and reproduction in any medium, provided the original work is properly cited and is not used for commercial purposes.(see below)

Creative Commons Attribution-Non-Commercial-NoDerivs License

The Creative Commons Attribution Non-Commercial-NoDerivs License (CC-BY-NC-ND) permits use, distribution and reproduction in any medium, provided the original work is properly cited, is not used for commercial purposes and no modifications or adaptations are made. (see below)

Use by commercial "for-profit" organizations

Use of Wiley Open Access articles for commercial, promotional, or marketing purposes requires further explicit permission from Wiley and will be subject to a fee.

Further details can be found on Wiley Online Library http://olabout.wiley.com/WileyCDA/Section/id-410895.html

Other Terms and Conditions:

v1.10 Last updated September 2015

Questions? customercare@copyright.com or +1-855-239-3415 (toll free in the US) or +1-978-646-2777.

For Figure 10a: Non-monotonic dependence of lignin rejection upon UF membrane MWCO (reprinted by permission of Taylor & Francis LLC [http://www.tandfonline.com] from Ref.[15])

Taylor & Francis
Taylor & Francis Group

Permissions

T & F Reference Number: P112415-03

11/24/2015

Nikita Kevlich
Georgia Institute of Technology
1950 Roswell Rd, Apt. 19-B5
Marietta, GA 30068
nkevlich3@gatech.edu

Dear Ms. Kevlich,

We are in receipt of your request to reproduce Figure 2. Lignin rejection coefficient as a function of membrane molecular weight cut off from the article

Marquita K. Hill, Dale A. Violette & Douglas L. Woerner (1988)
Lowering Kraft Black Liquor Viscosity by Ultrafiltration
Separation Science and Technology 23 (12-13): 1789-1798.
DOI: 10.1080/01496398808075663

For use in your thesis

Permission is granted to reproduce all editions in print and electronic.

We will be pleased to grant you permission free of charge on the condition that:

This permission is for non-exclusive English world rights.

This permission does not cover any third party copyrighted work which may appear in the material requested.

Full acknowledgement must be included showing article title, author, and full Journal title, reprinted by permission of Taylor & Francis LLC (http://www.tandfonline.com).

Thank you very much for your interest in Taylor & Francis publications. Should you have any questions or require further assistance, please feel free to contact me directly.

Sincerely,

Mary Ann Muller
Permissions Coordinator
Telephone: 215.606.4334
E-mail: maryann.muller@taylorandfrancis.com

For Figure 5: Flux and energy trends for different cross-flow velocities and TS at a TMP of 200 (filled-in points) and 300 kPa (unshaded points). From Ref.[79] (http://www.tandfonline.com)

Our Ref: LA/TDWT/P5739

26 November 2015

Dear Nikita Kevlich,

Material requested: Fig 9 from Anna-Karin Nordin & Ann-Sofi Jönsson (2009) Flux and energy requirement during ultrafiltration of a complex industrial process stream, Desalination and Water Treatment, 2:1-3, 326-334

Thank you for your correspondence requesting permission to reproduce the above mentioned material from our Journal in your printed thesis entitled 'Carbon Molecular Sieve And Ceramic Membranes For Black Liquor Concentration' and to be posted in your university's repository - Georgia Institute of Technology - SMARTech Repository.

We will be pleased to grant entirely free permission on the condition that you acknowledge the original source of publication and insert a reference to the Journal's web site: http://www.tandfonline.com

Please note that this licence does not allow you to post our content on any third party websites or repositories.

Thank you for your interest in our Journal.

Yours sincerely

Lee-Ann

Lee-Ann Anderson – Permissions & Licensing Administrator, Journals
Routledge, Taylor & Francis Group
3 Park Square, Milton Park, Abingdon, Oxon, OX14 4RN, UK.
Tel: +44 (0)20 7017 7932
Fax:+44 (0)20 7017 6336
Web: www.tandfonline.com
e-mail: lee-ann.anderson@tandf.co.uk

REFERENCES

1. Boniface, A., Introduction and Principals of Chemical Recovery. In *Chemical Recovery in the Alkaline Pulping Process, Third Edition*, Green, R. P.; Hough, G., Eds. TAPPI Press: Atlanta, GA, 1992.
2. Olsson, M. R. Simulations of Evaporation Plants in Kraft Pulp Mills: Including Lignin Extraction and Use of Excess Heat. Chalmers University of Technology, Göteborg, Sweden, 2009.
3. Forest Products Industry Technology Roadmap: Agenda 2020 www.agenda2020.org (accessed Oct. 4, 2015).
4. Dafinov, A.; Font, J.; Garcia-Valls, R., Processing of black liquors by UF/NF ceramic membranes. *Desalination* **2005,** *173* (1), 83-90.
5. Pettersen, R. C., The chemical composition of wood. In *The chemistry of solid wood.* , Rowell, R. M., Ed. American Chemical Society: Washington, DC, 1984; pp 57-126.
6. Alekhina, M.; Ershova, O.; Ebert, A.; Heikkinen, S.; Sixta, H., Softwood kraft lignin for value-added applications: Fractionation and structural characterization. *Industrial Crops and Products* **2015,** *66* (0), 220-228.
7. Wallberg, O.; Jonsson, A. S., Separation of lignin in kraft cooking liquor from a continuous digester by ultrafiltration at temperatures above 100 degrees C. *Desalination* **2006,** *195* (1-3), 187-200.
8. Keyoumu, A.; Sjodahl, R.; Henriksson, G.; Ek, M.; Gellerstedt, G.; Lindstrom, M. E., Continuous nano- and ultra-filtration of kraft pulping black liquor with ceramic filters - A method for lowering the load on the recovery boiler while generating valuable side-products. *Industrial Crops and Products* **2004,** *20* (2), 143-150.
9. Liu, G. L.; Liu, Y. S.; Ni, J. R.; Shi, H. C.; Qian, Y., Treatability of kraft spent liquor by microfiltration and ultrafiltration. *Desalination* **2004,** *160* (2), 131-141.
10. Xu, G.; Yan, G.-y.; Yang, J.-h., An Integrated Green Process for Beneficial Utilization of Pulping Black Liquor. *Waste Biomass Valor* **2012,** *4* (3), 497-502.
11. Toledano, A.; Garcia, A.; Mondragon, I.; Labidi, J., Lignin separation and fractionation by ultrafiltration. *Separation and Purification Technology* **2010,** *71* (1), 38-43.
12. Wang, Z.; Xue, J. W.; Zhang, J. S.; Liu, W. X., Ultrafiltration Treatment and Physical Properties of Ammonia Sulfite Pulping Liquor of Wheat Straw. In *Material Sciences and Technology, Pts 1 & 2*, Li, Y., Ed. Trans Tech Publications Ltd: Stafa-Zurich, 2012; Vol. 560-561, pp 909-913.
13. Jonsson, A. S.; Wallberg, O., Cost estimates of kraft lignin recovery by ultrafiltration. *Desalination* **2009,** *237* (1-3), 254-267.
14. Ross, D. F.; Cartwright, T. B.; Doshi, M. R.; Dugal, H. S., Ultrafiltration of kraft black liquor. In *IPST Technical Paper Series*, Technology, G. I. o., Ed. Appleton, Wisconsin, 1986.
15. Hill, M. K.; Violette, D. A.; Woerner, D. L., Lowering kraft black liquor viscosity by ultrafiltration. *Separation Science and Technology* **1988,** *23* (12-13), 1789-1798.

16. Arkell, A.; Olsson, J.; Wallberg, O., Process performance in lignin separation from softwood black liquor by membrane filtration. *Chemical Engineering Research & Design* **2014,** *92* (9), 1792-1800.
17. Hellstén, S.; Lahti, J.; Heinonen, J.; Kallioinen, M.; Mänttäri, M.; Sainio, T., Purification process for recovering hydroxy acids from soda black liquor. *Chemical Engineering Research and Design* **2013,** *91* (12), 2765-2774.
18. Cardoso, M.; de Oliveira, E. D.; Passos, M. L., Chemical composition and physical properties of black liquors and their effects on liquor recovery operation in Brazilian pulp mills. *Fuel* **2009,** *88* (4), 756-763.
19. Kirbawy, S. A.; Hill, M. K., Multivalent ion removal from kraft black liquor by ultrafiltration. *Industrial & Engineering Chemistry Research* **1987,** *26* (9), 1851-1854.
20. Worldwide Trends in Energy Use and Efficiency: Key Insights from IEA Indicator Analysis. 2008 ed.; International Energy Agency: France, 2008.
21. Jin, W.; Tolba, R.; Wen, J. L.; Li, K. C.; Chen, A. C., Efficient extraction of lignin from black liquor via a novel membrane-assisted electrochemical approach. *Electrochimica Acta* **2013,** *107* (0), 611-618.
22. Tomani, P., THE LIGNOBOOST PROCESS. *Cellulose Chemistry and Technology* **2010,** *44* (1-3), 53-58.
23. Ohman, F.; Theliander, H., Filtration properties of lignin precipitated from black liquor. *Tappi Journal* **2007,** *6* (7), 3-9.
24. Uloth, V. C.; Wearing, J. T., Kraft lignin recovery - acid precipitation versus ultrafiltration .1. Laboratory test-results. *Pulp & Paper-Canada* **1989,** *90* (9), 67-71.
25. Uloth, V. C.; Wearing, J. T., Kraft lignin recovery - acid precipitation versus ultrafiltration .2. Technology and economics. *Pulp & Paper-Canada* **1989,** *90* (10), T357-T360.
26. Kirkman, A. G.; Gratzl, J. S.; Edwards, L. L., Kraft lignin recovery by ultrafiltration - economic-feasibility and impact on the kraft recovery-system. *Tappi Journal* **1986,** *69* (5), 110-114.
27. De, S.; Bhattacharya, P. K., Recovery of water and inorganic chemicals from kraft black liquor using membrane separation processes. *Tappi Journal* **1996,** *79* (1), 103-111.
28. Lake, M. A. M. P., SC, US), Blackburn, John C. (Easley, SC, US) Process for producing furfural from black liquor. 2014.
29. Venkatesh, V.; Nguyen, X. N., Evaporation and concentration of Black Liquor. In *Chemical Recovery Process in the Alkaline Pulping Process, Third Edition*, Green, R. P.; Hough, G., Eds. TAPPI PRESS: Atlanta, GA, 1992.
30. Vakkilainen, E., Chemical recovery. In *Papermaking Science and Technology: Chemical Pulping*, Gullichsen, J. F., C.-J., Ed. Tappi Press: Finland, 1999; Vol. 6B.
31. Niemelä, K.; Alén, R., Characterization of Pulping Liquors. In *Analytical methods in wood chemistry, pulping and papermaking*, Sjöström, E. A., R., Ed. Springer: 1998.
32. Sjöström, E.; Alén, R., *Analytical methods in wood chemistry, pulping and papermaking*. Springer: 1998.
33. Liu, G. L.; Liu, Y. S.; Shi, H. C.; Qian, Y., Application of inorganic membranes in the alkali recovery process. *Desalination* **2004,** *169* (2), 193-205.
34. Brodin, I.; Sjoholm, E.; Gellerstedt, G., Kraft lignin as feedstock for chemical products: The effects of membrane filtration. *Holzforschung* **2009,** *63* (3), 290-297.

35. Niemelä, K.; Tamminen, T.; Ohra-aho, T. In *Black liquor components as potential raw materials*, 14th International Symposium on Wood, Fibre and Pulping Chemistry, Durban, South Africa, 2007; pp 25-28.
36. Reyes, P.; Teixeira Mendonça, R.; Rodríguez, J.; Fardim, P.; Vega, B., Characterization Of The Hemicellulosic Fraction Obtained After Pre-Hydrolysis Of Pinus Radiata Wood Chips With Hot-Water At Different Initial Ph. *Journal of the Chilean Chemical Society* **2013,** *58*, 1614-1618.
37. Pirttinen, E.; Stenius, P.; Kovasin, K., Surfactant phase equilibria and separation of amphiphilic extractives from black liquor in kraft cooking of wood. *Journal of Dispersion Science and Technology* **2007,** *28* (1), 5-10.
38. Hazlewood, P. E.; Singh, P. M.; Hsieh, J. S., Role of wood extractives in black liquor corrosiveness. *Corrosion* **2006,** *62* (10), 911-917.
39. Grace, T. M.; Sachs, D. G.; Grady, H. J., Determination of the inorganic composition of alkaline black liquors. *Tappi* **1977,** *60* (4), 122-125.
40. Brodin, I. Chemical properties and thermal behaviour of kraft lignins. Licentiate, KTH Royal Institute of Technology, Stockholm, Sweden, 2009.
41. Zabkova, M.; da Silva, E. A. B.; Rodrigues, A. E., Recovery of vanillin from lignin/vanillin mixture by using tubular ceramic ultrafiltration membranes. *Journal of Membrane Science* **2007,** *301* (1-2), 221-237.
42. Brunow, G.; Lundquist, K.; Gellerstedt, G., Lignin. In *Analytical methods in wood chemistry, pulping and papermaking*, Sjöström, E.; Alén, R., Eds. Springer: 1998.
43. Passinen, K. In *Chemical composition of spent liquors*, Symposium on Recovery of Pulping Chemicals, Helsinki, Finland, Kauppakirjapaino Oy: Helsinki, Finland, 1968.
44. Standards. http://www.tappi.org/Standards-TIPs.aspx (accessed Sep. 24,2014).
45. N series: (Procedures for non-fibrous materials). http://www.pfi.no/Info-Center/Scan-test-methods/N-series/ (accessed Sep. 24,2014).
46. Laboratory of Recovery Process. http://www.kclkymlab.fi/index.php/laboratory-of-recovery-process (accessed Sep. 24, 2014).
47. Yang, R. D.; Chen, K. F.; Liu, Y. L.; Chen, Q. F., Shear-thinning properties of non-wood kraft pulping waste liquor. *J. Cent. South Univ. Technol.* **2007,** *14*, 522-525.
48. Schäfer, A. I.; Fane, A. G.; Waite, T. D., *Nanofiltration: principles and applications*. Elsevier: 2005.
49. Seader, J. D.; Henley, E. J.; Roper, D. K., *Separation process principles*. Wiley: 2011.
50. Amjad, Z., *Reverse osmosis: membrane technology, water chemistry & industrial applications*. Chapman & Hall: 1993.
51. Yoon, S. Classification of membranes according to pore size. http://www.onlinembr.info/Membrane%20process/Pore%20size.htm (accessed March 18, 2015).
52. Membrane Filtration Guidance Manual. EPA, Ed. Office of Ground and Drinking Water: Cincinatti, OH, 2005.
53. Baker, R. W., Membrane Technology. In *Encyclopedia of Polymer Science and Technology*, John Wiley & Sons, Inc.: 2002.
54. Foley, G., *Membrane Filtration: A Problem Solving Approach with MATLAB®*. Cambridge University Press: 2013.

55. Causserand, C.; Rouaix, S.; Akbari, A.; Aimar, P., Improvement of a method for the characterization of ultrafiltration membranes by measurements of tracers retention. *Journal of Membrane Science* **2004,** *238* (1–2), 177-190.
56. Li, J.; Ohagan, T.; MacLeod, J. M., Using ultrafiltration to analyze the molar mass distribution of kraft lignin at pH 13. *Can. J. Chem. Eng.* **1996,** *74* (1), 110-117.
57. Rajnish; Bhattacharya, P. K., Ultrafiltrative solute rejection behavior of black liquor. *Acs Symposium Series* **1985,** *281*, 313-323.
58. Poddar, T. K.; Singh, R. P.; Bhattacharya, P. K., Ultrafiltration flux and rejection characteristics of black liquor and polyethylene-glycol. *Chem. Eng. Commun.* **1989,** *75*, 39-56.
59. Bhattacharjee, C.; Bhattacharya, P. K., Prediction of Limiting Flux in Ultrafiltration of Kraft Black Liquor. *Journal of Membrane Science* **1992,** *72* (2), 137-147.
60. Bhattacharjee, C.; Bhattacharya, P. K., Flux Decline Analysis in Ultrafiltration of Kraft Black Liquor. *Journal of Membrane Science* **1993,** *82* (1-2), 1-14.
61. Satyanarayana, S. V.; Bhattacharya, P. K.; De, S., Flux decline during ultrafiltration of kraft black liquor using different flow modules: a comparative study. *Separation and Purification Technology* **2000,** *20* (2-3), 155-167.
62. Bhattacharjee, C.; Bhattacharya, P., Ultrafiltration of black liquor using rotating disk membrane module. *Separation and Purification Technology* **2006,** *49* (3), 281-290.
63. Bhattacharjee, S.; Datta, S.; Bhattacharjee, C., Performance study during ultrafiltration of Kraft black liquor using rotating disk membrane module. *Journal of Cleaner Production* **2006,** *14* (5), 497-504.
64. Bhattacharjee, C.; Sarkar, P.; Datta, S.; Gupta, B. B.; Bhattacharya, P. K., Parameter estimation and performance study during ultrafiltration of Kraft black liquor. *Separation and Purification Technology* **2006,** *51* (3), 247-257.
65. De, S.; Bhattacharya, P. K., Flux prediction of black liquor in cross flow ultrafiltration using low and high rejecting membranes. *Journal of Membrane Science* **1996,** *109* (1), 109-123.
66. Adikane, H. V.; Thakar, D. M.; Nene, S. N., Optimisation of colour and sugar rejection of black liquor using membranes. *Separation and Purification Technology* **2004,** *36* (3), 229-234.
67. Niemi, H.; Lahti, J.; Hatakka, H.; Karki, S.; Rovio, S.; Kallioinen, M.; Manttari, M.; Louhi-Kultanen, M., Fractionation of Organic and Inorganic Compounds from Black Liquor by Combining Membrane Separation and Crystallization. *Chemical Engineering & Technology* **2011,** *34* (4), 593-598.
68. Olsen, O., Membrane Technology in the Pulp and Paper-Industry. *Desalination* **1980,** *35* (1-3), 291-302.
69. Tanistra, I.; Bodzek, M., Preparation of high-purity sulphate lignin from spent black liquor using ultrafiltration and diafiltration processes. *Desalination* **1998,** *115* (2), 111-120.
70. Wang, Z.; Li, Z. Z., *Effect of ultrafiltration on the physical and chemical properties of ammonia sulfite pulping black liquor*. China Light Industry Press: Beijing, 2008; p 1075-1077.

71. Danielsson, L. G.; Yang, X. T., Transport of low molecular weight anions through a Nafion ionomer membrane: Application to kraft cooking liquors. *Analytical Chemistry* **2000,** *72* (7), 1564-1568.
72. Cortinas, S.; Luque, S.; Alvarez, J. R.; Canaval, J.; Romero, J., Microfiltration of kraft black liquors for the removal of colloidal suspended matter (pitch) (vol 147, pg 49, 2002). *Desalination* **2003,** *151* (3), 309-310.
73. Cortinas, S.; Luque, S.; Alvarez, J. R.; Canaval, J.; Romero, J., Microfiltration of kraft black liquors for the removal of colloidal suspended matter (pitch). *Desalination* **2002,** *147* (1-3), 49-54.
74. Holmqvist, A.; Wallberg, O.; Jonsson, A. S., Ultrafiltration of kraft black liquor from two Swedish pulp mills. *Chemical Engineering Research & Design* **2005,** *83* (A8), 994-999.
75. Wallberg, O.; Jonsson, A. S., Influence of the membrane cut-off during ultrafiltration of kraft black liquor with ceramic membranes. *Chemical Engineering Research & Design* **2003,** *81* (A10), 1379-1384.
76. Wallberg, O.; Jonsson, A. S.; Wimmerstedt, R., Fractionation and concentration of kraft black liquor lignin with ultrafiltration. *Desalination* **2003,** *154* (2), 187-199.
77. Wallberg, O.; Jonsson, A. S.; Wimmerstedt, R., Ultrafiltration of kraft black liquor with a ceramic membrane. *Desalination* **2003,** *156* (1-3), 145-153.
78. Jonsson, A. S.; Nordin, A. K.; Wallberg, O., Concentration and purification of lignin in hardwood kraft pulping liquor by ultrafiltration and nanofiltration. *Chemical Engineering Research & Design* **2008,** *86* (11A), 1271-1280.
79. Nordin, A. K.; Jonsson, A. S., Flux and energy requirement during ultrafiltration of a complex industrial process stream. *Desalination and Water Treatment* **2009,** *2* (1-3), 317-324.
80. Rojas, O.; Song, J.; Argyropoulos, D.; Bullón, J., Lignin separation from kraft black liquors by tangential ultrafiltration. *La Chimica e IIndustria* **2006**, 88-95.
81. Sridhar, S.; Bhattacharya, P. K., Limiting Flux Phenomena in Ultrafiltration of Kraft Black Liquor. *Journal of Membrane Science* **1991,** *57* (2-3), 187-206.
82. Jonsson, A. S.; Wimmerstedt, R., The Application of Membrane Technology in the Pulp and Paper-Industry. *Desalination* **1985,** *53* (1-3), 181-196.
83. Kang, I. J.; Yoon, S. H.; Lee, C. H., Comparison of the filtration characteristics of organic and inorganic membranes in a membrane-coupled anaerobic bioreactor. *Water Res.* **2002,** *36* (7), 1803-1813.
84. Thormann, A.; Teuscher, N.; Pfannmöller, M.; Rothe, U.; Heilmann, A., Nanoporous Aluminum Oxide Membranes for Filtration and Biofunctionalization. *Small* **2007,** *3* (6), 1032-1040.
85. Gargulak, J. D.; Lebo, S. E., Commercial Use of Lignin-Based Materials. In *Lignin : historical, biological, and materials perspectives*, Northey, R. A.; Glasser, W. G.; Schultz, T. P., Eds. American Chemical Society: Washington, D.C. , 2000; pp 304-320.
86. Holmbom, B., Extractives. In *Analytical methods in wood chemistry, pulping and papermaking*, Sjöström, E.; Alén, R., Eds. Springer: 1999.
87. Ban, W.; Van Heiningen, A., Adsorption of Hemicellulose Extracts From Hardwood Onto Cellulosic Fibers: I. Effects of Adsorption and Optimization Factors. *Cellulose Chemistry and Technology* **2011,** *45* (1-2), 57-65.

88. Mamman, A. S.; Lee, J.-M.; Kim, Y.-C.; Hwang, I. T.; Park, N.-J.; Hwang, Y. K.; Chang, J.-S.; Hwang, J.-S., Furfural: Hemicellulose/xylosederived biochemical. *Biofuels, Bioproducts and Biorefining* **2008,** *2* (5), 438-454.
89. Furfural Market Analysis By Application (Furfuryl Alcohol, Solvent) And Segment Forecasts To 2020. http://www.grandviewresearch.com/industry-analysis/furfural-market (accessed Oct. 9, 2015).
90. Ziesig, R.; Tomani, P.; Theliander, H., Production of a pure lignin product part 2: Separation of lignin from membrane filtration permeates of black liquor. *Cellulose Chemistry and Technology* **2014,** *48* (9-10), 805-811.
91. Wallberg, O.; Holmqvist, A.; Jonsson, A. S., Ultrafiltration of kraft cooking liquors from a continuous cooking process. *Desalination* **2005,** *180* (1-3), 109-118.
92. Bhattacharjee, C.; Sen, D., Treatment of Kraft Black Liquor Using Membrane-Based Separation Process. In *Membrane technologies and applications* Mohanty, K.; Purkait, M. K., Eds. CRC Press: Boca Raton , FL, 2012.
93. Fritzmann, C.; Lowenberg, J.; Wintgens, T.; Melin, T., State-of-the-art of reverse osmosis desalination. *Desalination* **2007,** *216* (1-3), 1-76.
94. Spiegler, K. S.; Kedem, O., Thermodynamics of hyperfiltration (reverse osmosis): criteria for efficient membranes. *Desalination* **1966,** *1* (4), 311-326.
95. Blatt, W. F.; Dravid, A.; Michaels, A. S.; Nelsen, L., Solute polarization and cake formation in membrane ultrafiltration: causes, consequences, and control techniques. In *Membrane science and technology*, Springer: 1970; pp 47-97.
96. Jonsson, A. S.; Tragardh, G., Fundamental principles of ultrafiltration. *Chem. Eng. Process.* **1990,** *27* (2), 67-81.
97. Feher, J. J.; Ford, G. D., A simple student laboratory on osmotic flow, osmotic pressure, and the reflection coefficient. *The American journal of physiology* **1995,** *268* (6 Pt 3), S10-20.
98. Wijmans, J.; Nakao, S.; Smolders, C., Flux limitation in ultrafiltration: osmotic pressure model and gel layer model. *Journal of membrane science* **1984,** *20* (2), 115-124.
99. Cheryan, M., *Ultrafiltration and Microfiltration Handbook*. CRC Press: Lancaster, Pa, 1998.
100. Cheryan, M., *Ultrafiltration handbook*. Lancaster, Pa.: Technomic Pub. Co., 1986.
101. Kedem, O. t.; Katchalsky, A., Thermodynamic analysis of the permeability of biological membranes to non-electrolytes. *Biochimica et biophysica Acta* **1958,** *27*, 229-246.
102. Thiel, S. W.; Lloyd, D. R., Application Of The Stefan-Maxwell Equations To The Pressure-Driven Membrane Separation Of Dilute Multicomponent Solutions Of Nonelectrolytes. *Journal of Membrane Science* **1988,** *37* (3), 233-249.
103. Williams, M. E. A Review of Reverse Osmosis Theory 2003. http://www.eetcorp.com/heepm/RO_TheoryE.pdf (accessed Oct. 11, 2015).
104. Zeman, L. J., *Microfiltration and ultrafiltration : principles and applications*. New York: Marcel Dekker, 1996.
105. Nakao, S.; Kimura, S., Analysis Of Solutes Rejection In Ultrafiltration. *J. Chem. Eng. Jpn.* **1981,** *14* (1), 32-37.

106. Ganguly, S.; Bhattacharya, P. K., Development of concentration profile and prediction of flux for ultrafiltration in a radial cross-flow cell. *Journal of Membrane Science* **1994,** *97* (0), 185-198.
107. Saufi, S. M.; Ismail, A. F., Fabrication of carbon membranes for gas separation—a review. *Carbon* **2004,** *42* (2), 241-259.
108. Rungta, M. Carbon Molecular Sieve Dense Film Membranes For Ethylene/Ethane Separations. Georgia Institute of Technology, Atlanta, GA, 2012.
109. Zhang, Y.; Musselman, I. H.; Ferraris, J. P.; Balkus Jr, K. J., Gas permeability properties of Matrimid® membranes containing the metal-organic framework Cu–BPY–HFS. *Journal of Membrane Science* **2008,** *313* (1–2), 170-181.
110. Vu, D. Q.; Koros, W. J.; Miller, S. J., Mixed matrix membranes using carbon molecular sieves: I. Preparation and experimental results. *Journal of Membrane Science* **2003,** *211* (2), 311-334.
111. Tin, P. S.; Lin, H. Y.; Ong, R. C.; Chung, T. S., Carbon molecular sieve membranes for biofuel separation. *Carbon* **2011,** *49* (2), 369-375.
112. Gullichsen, J.; Fogelholm, C.-J., *Papermaking Science and Technology: Chemical Pulping*. Tappi Press: Finland, 1999; Vol. 6B.
113. Fuertes, A. B.; Centeno, T. A., Preparation of supported carbon molecular sieve membranes. *Carbon* **1999,** *37* (4), 679-684.
114. Tin, P. S.; Xiao, Y. C.; Chung, T. S., Polyimide-carbonized membranes for gas separation: Structural, composition, and morphological control of precursors. *Sep. Purif. Rev.* **2006,** *35* (4), 285-318.
115. Jiang, L. Y.; Chung, T.-S.; Rajagopalan, R., Dehydration of alcohols by pervaporation through polyimide asymmetric hollow fibers with various modifications. *Chem. Eng. Sci.* **2008,** *63* (1), 204-216.
116. Chung, T.-S.; Guo, W. F.; Liu, Y., Enhanced Matrimid membranes for pervaporation by homogenous blends with polybenzimidazole (PBI). *Journal of Membrane Science* **2006,** *271* (1–2), 221-231.
117. Rasband, W. S. ImageJ. http://imagej.nih.gov/ij/.
118. Wei, W.; Xia, S.; Liu, G.; Gu, X.; Jin, W.; Xu, N., Interfacial Adhesion Between Polymer Separation Layer and Ceramic Support for Composite Membrane. *Aiche J.* **2010,** *56* (6), 1584-1592.
119. Benito, J. M.; Conesa, A.; Rodriguez, M. A., Preparation of multilayer ceramic systems for deposition of mesoporous membranes. *Journal of Materials Science* **2005,** *40* (23), 6105-6112.
120. Fuertes, A. B.; Centeno, T. A., Carbon molecular sieve membranes from polyetherimide. *Microporous and Mesoporous Materials* **1998,** *26* (1-3), 23-26.
121. Wang, C.; Hu, X.; Yu, J.; Wei, L.; Huang, Y., Intermediate gel coating on macroporous Al2O3 substrate for fabrication of thin carbon membranes. *Ceramics International* **2014,** *40* (7), 10367-10373.
122. Fuertes, A. B.; Centeno, T. A., Preparation of supported asymmetric carbon molecular sieve membranes. *Journal of Membrane Science* **1998,** *144* (1-2), 105-111.
123. Hedlund, J.; Sterte, J.; Anthonis, M.; Bons, A.-J.; Carstensen, B.; Corcoran, N.; Cox, D.; Deckman, H.; De Gijnst, W.; de Moor, P.-P.; Lai, F.; McHenry, J.; Mortier, W.; Reinoso, J.; Peters, J., High-flux MFI membranes. *Microporous and Mesoporous Materials* **2002,** *52* (3), 179-189.

124. Evans, J. R. G.; Edirisinghe, M. J., Interfacial factors affecting the incidence of defects in ceramic mouldings. *Journal of Materials Science* **1991,** *26* (8), 2081-2088.
125. Manjula, S.; Kumar, S. M.; Raichur, A. M.; Madhu, G. M.; Suresh, R.; Raj, M. A. L. A., A sedimentation study to optimize the dispersion of alumina nanoparticles in water. *Cerâmica* **2005,** *51*, 121-127.
126. Singh, B. P.; Menchavez, R.; Takai, C.; Fuji, M.; Takahashi, M., Stability of dispersions of colloidal alumina particles in aqueous suspensions. *J. Colloid Interface Sci.* **2005,** *291* (1), 181-186.
127. Bertazzo, S.; Rezwan, K., Control of α-Alumina Surface Charge with Carboxylic Acids. *Langmuir* **2010,** *26* (5), 3364-3371.
128. Chen, X.; Zhang, W.; Lin, Y.; Cai, Y.; Qiu, M.; Fan, Y., Preparation of high-flux gamma-alumina nanofiltration membranes by using a modified sol-gel method. *Microporous and Mesoporous Materials* **2015,** *214*, 195-203.
129. Ma, X.; Lin, B. K.; Wei, X.; Kniep, J.; Lin, Y. S., Gamma-Alumina Supported Carbon Molecular Sieve Membrane for Propylene/Propane Separation. *Industrial & Engineering Chemistry Research* **2013,** *52* (11), 4297-4305.
130. Schaep, J.; Vandecasteele, C.; Peeters, B.; Luyten, J.; Dotremont, C.; Roels, D., Characteristics and retention properties of a mesoporous gamma-Al2O3 membrane for nanofiltration. *Journal of Membrane Science* **1999,** *163* (2), 229-237.
131. Kassaee, M. H. Internal surface modification of zeolite MFI particles and membranes for gas separation. Dissertation, Georgia Institute of Technology, Atlanta, GA, 2012.
132. Kumar, P.; Ida, J.; Kim, S.; Guliants, V. V.; Lin, J. Y. S., Ordered mesoporous membranes: Effects of support and surfactant removal conditions on membrane quality. *Journal of Membrane Science* **2006,** *279* (1–2), 539-547.
133. Khalili, M.; Sabbaghi, S.; Daneshmand, H.; Zerafat, M., Synthesis and characterization of [alpha]-Alumina membrane supports and the binding effect of Poly (Vinyl Alcohol). *International Journal of Nano Dimension* **2014,** *5* (4), 393.
134. Shevade, S.; Ford, R. G., Use of synthetic zeolites for arsenate removal from pollutant water. *Water Res.* **2004,** *38* (14–15), 3197-3204.
135. Best, D. F. Urea rejuvenation of catalysts. 1987.
136. Arhippainen, B.; Jungerstam, B. In *Kraft Liquor Evaporation*, Symposium on Recovery of Pulping Chemicals, Helsinki, Finland, Kauppakirjapaino Oy: Helsinki, Finland, 1968.
137. Zhu, W.; Westman, G.; Theliander, H., The molecular properties and carbohydrate content of lignins precipitated from black liquor. *Holzforschung* **2014,** *0* (0).
138. Arkell, A.; Olsson, J.; Wallberg, O., Process performance in lignin separation from softwood black liquor by membrane filtration. *Chemical Engineering Research and Design* **2013,** (0).
139. Aldaeus, F.; Schweinebarth, H.; Torngren, P.; Jacobs, A., Simplified determination of total lignin content in kraft lignin samples and black liquors. *Holzforschung* **2011,** *65* (4), 601-604.
140. Easty, D. B.; Borchardt, M. L.; Webb, A. A., Analysis of pulping liquors by ion chromatography: evaluation and validation. **1984**.
141. Xu, K. M.; Liu, H. Y.; Dong, L.; Tong, S.; Liu, Y. J., Lignin recovery from the black liquor of Reed pulping. In *Renewable and Sustainable Energy Ii, Pts 1-4*, Ren, N.;

Che, L. K.; Jin, B.; Dong, R.; Su, H., Eds. Trans Tech Publications Ltd: Stafa-Zurich, 2012; Vol. 512-515, pp 2376-2380.
142. Helander, M.; Theliander, H.; Lawoko, M.; Henriksson, G.; Zhang, L. M.; Lindstrom, M. E., Fractionation of Technical Lignin: Molecular Mass and pH Effects. *Bioresources* **2013,** *8* (2), 2270-2282.
143. Manttari, M.; Lahti, J.; Hatakka, H.; Louhi-Kultanen, M.; Kallioinen, M., Separation phenomena in UF and NF in the recovery of organic acids from kraft black liquor. *Journal of Membrane Science* **2015,** *490*, 84-91.